UNIVERSIDADE DE LISBOA

FACULDADE DE MEDICINA VETERINÁRIA

DESCRIPTIVE ANALYSIS OF LOW-FIELD MAGNETIC RESONANCE IMAGING FINDINGS IN THE FOOT OF 149 HORSES

TERESA COELHO REIS ARAÚJO

ORIENTADORA:
Doutora Katherine Arlene Robinson

COORIENTADOR:
Doutor Luís Ressano Garcia Pardon Lamas

2025

UNIVERSIDADE DE LISBOA

FACULDADE DE MEDICINA VETERINÁRIA

DESCRIPTIVE ANALYSIS OF LOW-FIELD MAGNETIC RESONANCE IMAGING FINDINGS IN THE FOOT OF 149 HORSES

TERESA COELHO REIS ARAÚJO

DISSERTAÇÃO DE MESTRADO INTEGRADO EM MEDICINA VETERINÁRIA

JÚRI
PRESIDENTE:
Doutor António José de Almeida Ferreira

VOGAIS:
Doutora Paula Alexandra Botelho Garcia de Andrade Pimenta Tilley
Doutor Luís Ressano Garcia Pardon Lamas

ORIENTADORA:
Doutora Katherine Arlene Robinson

COORIENTADOR:
Doutor Luís Ressano Garcia Pardon Lamas

2025

DECLARAÇÃO RELATIVA ÀS CONDIÇÕES DE REPRODUÇÃO DA DISSERTAÇÃO

Nome: Teresa Coelho Reis Araújo

Título da Tese ou Dissertação: Descriptive analysis of low-field magnetic resonance imaging findings in the foot of 149 horses

Ano de conclusão (indicar o da data da realização das provas públicas): 2025

Designação do curso de Mestrado ou de Doutoramento: Mestrado Integrado em Medicina Veterinária

Área científica em que melhor se enquadra (assinale uma):

☒ Clínica ☐ Produção Animal e Segurança Alimentar
☐ Morfologia e Função ☐ Sanidade Animal

Declaro sobre compromisso de honra que a tese ou dissertação agora entregue corresponde à que foi aprovada pelo júri constituído pela Faculdade de Medicina Veterinária da ULISBOA.

Declaro que concedo à Faculdade de Medicina Veterinária e aos seus agentes uma licença não-exclusiva para arquivar e tornar acessível, nomeadamente através do seu repositório institucional, nas condições abaixo indicadas, a minha tese ou dissertação, no todo ou em parte, em suporte digital.

Declaro que autorizo a Faculdade de Medicina Veterinária a arquivar mais de uma cópia da tese ou dissertação e a, sem alterar o seu conteúdo, converter o documento entregue, para qualquer formato de ficheiro, meio ou suporte, para efeitos de preservação e acesso.

Retenho todos os direitos de autor relativos à tese ou dissertação, e o direito de a usar em trabalhos futuros (como artigos ou livros).

Concordo que a minha tese ou dissertação seja colocada no repositório da Faculdade de Medicina Veterinária com o seguinte estatuto (assinale um):

1. ☒ Disponibilização imediata do conjunto do trabalho para acesso mundial;
2. ☐ Disponibilização do conjunto do trabalho para acesso exclusivo na Faculdade de Medicina Veterinária durante o período de ☐ 6 meses, ☐ 12 meses, sendo que após o tempo assinalado autorizo o acesso mundial*;

* Indique o motivo do embargo (OBRIGATÓRIO)

Nos exemplares das dissertações de mestrado ou teses de doutoramento entregues para a prestação de provas na Universidade e dos quais é obrigatoriamente enviado um exemplar para depósito na Biblioteca da Faculdade de Medicina Veterinária da Universidade de Lisboa deve constar uma das seguintes declarações (incluir apenas uma das três):

1. É AUTORIZADA A REPRODUÇÃO INTEGRAL DESTA TESE/TRABALHO APENAS PARA EFEITOS DE INVESTIGAÇÃO, MEDIANTE DECLARAÇÃO ESCRITA DO INTERESSADO, QUE A TAL SE COMPROMETE.
2. É AUTORIZADA A REPRODUÇÃO PARCIAL DESTA TESE/TRABALHO (indicar, caso tal seja necessário, nº máximo de páginas, ilustrações, gráficos, etc.) APENAS PARA EFEITOS DE INVESTIGAÇÃO, MEDIANTE DECLARAÇÃO ESCRITA DO INTERESSADO, QUE A TAL SE COMPROMETE.
3. DE ACORDO COM A LEGISLAÇÃO EM VIGOR, (indicar, caso tal seja necessário, nº máximo de páginas, ilustrações, gráficos, etc.) NÃO É PERMITIDA A REPRODUÇÃO DE QUALQUER PARTE DESTA TESE/TRABALHO.

Faculdade de Medicina Veterinária da Universidade de Lisboa, 03 de Outubro de 2025

Assinatura: Teresa Araújo.

ACKNOWLEDGEMENTS

Firstly, I would like to thank my supervisors, who generously dedicated their time and expertise to support me throughout the development of this dissertation. Dr. Kate Robinson, for her kind mentorship and guidance throughout my traineeship at McKee-Pownall Equine Services and beyond; and Professor Luís Lamas, who first welcomed me to the world of equine veterinary practice and has taught me so much over the years. I am also grateful to Professor Rita Pequito, who encouraged and guided me through the initial stages of this project.

A huge thank you to the entire team at MPES for providing such a rich, fun, and supportive learning environment, and for making me feel right at home in their practice (and in Canada!). Special thanks to Dr. Alejandra Garza, Dr. Rafael Gomez, Dr. Andrea Dubé, and the rest of the wonderful team at Caledon for their support, patience and for sharing their knowledge; to Dr. Tara Richards for kindly allowing me to join her ophthalmology consultations; to Stacey Thompson, for taking the time to introduce me to MRI and for her essential help in gathering the data for this study; and to Jeff, for his generosity and for kindly sharing his fond memories of Portugal with me. Finally, I'm deeply grateful for Dr. Mike Pownall, who made this and so many other invaluable learning opportunities possible.

I would also like to extend my genuine gratitude to the whole team at the Equine Emergency and Surgery Service of the University of Lisbon (SCUE), who played such a fundamental role in my clinical training. A special thank you to Dr. Teresa Rosa, Dr. Mariana Magalhães, Dr. Gonçalo Silva, and Dr. Deborah Dias for all their patience, for giving me the opportunity to learn from them, and for being incredible role models to look up to since the very beginning of my veterinary journey. I would also like to thank all the interns, externs, and volunteers I've had the pleasure of working alongside over the years, and who helped make this journey so memorable.

To my classmates and fellow *Scueteiros*, especially Carolina, Alice, Sofia, Catarina, Carra, Cláudia, João, Laura, Salvador, Carol, Maria Rita, Maria e Cerca, without whom I truly could not have done it. Thank you for being there then and always!

To my dear friends Chica, Catarina, Madalena, Inês, Pat, Bia e Mara, who have supported me in more ways than they know, thank you for everything.

And last, but most definitely not least, to my family, especially my dear parents and siblings, for their unwavering love and support throughout all aspects of life. I am endlessly grateful for everything you do for me.

My sincere gratitude to all those that in one way or another were part of this long, challenging, yet incredibly rewarding journey to becoming a Doctor of Veterinary Medicine.

Obrigada!

RESUMO

ANÁLISE DESCRITIVA DOS SINAIS IMAGIOLÓGICOS DE RESSONÂNCIA MAGNÉTICA DE BAIXO CAMPO NO CASCO DE 149 CAVALOS

A claudicação com origem no casco é um dos casos mais frequentes em clínica de equinos, sendo a ressonância magnética (RM) considerada o *gold standard* para a sua avaliação por superar as limitações das modalidades imagiológicas convencionais. Este estudo retrospetivo analisou a aplicação clínica de RM de baixo campo realizada com o cavalo em estação, ao longo de três anos, numa população predominantemente composta por cavalos de desporto na província de Ontário, no Canadá. Teve ainda como objetivos caracterizar a prevalência, natureza e padrões de coocorrência das alterações detetadas no casco do membro torácico, e explorar possíveis associações com fatores demográficos (idade, sexo, raça e disciplina).

Foram analisados os registos clínicos de 185 cavalos que realizaram exames de RM de baixo campo em estação, numa única clínica, com o objetivo de descrever a casuística geral. Um subgrupo de 149 cavalos com exame ao casco do membro torácico foi selecionado para análise detalhada. As alterações registadas referem-se aos membros com claudicação, tendo sido assinaladas as estruturas afetadas, o tipo de lesão e a sua relevância clínica, segundo a interpretação do autor do relatório.

A maioria dos exames foi realizada no verão (32.6%) e outono (30.8%) para investigar claudicação dos membros torácicos, e o casco foi a região mais frequentemente examinada. Entre os 149 cavalos (179 membros afetados), os sinais imagiológicos clinicamente significativos mais prevalentes foram a tendinopatia do tendão flexor digital profundo (TFDP) e padrão de lesão medular do osso navicular (46.4%). Embora a distensão da articulação interfalângica distal (86%) e da bursa navicular (60.3%) tenham sido as alterações mais comuns, estas foram frequentemente consideradas secundárias ou incidentais. Identificaram-se associações significativas entre: tendinopatia do TFDP e alterações do osso e da bursa navicular; e entre alterações do osso navicular e bursite, e entesopatia do ligamento ímpar. Verificou-se ainda que lesões da falange distal foram mais prevalentes em machos castrados, e lesões da articulação interfalângica proximal em cavalos mais velhos (16–20 anos).

Estes resultados reforçam a utilidade diagnóstica da RM e contribuem para uma melhor compreensão dos padrões de patologia do casco nesta população. A elevada prevalência de alterações concomitantes em estruturas ósseas e de tecidos moles realça a importância de uma avaliação completa por RM. O reconhecimento de tendências demográficas pode ajudar na identificação precoce e na prevenção destas patologias.

Palavras-chave: equino; ressonância magnética; casco; claudicação.

ABSTRACT

DESCRIPTIVE ANALYSIS OF LOW-FIELD MAGNETIC RESONANCE FINDINGS IN THE FOOT OF 149 HORSES

Foot-related lameness is one of the most common clinical presentations in equine practice, with magnetic resonance imaging (MRI) overcoming the limitations of conventional imaging modalities and serving as the gold standard for comprehensive evaluation of the foot. This retrospective study analyzed the clinical application of standing low-field MRI over a three-year period in a predominantly sport horse population in Ontario, Canada. It further aimed to characterize the prevalence, nature, and co-occurrence of MRI findings in the forelimb foot, and to explore associations with demographic factors (age, sex, breed, discipline).

Medical records of 185 horses that underwent standing low-field MRI at a single equine practice were reviewed to provide an overview of the MRI caseload. A subset of 149 horses with forelimb lameness that underwent foot imaging was selected for detailed analysis of MRI findings. Abnormalities were extracted from MRI reports for clinically lame limbs, with each affected structure and lesion type recorded. Clinical significance was determined based on the original report author's interpretation.

MRI was primarily used in the summer (32.6%) and fall (30.8%) to investigate forelimb lameness, with the foot being the most frequently imaged region. Among the 149 horses (179 lame limbs) that underwent forelimb foot imaging, the most prevalent clinically significant findings were deep digital flexor tendon (DDFT) tendinopathy (49.2%) and navicular bone marrow lesions (46.4%). Although distal interphalangeal (DIP) joint effusion (86%) and navicular bursitis (60.3%) were the most frequent findings overall, these were often interpreted as secondary or incidental. Significant associations were identified between: DDFT tendinopathy and both navicular bone and bursa pathology; and, navicular bone pathology and both navicular bursitis and distal sesamoidean impar ligament (DSIL) enthesopathy. Additionally, distal phalanx pathology was significantly more prevalent in geldings, and proximal interphalangeal (PIP) joint pathology in older horses (16-20 years).

These findings support the diagnostic utility of MRI in equine practice and contribute to a better understanding of foot pathology patterns in this population. The high prevalence of concurrent osseous and soft tissue abnormalities underscores the importance of comprehensive MRI evaluation. Awareness of demographic trends may aid in early recognition and more targeted management of foot-related lameness.

Key words: equine; magnetic resonance imaging; foot; forelimb lameness.

TABLE OF CONTENTS

TABLE INDEX

FIGURE INDEX

LIST OF ABBREVIATIONS

ACVR	American College of Veterinary Radiology
CLs	Collateral Ligaments
CSL	Collateral Sesamoidean Ligaments
CT	Computed Tomography
DDAL	Distal Digital Annular Ligament
DDFT	Deep Digital Flexor Tendon
DIP	Distal Interphalangeal Joint
DSIL	Distal Sesamoidean Impar Ligament
FSE/TSE	Fast Spin Echo / Turbo Spin Echo
GE/GRE	Gradient (Recalled) Echo
SPGR	Spoiled Gradient Echo
IR	Inversion Recovery
LF	Left Front (limb)
MHz	Megahertz
MPES	McKee-Pownall Equine Services
MRI	Magnetic Resonance Imaging
NB	Navicular Bone
NBU	Navicular Bursa
NEHS	National Equine Health Survey
OCLL	Osseous Cyst-Like Lesion
P2	Middle Phalanx
P3	Distal Phalanx
PD	Proton Density
PIP	Proximal Interphalangeal Joint
RF	Radiofrequency
RF	Right Front (limb)
RVT	Registered Veterinary Technician
SE	Spin Echo
SDFT	Superficial Digital Flexor Tendon
SI	Signal Intensity
STIR	Short-Tau Inversion Recovery
T1	T1-weighted images
T2	T2-weighted images
T2*	T2-star weighted images
TE	Time of Echo
TR	Time of Repetition
UC	Ungual Cartilages

I. CURRICULAR TRAINEESHIP

My curricular traineeship in clinical practice took place at McKee-Pownall Equine Services (MPES) in Ontario, Canada, between September 19 and December 16 of 2022. MPES is a full-service ambulatory equine practice with a strong focus on lameness, sport horse medicine, pre-purchase exams, dentistry, and preventative care, operating across three locations in the Greater Toronto Area. During this period, I was primarily based at the Reproduction and Rehabilitation Farm (now known as the Performance Centre), under the supervision of Dr. Kate Robinson. I also had the opportunity to learn from a team of experienced equine practitioners, including Dr. Alejandra Garza, Dr. Rafael Gomez, and Dr. Andrea Dubé, as well as from a wonderful team of veterinary technicians and assistants. At the time, the Reproduction and Rehabilitation Farm provided in-clinic treatment for horses recovering from surgery, injury, or conditions requiring intensive medical care not easily managed at home, in addition to outpatient ambulatory services in the surrounding areas. Although breeding services were available at this facility, the traineeship took place during the off-season, so I only witnessed a few outpatient pregnancy checks.

My daily routine began with morning rounds, where I participated in the discussion, monitoring, and treatment of hospitalized patients. This was followed by ambulatory appointments, during which I was exposed to a wide range of clinical cases and services, offering a well-rounded understanding of the day-to-day responsibilities of an equine primary care practitioner. Patients ranged from pleasure to elite sport horses, and the cases included wellness care (vaccinations, bloodwork, coggins testing, insurance forms), dentistry work, sports medicine (lameness examinations including diagnostic analgesia and imaging, joint injections, laser and shockwave therapy), bodywork (chiropractic, osteopathy, acupuncture, massage therapy, etc), elective field surgeries (castration, enucleation), and emergency care (colic, lacerations, esophageal obstruction). Once a week, I had the privilege of shadowing Dr. Tara Richards, a board-certified ophthalmologist, who consults for MPES and receives referral cases from across Ontario. This experience significantly broadened my knowledge of equine ophthalmology, as I assisted in the diagnosis and management of various ocular conditions. Additionally, I visited the Campbellville clinic on two occasions to observe standing MRI examinations. Under the guidance of Stacey Thompson, RVT, I was introduced to the principles of magnet preparation, patient positioning, sedation protocols, and the basics of image acquisition and interpretation.

Beyond the clinical experience, I had the opportunity to receive business training from Dr. Mike Pownall, co-founder of MPES and an MBA graduate. These sessions were built around general case studies to explore core business concepts and discuss how those principles could be applied to the management of a modern veterinary practice.

II. LITERATURE REVIEW

1. Introduction

Lameness is the most prevalent health concern in equine veterinary practice, not only impacting horse welfare and performance, but also carrying social and economic implications (NEHS 2016). It is defined as an abnormal gait or stance resulting from a structural disorder, a mechanical defect, or neuromuscular dysfunction (Ross 2011a). Regardless of its underlying cause, most cases of lameness are a manifestation of pain in one or more limbs, characterized by an asymmetric gait (or limping), with its severity ranging from subtle performance limitations to complete loss of function (Baxter 2022).

Beyond its implications for equine welfare, lameness has been shown to be the leading cause of decreased performance in athletic horses, contributing to lost training days, reduced competition opportunities, and early retirement (Egenvall et al. 2013; Swor et al. 2019; Boorman et al. 2021). Additionally, veterinary care and periods of inactivity following lameness episodes represent considerable financial burdens for owners (Egenvall et al. 2008; Uprichard et al. 2014).

Several factors contribute to a horse's susceptibility to lameness, including intrinsic factors such as age, gender, breed, and conformation, as well as extrinsic factors like sport discipline, training intensity, or environmental conditions (Baxter 2022). Consequently, the type and anatomical location of musculoskeletal issues may be influenced by these factors, with certain injuries being linked to specific groups. For instance, younger horses are more likely to present with lameness due to developmental orthopaedic disease (Lepeule et al. 2011), while older horses are more likely to develop osteoarthritis and chronic laminitis (Van Weeren and Back 2016). Similarly, abnormal hoof conformation has been shown to be associated with the presence of lameness, as horses with an upright heel or broken-back hoof-pastern axis conformation are more likely to experience lameness (Mata et al. 2024).

Understanding these risk factors is critical for developing effective prevention strategies and enabling early detection of abnormalities. Early intervention is essential to mitigate the progression of minor issues that, if left unaddressed, can lead to chronic pain or irreversible damage (Weishaupt 2008). Accurate diagnosis is equally essential, as effective management depends on identifying the root cause of lameness rather than merely addressing the clinical signs (Davidson 2018). In this context, advanced imaging modalities such as magnetic resonance imaging (MRI) play a fundamental role in identifying and diagnosing subtle or complex pathologies, particularly in the foot, where traditional imaging techniques may be less effective (Barrett et al. 2017a; Gallastegui 2021).

2. Magnetic Resonance Imaging

2.1. Image Acquisition

MRI is based on the physical phenomenon of nuclear magnetic resonance, which relies on the principle that certain atomic nuclei have magnetic properties, and can therefore be manipulated by an external magnetic field and radiofrequency (RF) pulses to generate signals (Bolas 2010). In a clinical context, MRI leverages the inherent magnetic properties (spin) of hydrogen protons and their natural abundance in body tissues, particularly in water and fat, to generate strong detectable signals (Bolas 2010).

An MRI system consists of a large magnet, magnetic field gradients, transmitter and receiver RF coils, and a computer with a dedicated software (Murray and Mair 2005; Werpy et al. 2006). The imaging process involves a complex interaction between these components and the tissues being examined.

The large magnet in the MRI scanner generates a strong, uniform magnetic field. When a horse's limb is placed within this field, the hydrogen protons in the tissues undergo two processes: alignment and precession (Werpy et al. 2006; Bolas 2010). Firstly, the protons align parallel to the main magnetic field in a low-energy state, behaving like tiny bar magnets. They then start to precess, or rotate, around the axis of the magnetic field at a specific speed or frequency. This frequency is directly proportional to the strength of the magnetic field and falls within the megahertz (MHz) range of radio frequencies at the typical field strengths used in clinical MRI systems (Bolas 2010).

To generate a signal, an RF coil positioned around the scanned region applies short radiofrequency pulses that must match the frequency of the precessing protons (Werpy et al. 2006; Bolas 2010). Each RF pulse causes the protons to absorb energy and transition to a higher-energy state (excitation), changing their orientation while synchronizing their precession (resonance). Once the RF pulse stops, the protons gradually return to their original alignment, releasing the absorbed energy and losing synchronization (relaxation). This emitted energy is detected by the RF coil, converted into an electrical signal, and processed by the computer software to generate an image (Werpy et al. 2006; Bolas 2010).

To determine the location of the received signals and construct a three-dimensional (3D) representation of the tissues, additional magnetic field gradients are applied using gradient coils inbuilt in the scanner (Bolas 2010). These gradient magnets create small variations in the field strength across the scanned region in the sagittal, transverse, and dorsal planes, causing the protons in different locations to precess at slightly different frequencies. This frequency variation allows the system to spatially encode the emitted and received signals, mapping them to specific locations based on their frequency (Werpy et al. 2006; McKnight 2012a).

2.2. Pulse Sequences

While the principles of MR image acquisition are always the same, several different acquisition, or pulse, sequences are often necessary to achieve useful diagnostic images (Murray and Mair 2005). Pulse sequences are a series of RF pulses and magnetic field gradients applied in a specific order to manipulate the magnetic properties of protons in the tissues (Bolas 2010). These sequences dictate how signals are generated and collected, influencing image appearance, resolution, and scan times (Jaskólska et al. 2013). There is a wide range of pulse sequences available to choose from, and the choice is mostly determined by which one offers the optimal diagnostic utility depending on the structure of interest (Murray and Mair 2005).

There are three main categories of sequences used: spin echo (SE), gradient echo (GRE), and inversion recovery (IR). The main difference between them is that SE sequences use two RF pulses, while GRE uses a magnetic gradient along with a single RF pulse to form an echo and strengthen the detected signal; IR sequences use an initial inverting RF pulse to nullify the signal from specific tissue types (Werpy et al. 2006; Jaskólska et al. 2013).

SE sequences are advantageous due to their high signal-to-noise ratio[1] (SNR) and consistent image quality. They produce images with higher contrast resolution, making them particularly useful for defining soft-tissue margins (Jaskólska et al. 2013). However, they require long scan times, making them less suitable for clinical scenarios where patient motion or time under general anesthesia is a concern (Murray and Mair 2005). Therefore, fast spin echo (FSE) sequences have been developed to acquire multiple echoes within a single pulse, decreasing acquisition time but slightly trading off image quality (Werpy et al. 2006).

GRE sequences offer faster acquisition times compared to SE-based techniques. They acquire information in a volume, allowing for the production of thin tissue slices with good anatomic detail, making them advantageous for three-dimensional reconstruction of images (Tucker and Sampson 2007). However, they have increased susceptibility to artifacts from magnetic field inhomogeneities and decreased soft-tissue contrast (Werpy et al. 2006).

IR sequences are designed to enhance image contrast by selectively supressing signals from other tissues (Bolas 2010). A commonly used IR technique is short tau inversion recovery (STIR), which highlights fluid by supressing the signal from fat, which is relatively high on all sequences (Werpy et al. 2006). This makes STIR particularly useful for detecting early and subtle pathological changes in bone and soft-tissue structures, but tends to have relatively low detail and longer acquisition times (Murray and Mair 2005).

[1] Signal-to-Noise Ratio (SNR) – measure of strength of the signal generated by the tissues relative to the signal generated by background noise (Winter 2012).

2.3. Image Appearance and Contrast Optimization

MR images are displayed in shades of gray, where different tissues appear as varying levels of brightness, or signal intensity. The signal intensity received from protons varies based on the tissue type, as differences in tissue composition and molecular structure influence the availability of protons and their response to pulse sequences (Bolas 2010). Tissues with high signal intensity appear white (hyperintense), those with low signal intensity appear black (hypointense), and intermediate signals appear gray (isointense) (Werpy et al. 2006).

To comprehensively evaluate the tissues, it is often necessary to obtain multiple images of the same structures with different contrasts and compare them. A balanced image contrast is desired for general tissue differentiation, but certain tissue properties may need to be emphasized over others to effectively detect and characterize abnormalities (Winter 2012). While pulse sequences dictate the method of acquisition, adjusting certain acquisition parameters like echo time[2] (TE) and repetition time[3] (TR), allows for manipulation of image contrast, a technique known as image weighting (Bolas 2010) (**Table 1**).

As mentioned earlier, the produced signal is measured once the RF pulse is discontinued and proton relaxation occurs. The amount of signal produced is directly influenced by the number of hydrogen protons in a tissue (proton density, PD), with tissues with high proton density (e.g. water- and fat-rich tissues) producing stronger signals, and vice versa. Additionally, during the relaxation process, two time constants are measured: T1 relaxation, the time it takes for protons to release the absorbed energy and realign with the magnetic field; and T2 relaxation, the time it takes for protons to lose phase synchronization with each other. Different tissues have unique combinations of PD, T1, and T2 relaxation times, and these are the tissue properties that can be given emphasis in different sequences to obtain the desired image contrast (**Table 2**). In addition to TR and TE, other parameters, such as inversion time (TI) in IR sequences and flip angle in GE sequences, further refine contrast and diagnostic utility (Winter 2012).

Table 1 – Time of Repetition (TR) and Time of Echo (TE) settings for image weighting.

	TR	TE
T1-weighted	Short	Short
T2-weighted	Long	Long
PD-weighted	Long	Short

T1-weighted images offer high anatomical detail, being useful for evaluating bone and soft-tissue, but have lower contrast compared to other weightings. T2-weighted images have slightly less resolution but higher contrast, and are valuable for assessing bone and soft-tissue,

[2] Time of Echo (TE) – the interval between the initial RF pulse and the peak of the received signal echo.
[3] Time of Repetition (TR) – the interval between successive applications of the same RF pulse.

and identifying pathological processes involving fluid accumulation. PD-weighted images primarily reflect proton concentration in the tissues, offering a balanced visualization of structures with good anatomical detail (Tucker and Sampson 2007).

Table 2 – Appearance of different tissues on T1-, T2-, and PD-weighted images.

	Fluid	Fat	Tendons/ Ligaments	Cortical Bone	Trabecular Bone	Cartilage
T1-weighted	Black	White	Black	Black	White	Gray
T2-weighted	White	White	Black	Black	Gray	Black
PD-weighted	Light Gray	Light Gray	Dark Gray	Black	Light Gray	Gray

Figure 1 – (A) T1-weighted, (B) T2-weighted, and (C) PD SE sagittal images of a normal foot.

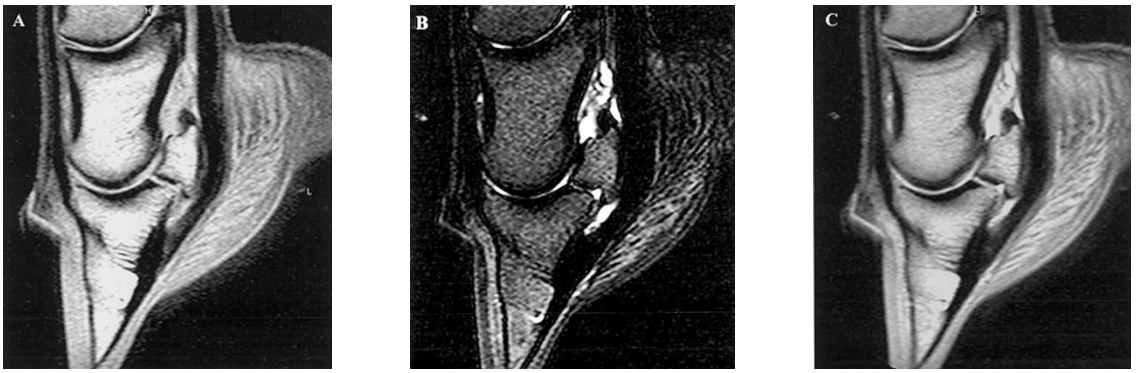

Adapted from: Werpy NM. 2004. Magnetic Resonance Imaging for Diagnosis of Soft Tissue and Osseous Injuries in the Horse. Clinical Techniques in Equine Practice. 3(4):389–398. Original figure 2.

By selecting an appropriate combination of pulse sequences and weighting parameters, MR images provide visualization of both bone and soft-tissue structures with great detail, allowing for identification of early and subtle lesions, as well as characterization of the severity and activity of lesions (Murray and Mair 2005; Winter 2012). **Table 3** summarizes common pulse sequences and image weightings used in equine musculoskeletal MRI scans.

Table 3 – Common pulse sequences used in equine musculoskeletal MRI scans.

	Common abbreviations	General speed acquisition	Primary image weighting
Spin echo	SE	Very slow	T1, T2, PD, dual-echo
Fast spin echo	FSE/TSE	Intermediate	T1, T2, PD, dual-echo
Gradient echo	GE, GRE, SPGR	Very fast	T1, T2*, PD
Short tau inversion recovery	STIR	Intermediate	Fat suppression

Adapted from: Murray R, Mair T. 2005. Use of magnetic resonance imaging in lameness diagnosis in the horse. In Practice. 27(3):138–146.

2.4. High-field and Low-field MRI

While pulse sequences and image weighting aid image interpretation by enhancing contrast, the strength of the magnetic field is what most influences the overall image resolution, signal quality, and, in some cases, diagnostic accuracy. The strength of the magnetic field, measured in Tesla (T), categorizes MRI systems into low-field (<0.3T) and high-field (≥1.5T)

units (Bolas 2010). Both are used in equine practice, each offering distinct advantages and limitations. Understanding these differences is important to appropriately refer cases, as some may benefit more from one modality over the other (Garrett 2015).

Signal strength is proportional to the strength of the magnetic field. Therefore, regarding image quality, high-field systems provide superior SNR, contrast, and resolution, leading to better visualization of small structures and subtle lesions (Werpy 2007). In low-field systems, these limitations may lead to less reliable representations of the articular cartilage, the flexor surface of the navicular bone, and the distal sesamoidean impar ligament (Bolen et al. 2010; Dyson et al. 2010; Smith et al. 2012; Berner et al. 2020; Baker et al. 2023). Despite being inferior in these aspects, several studies have shown that low-field magnets are still valuable for producing adequate diagnostic quality images of the distal limb up to the carpus/tarsus (Murray et al. 2009; Nagy and Dyson 2011; Labens et al. 2020; Doll et al. 2022).

Regarding practicality, the design and operational setup of MRI systems impacts their accessibility, cost, and clinical utility. High-field MRI units use a superconducting magnet with a closed-bore cylindrical design (**Figure 2**), which significantly increases installation and maintenance costs, limiting their access for many practices (Werpy 2007). These systems are also designed for use in recumbent horses under general anaesthesia, introducing additional risks and logistical challenges (Dugdale and Taylor 2016; Morgan et al. 2024a). Conversely, most low-field MRI units feature an open, U-shaped design (**Figure 3**), allowing easier positioning and enabling the horse to be imaged while standing and sedated, thus eliminating the need for general anesthesia and improving patient safety (Werpy 2007). These systems are also easier to integrate into an existing practice due to their smaller size, and installation and maintenance requirements, making them more affordable and accessible (Werpy 2007). However, image acquisition times can be longer with low-field systems due to the need for additional sequences to compensate for the smaller field of view and increased motion artifacts (Werpy 2007; Garrett 2015).

Figure 2 – High-field MRI system.

Reprinted from: *The Horse, https://thehorse.com/126307/review-of-available-mri-systems/)*

Figure 3 – Low-field MRI system.

Reprinted from: *Hallmarq Veterinary Imaging, https://hallmarq.net/2024/09/05/)*

3. The Role of MRI in Lameness Diagnosis

Lameness, defined as an abnormal stance or gait, is not a disease itself but rather a clinical sign indicative of an underlying disorder affecting the locomotor system (Davidson 2018; Baxter 2022). While lameness may arise from functional disorders such as neurological dysfunction, it most frequently results from pain associated with structural pathology of the musculoskeletal system (Baxter 2022). In these cases, lameness reflects the horse's adaptive strategies to offload the affected limb(s) and minimize discomfort (Weishaupt 2008).

Forelimb lameness is generally more prevalent than hindlimb lameness, as the forelimbs serve as the primary shock absorbers and support approximately 60-65% of the horse's body weight, with the rider's weight further contributing to this imbalance (Ross 2011a; Baxter 2022). Within the forelimb, the distal limb is particularly prone to injury, with an estimated 95% of forelimb lameness originating at or below the carpus (Baxter 2022). Among these cases, foot pain is a very common cause, particularly in sport horses whose training regimes place substantial strain on the structures enclosed within the hoof (Baxter et al. 2020).

Accurate diagnosis of lameness and the development of effective rehabilitation strategies remain a challenging and clinically significant aspect of equine practice. This process requires a thorough and systematic investigation, guided by both clinical findings and imaging results. While the introduction of MRI revolutionized our understanding of foot biomechanics, injury patterns, and disease processes, not every case of foot-related lameness warrants the use of MRI (Sue Dyson and Murray 2007). Therefore, a solid understanding of the foot's anatomy, its biomechanical function, and its susceptibility to injury is essential for selecting the most appropriate imaging modality and accurately interpreting its findings.

3.1. Functional Anatomy of the Equine Foot

The foot is composed of three primary bones: the distal phalanx (P3), the distal aspect of the middle phalanx (P2), and the navicular bone (Dyce et al. 2017; Gerard 2021). These bones articulate at the distal interphalangeal (DIP) joint, a hinge-like joint that allows for limited flexion and extension of the foot (Dyce et al. 2017; Fails 2020). Articular cartilage overlays the subchondral bone and protects the articular surfaces, while the fluid-filled synovial cavity between them ensures a smooth, frictionless movement of the joint (Van Weeren 2016). Two collateral ligaments (CLs) span between the middle and distal phalanges on each side to provide medial and lateral support to the joint (Van Weeren 2016; Dyce et al. 2017). Additionally, the podotrochlear apparatus, along with the distal digital annular ligament (DDAL), provides palmar stability (Dyson 2011; Wilson and Weller 2011; Parks 2012).

The podotrochlear apparatus consists of the navicular bone, navicular bursa, collateral sesamoidean ligaments (CSL), distal sesamoidean impar ligament (DSIL), and the distal portion of the deep digital flexor tendon (DDFT) (Dyson 2011). The DDFT plays a key role in

resisting hyperextension of the DIP joint during the stance phase of the stride by pulling on the palmar aspect of the distal phalanx to flex the joint (Dyson 2011). As the foot touches the ground, the DIP joint naturally extends, causing the DDFT to stretch and store elastic energy; when the heel lifts, this stored energy is released, assisting in forward propulsion (Smith et al. 2024). This spring-like function of the DDFT contributes to energy-efficient movement and helps dissipate concussive forces upon landing (Smith et al. 2024).

The navicular bone serves as the distal sesamoid for the DDFT as the tendon passes over its palmar (flexor) surface before inserting on the distal phalanx (Fails 2020). It acts as a fulcrum, ensuring a consistent angle of insertion and maintaining optimal tension throughout the stride (Dyson 2011). Therefore, during weight-bearing and joint extension, the navicular bone helps dissipate focal pressure, preventing excessive strain on both the tendon and distal phalanx; and, as the joint transitions into flexion, the angle of insertion remains unchanged, preserving tension for effective movement (Durham and Dyson 2011). To prevent excessive friction, a fibrocartilaginous layer covers the flexor cortex of the navicular bone (Durham and Dyson 2011), while the navicular bursa, a small synovial sac interposed between the bone and tendon, provides lubrication to facilitate smooth tendon gliding (Durham and Dyson 2011). At the insertion level, the DDFT is no longer enclosed within the digital flexor tendon sheath, but is instead supported palmarly by the DDAL (Fails 2020).

The CSL and DSIL constitute the navicular suspensory apparatus, which maintains the navicular bone in place (Bowker 2011). The CSLs are paired ligaments originating from each side of the distal aspect of the proximal phalanx and inserting on the proximal border of the navicular bone (Dyce et al. 2017). They have additional attachments to the middle and distal phalanges, as well as the foot cartilages, providing proximal and medial-lateral support for the navicular bone (Bowker 2011; Dyce et al. 2017). The DSIL is a short, strong ligament that connects the distal border of the navicular bone to the palmar aspect of the distal phalanx, just proximal to the DDFT insertion (Bowker 2011; Dyce et al. 2017). Its key role is to stabilize the navicular bone in relation to the distal phalanx, preventing dorsal displacement, especially when the heel lifts from the ground (Bowker 2011).

The distal phalanx is completely enclosed within the hoof, with its dorsal surface suspended from the inner hoof wall via strong interdigitations of laminar layers (Gerard 2021). The extensor process, a central prominence on its dorsoproximal aspect, serves as the insertion site for the common digital extensor tendon (Gerard 2021). Extending proximally from each palmar process of the distal phalanx, are the ungual or collateral cartilages of the foot, which are supported by several small ligaments attached to the digital bones (Fails 2020). These cartilages work in close association with the fibroelastic digital cushion, which lies between them and the solar surface of the distal phalanx, contributing to absorbing and dissipating forces during locomotion (Bowker 2011).

Figure 4 – Anatomical structures of the equine foot.

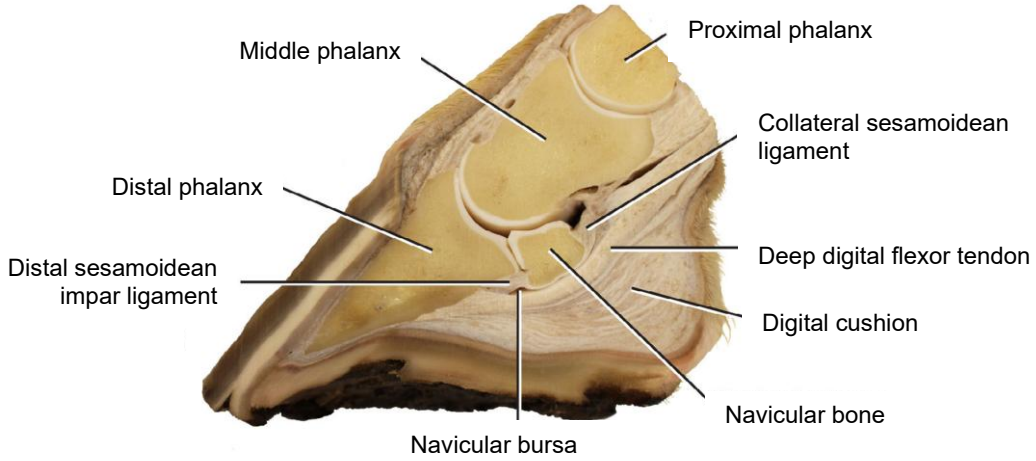

Adapted from: Osborn ML, Cornille JL, Blas-Machado U, Uhl EW. The equine navicular apparatus as a premier enthesis organ: functional implications. *Vet Surg*. 2021;50(4):713–728. doi:10.1111/vsu.13620. Original figure 2.

3.2. Biomechanical Susceptibility to Injury

Biological tissues have the ability to adapt and repair to mechanical stress through remodeling, provided the stimulation is appropriate and enough time is allowed for recovery (Wilson and Weller 2011). For example, in areas subjected to higher loads bone may become denser, tendons and ligaments can increase collagen production and improve fiber alignment, synovial membranes may increase fluid secretion, and cartilage may show variations in cell morphology and matrix composition across articular surfaces (McIlwraith et al. 2020). While these changes are typically beneficial, the same adaptive mechanisms can, under certain conditions, lead to abnormal and even irreversible changes. Aside from congenital or developmental disorders, musculoskeletal pathological changes typically result from a single traumatic event that exceeds a structure's mechanical capacity or, more commonly, from chronic stress, where repeated low-grade trauma gradually surpasses the tissue's ability to adapt and repair, culminating in structural damage (Wilson and Weller 2011).

Under normal conditions, forces are transmitted through the foot in a coordinated way, with the various structures working together as a unit to absorb impact and maintain stability, while undergoing inherent adaptive changes in response to the biomechanical stress they endure during daily activities (Dyson et al. 2011; Parks 2012). However, when force distribution becomes imbalanced, whether it be due to excessive loads, abnormal conformation, or other factors, certain structures may experience increased stress, causing adaptation to shift from beneficial to pathological over time (Dyson et al. 2011). The nature and severity of the resulting changes depend on the magnitude, duration, and type of stress, along with individual factors such as genetics, age, and overall health. In athletic horses, the specific characteristics of the stress are often dictated by the demands of the discipline they train for (Dyson 2002; Murray et al. 2006a). As a result, different sports predispose horses to specific injuries in specific anatomical locations, often correlating with performance levels (Murray et al. 2006a). Breed

also plays a role, with hoof conformation influencing weight distribution and the ability to dissipate forces effectively (Dyson et al. 2011; Mata et al. 2024), and breed-specific genetics having been linked to the presence or absence of certain musculoskeletal disorders (Metzger and Distl 2020). Additionally, the regenerative capacity of tissues tends to decline with age, increasing susceptibility to chronic stress-related pathology (Van Weeren and Back 2016).

Given the functional interplay between anatomical structures of the foot, injury to a single structure rarely occurs in isolation. Instead, biomechanical imbalances often trigger a cascade of compensatory changes, altering the distribution of forces across the foot and predisposing adjacent structures to secondary injury (Dyson et al. 2011). This is particularly evident in the podotrochlear apparatus, where the navicular bone, as the central component, is subjected to significant forces from multiple directions, making it highly susceptible to injury (Dyson et al. 2011; Osborn et al. 2021). Each time the horse bears weight and the DDFT is under tension, the tendon compresses the navicular bone, particularly during the propulsive phase of the stride (Dyson et al. 2011; Osborn et al. 2021). At the same time, tensile forces from the CSL and DSIL work to prevent displacement of the bone, while shear forces arise from its articulation with the middle and distal phalanges (Dyson et al. 2011; Osborn et al. 2021). Injury to the navicular bone was historically referred to as “navicular disease” and thought to be a primary bone disorder; however, advances in diagnostic imaging, particularly MRI, have revealed that navicular pathology is frequently accompanied by abnormalities in the surrounding structures of the podotrochlear apparatus, leading to the more accurate term, podotrochlosis (Dyson and Murray 2007; Dyson et al. 2011; Osborn et al. 2021). Nonetheless, primary or isolated pathological changes can still occur in any individual structure within the foot.

Structural abnormalities in any component of the foot can lead to pain, which in turn manifests clinically as lameness (Baxter 2022). While acute injuries may present with a sudden onset of lameness and are often more readily recognized, chronic injuries often develop insidiously, progressively compromising function and predisposing the foot to degenerative changes (Wilson and Weller 2011). This highlights the importance of early and accurate diagnosis, allowing for timely intervention and prevention of long-term structural damage.

3.3. Indications for MRI

A comprehensive lameness investigation typically begins with obtaining a detailed clinical history to assess risk factors and narrow down potential causes, followed by a physical examination and gait evaluation to identify the affected limb(s). Flexion tests and limb manipulation techniques, in conjunction with diagnostic anesthesia, are then used to localize the source of pain. Ultimately, diagnostic imaging is employed to determine the specific underlying pathology (Davidson 2018; Baxter 2022).

As an imaging modality, MRI is highly valuable for detecting musculoskeletal pathology from the foot to the carpus and tarsus (Werpy 2004; Murray and Mair 2005; A. McKnight 2012a). Some studies have also reported successful assessment of the stifle using rotating low-field units designed for recumbent horses under general anesthesia (McKnight 2012b; Waselau et al. 2020). Despite its clinical application in multiple regions of the limb, MRI is expensive, time-consuming, not as readily available as more conventional imaging modalities, and may involve risks associated with general anesthesia (Schramme and Zimmerman 2022). Therefore, it is not practical for routine screening of the entire limb, nor is it a substitute for in-depth clinical investigation and traditional imaging techniques (Schramme and Zimmerman 2022). In fact, the decision to pursue MRI and its interpretation relies heavily on the clinical context provided. Consequently, as an advanced imaging modality, MRI is warranted when pain has been successfully localized through diagnostic anesthesia, yet radiographs or ultrasound have failed to reveal abnormalities; when lameness is persistent and unresponsive to treatment and imaging findings do not justify the clinical signs; when pathology has been identified but requires further characterization; or when multiple structure involvement is suspected (Garrett 2022; Schramme and Zimmerman 2022).

3.3.1. Diagnostic Imaging of the Equine Foot

Once the source of pain has been localized to a specific area within the limb, diagnostic imaging is then used to pinpoint the underlying pathology. Therefore, prior to diagnostic imaging, diagnostic anesthesia is an essential step of the lameness work-up, as it guides the selection of the relevant anatomical region to image and facilitates the interpretation of how imaging findings relate to the presenting lameness based on their location (Giorio 2018; Garrett 2022). This step is particularly relevant for MRI, which requires targeted imaging to minimize procedure duration and the associated risks and costs (Giorio 2018; Garrett 2022). However, caution is warranted when interpreting the results of diagnostic anesthesia, as anesthetic diffusion beyond the intended site is common. A palmar digital nerve block which is used to anesthetize most of the foot, may extend proximally to the pastern or fetlock, and an intra-articular block of the DIP joint may desensitize the entire podotrochlear apparatus and even portions of the sole (Nagy and Malton 2015; Pilsworth and Dyson 2015). To account for potential diffusion-related inaccuracies, the pastern and fetlock are often included in the imaging plan (Dyson 2013; Giorio 2018; Garrett 2022). In the context of high-field MRI, to avoid prolonged anesthesia, it is helpful to have the images reviewed as the scan progresses to determine this need for additional scans, while with standing MRI it is easier to obtain additional images later on if necessary (Porter and Werpy 2014; Garrett 2022).

Radiography and ultrasonography are the primary imaging modalities used in both ambulatory and hospital settings due to their accessibility, affordability, and capacity to detect

a wide range of pathologies (Gallastegui 2021; Garrett 2022). Radiography is often the first-line imaging tool and is effective for identifying osseous abnormalities such as fractures, subtle bone contour changes (e.g., osteophytes, enthesophytes, small osteochondral fragments), and alterations in bone density and alignment (Schramme and Segard-Weisse 2020). Ultrasonography typically complements it by providing real-time visualization of soft tissue and synovial structures (Schramme and Segard-Weisse 2020). However, when assessing the foot, the hoof capsule presents a significant limitation by preventing direct visualization of deeper structures (Werpy 2010; Garrett 2022). Although two possible transducer approaches have been described, they only allow limited examination of some structures, which often require significant changes to be detected (Gallastegui 2021). Additionally, obtaining reliable images can be challenging, as ultrasonography is highly dependent on the operator's skill. Image quality and diagnostic accuracy are directly influenced by transducer positioning, pressure, and angle, which, if not properly applied, can create artifacts that obscure or mimic pathology (Werpy 2010; Schramme and Segard-Weisse 2020). Consequently, when high-quality radiographs of the foot fail to reveal significant abnormalities, ultrasound is often bypassed, as it rarely provides a definitive or complete diagnosis. In such cases, MRI is typically considered the second-line imaging modality (Schramme and Zimmerman 2022).

Unlike radiography, MRI can detect cartilage abnormalities and identify subtle, early-stage lesions by visualizing fluid in the subchondral and trabecular bone (Schramme and Zimmerman 2022). This ability allows MRI to reveal conditions such as inflammation, contusion, subtle or focal resorption, and trabecular microfractures, which may not be visible on radiographs until significant structural changes occur (Werpy 2010; Schramme and Zimmerman 2022). Additionally, MRI offers cross-sectional imaging, overcoming the limitations associated with superimposition of anatomical structures inherent to radiography, particularly in complex regions like the foot (Werpy 2010; Smith 2015). MRI also provides superior soft tissue contrast and is more sensitive than ultrasound for detecting subtle injuries (Werpy 2010; Schramme and Zimmerman 2022). Because of its unique ability to visualize osseous, soft tissue, articular, and synovial structures in a single scan and across multiple planes, MRI is considered the gold standard for diagnosing equine foot pathology (Dyson and Murray 2007; Smith 2015; Gallastegui 2021; Schramme and Zimmerman 2022).

While both low-field and high-field MRI systems provide diagnostic quality images, high-field units offer superior image resolution, making them more sensitive for identifying small lesions and preferable for detailed evaluation of small anatomical structures, such as the DSIL and the CLs of the DIP joint (Byrne et al. 2021). Moreover, although evaluating articular cartilage may be challenging with MRI in general, high-field systems are significantly more effective at detecting cartilage defects (Smith et al. 2012). However, factors such as cost, availability, and patient safety must also be considered. Therefore, in most clinical scenarios,

standing low-field MRI is the preferred modality, while high-field MRI may be better indicated when image quality is a priority (Byrne et al. 2021).

When MRI does not reveal significant pathology in the foot, and additional scans of the pastern or fetlock remain inconclusive, alternative strategies may be necessary. These include re-evaluating lameness localization, implementing a rest period followed by repeat imaging (to account for delay in appearance of signal abnormalities), or considering other advanced modalities such as contrast-enhanced computed tomography (CT) or positron emission tomography (PET) (Schramme and Zimmerman 2022).

3.3.2. Recheck Examination

Beyond its primary role in diagnosing cases with inconclusive radiographic or ultrasonographic findings, MRI is also useful for monitoring injury progression.

Follow-up examinations are essential for effectively managing injuries, as they provide critical information regarding injury progression and allow for timely adjustments in treatment and rehabilitation strategies (Werpy 2012; Horne and Tufts 2023). While radiography and ultrasound are recommended for more frequent assessments at a lower cost, certain lesion types and locations require a recheck MRI for a comprehensive evaluation of the dynamic nature of injuries, ensuring that treatment plans are based on the most current information available (Werpy 2012). For instance, distinguishing whether bone fluid observed on an initial scan is transient, indicative of a contusion or physiological stress, or permanent, suggesting a more serious or degenerative injury, is crucial for appropriate management (Werpy 2012). Additionally, in cases where multiple abnormalities are present or a combination of acute and chronic lesions is observed, a recheck MRI is invaluable in clarifying their clinical significance (Horne and Tufts 2023).

4. MRI: The Gold Standard for Diagnosing Foot Pathology

Given the high prevalence of foot lameness in horses and the inherent limitations of radiography and ultrasonography for visualizing the complex anatomy of the foot, MRI has become the gold standard for diagnosing equine foot-related lameness (Gallastegui 2021; Garrett 2022). The introduction of standing MRI has further revolutionized clinical practice by making MRI much more accessible, thereby rapidly advancing our understanding of foot-related pain (Mair et al. 2005; Porter and Werpy 2014). The ability to visualize multiplanar images of bone, tendon, ligament, and synovial structures of the foot, has allowed us to specifically identify the affected anatomical structures and their pathological changes with great detail (Dyson 2011; Osborn et al. 2021). Furthermore, MRI provides important information regarding the activity and severity of lesions, which is essential for managing treatment strategies and assessing prognosis (Werpy 2012; Barrett et al. 2017a).

4.1. Identification of Pathological Change

MRI protocols produce hundreds to thousands of images, using multiple imaging planes and pulse sequences to effectively characterize the various tissue types and potential pathological changes (Tucker and Sampson 2007; Winter 2012; Jaskólska et al. 2013). Typically, imaging planes include sagittal, transverse and dorsal views, and those that are perpendicular to the structure being examined are generally best for characterizing changes (Winter 2012). To distinguish an actual lesion from an artifact, the abnormality must be identified in at least two imaging planes and two contrast-weightings (Schramme and Segard-Weisse 2020). Additionally, findings may be compared to images of the contralateral limb, if presumably sound, to distinguish true pathological changes from normal anatomical variations (Porter and Werpy 2014).

A standard standing low-field MRI protocol for the foot includes 3D T1 GE, 3D T2* GE, PD FSE, T2 FSE and STIR FSE sequences (Mair et al. 2005; Gold 2015). Additional sequences may be employed if deemed necessary to further evaluate certain structures (Jaskólska et al. 2013). The identification of abnormalities on MRI relies on the detection of changes in signal intensity, size, shape, and contour of anatomical structures when compared to their normal appearance (Schramme and Segard-Weisse 2020). Pathological processes in the equine foot frequently involve an increase in fluid within and around affected tissues, which can be a hallmark of inflammation, edema, or active injury process. Fluid typically manifests on MRI as increased signal intensity on T2-weighted and STIR images, and decreased signal intensity on T1-weighted images (Murray and Dyson 2007). In general, T1-weighted images are better for assessing tissue anatomy and contours, and more chronic changes (Murray and Dyson 2007). A summary of common pathological changes identified on MRI is presented in **Table 4**.

Table 4 – Common pathological changes and their typical MRI findings by tissue type.

Pathological Change	MRI Signal Characteristics
Bone	
Bone Marrow Lesion	Increased T2 and STIR signal; decreased T1 signal.
Bone Sclerosis	Low T1, T2, and STIR signal; appears hypointense within high signal fatty marrow on T1/PD.
Fracture	Altered bone contour/structure; may show as line of increased T2 signal, with associated fluid/sclerosis signal in adjacent bone.
Periosteal Reaction	Altered surface contour/thickening, often with increased T2/STIR signal.
OCLL	Focal, well-defined lesions, typically fluid-like but signal can vary depending on content; often in the subchondral bone or at tendon/ligaments insertion sites.
Osteophytes	Altered surface contour; bony (low signal) projections that form along the edges of joints.
Hemorrhage	Variable, but often increased T1, T2, and STIR signal.

Tendon / Ligament	
Inflammation	Swelling/thickening; increased PD/T1 and T2/STIR signal; associated with acute injury.
Fibrosis	Thickening/irregular shape; low PD and T2 signal, T1 signal remains higher than normal tendon; associated with chronic injury. Mature scar: low signal on all sequences, may form adhesions.
Degeneration	Increased signal on T1, and only minimal on PD and T2, but variable depending on severity; irregular fiber pattern.
Tear	Marked thinning or discontinuity of the tendon/ligament contour (partial); completely interrupted contour (complete), with focal fluid signal at the site.
Peritendinous/ligamentous changes	Edematous changes in surrounding soft-tissues; increased T2/STIR signal.
Enthesopathy	Thickening/irregular shape and signal changes near origin/insertion; bone changes: altered contour (enthesophyte formation, focal resorption, OCLL), and fluid-like signal.
Articular Cartilage	
Inflammation	Swelling/Thickening; increased PD/T2/STIR signal, potentially decreased T1 signal (increased water content).
Fibrillation	Altered contour: surface irregularity/superficial defects.
Fissure	Linear defect (loss of signal) or linear T2 signal intensity.
Full-thickness Defect	Complete focal signal loss, may allow synovial fluid to pool within them (increased T2/STIR signal; low T1 signal); often with associated subchondral bone changes (thickening, altered contour, focal fluid-like signal).
Synovial Fluid / Synovium / Joint Capsule	
Synovial Effusion	Distension/displacement of capsular margin; increased T2/STIR signal, low T1 signal.
Inflammation/Hemorrhage	Increased T2/STIR signal, increased T1 signal compared to normal fluid (increased protein).
Synovial Proliferation	Thickening with or without irregular margins; chronic proliferation: increased T1 signal, and decreased T2 signal (fibrosis), with reduced fluid content.
Capsular Rupture	Break in capsular margin with extravasation (leakage) of fluid.

Abbreviations: PD, proton density-weighted images; **T1**, T1-weighted images; **T2**, T2-weighted imaged; **STIR**, short tau inversion recovery; **OCLL**, osseous cyst-like lesion. **Based from:** (Murray and Dyson, 2007) *Image Interpretation and Artifacts;* and, (Jaskólska et al, 2013) *Magnetic resonance protocols in equine lameness examination, used sequences, and interpretation*.

4.2. Prevalence of MRI-detected Foot Injuries

Over the past two decades, several studies have investigated the spectrum of injuries that can be detected using MRI in horses with foot-related lameness, establishing their relative prevalence, and correlating these imaging findings with observed clinical signs and the outcomes of various treatment interventions (Dyson et al. 2005; Mitchell et al. 2006; S. Dyson and Murray 2007; Sherlock et al. 2007; Sampson et al. 2009; Gutierrez-Nibeyro et al. 2012; Gutierrez-Nibeyro et al. 2020). A comparative summary of reported lesion frequencies detected with standing low-field MRI is presented in **Table 5**.

Across these studies, the navicular bone was consistently the most frequently affected structure, with reported prevalence ranging between 74-78%. Other commonly affected structures included the DIP joint (53-68%), DDFT (47-64%), and navicular bursa (48-57%).

Lesions of the CLs of the DIP joint were moderately prevalent (21-39%), while injury to the CSL (13-24%), DSIL (4-30%), and distal and middle phalanges (4-24%) was less frequently observed. Prevalence of pathological changes of the ungual cartilages and DDAL were rarely reported in these studies, but the available data indicated 10-16% and 11% prevalence, respectively.

In contrast, a study using high-field MRI in 199 horses found that DDF tendinopathy was the most common injury (59%), followed by desmitis of the CLs of the DIP joint (31%), and navicular bone abnormalities (22%) (Dyson et al. 2005). Similarly, another high-field MRI study evaluating 264 horses also identified DDFT lesions as the most prevalent finding (82%), followed by changes in the navicular bursa (50%) and DIP joint (42%) (Dyson and Murray 2007). Overall, both low-field and high-field MRI studies identify the navicular bone and DDFT as commonly affected structures in horses with foot lameness, but there is considerable variability in the reported prevalence of foot injuries across different studies.

Table 5 – Prevalence (%) of MRI findings in the equine foot reported in standing low-field MRI (0.27T) retrospective studies (Mitchell et al. 2006; Gutierrez-Nibeyro et al. 2012; Gutierrez-Nibeyro et al. 2020).

MRI Abnormalities (% total prevalence)	**N=98**	**N=79**	**N=550**
Navicular Bone	77	78	74
Navicular Bursa	49	57	48
DSIL	4	30	24
CSL	13	24	16
DDFT	64	54	47
DIP Joint	68	53	66
CLs of DIP Joint	21	39	31
Distal and Middle Phalanges	4	24	7
DDAL	-	11	-
Ungual Cartilages	-	10	16

Abbreviations: DSIL, distal sesamoidean impar ligament; **CSL**, collateral sesamoidean ligament; **DDFT**, deep digital flexor tendon; **DIP**, distal interphalangeal**, CLs**, collateral ligaments; **DDAL**, distal digital annular ligament.

A common finding across these studies is the frequent occurrence of concurrent injuries involving multiple structures within the equine foot. Research suggests that approximately 30% of horses diagnosed with foot lameness based on MRI findings exhibit a combination of lesions affecting different anatomical structures (Sherlock 2015). It is important to note, however, some detected abnormalities may not be the primary cause of the horse's current lameness or may even be incidental findings. Therefore, clinical significance of MRI findings should be prioritized based on the lameness presentation, the results obtained from other diagnostic procedures, and known associations between specific MRI findings and lameness (Schramme and Segard-Weisse 2020).

III. RETROSPECTIVE STUDY

1. Introduction and Aims

Musculoskeletal issues are among the most common concerns in equine veterinary practice (Ribitsch et al. 2021), with the distal limb region being particularly susceptible to injury due to the high biomechanical stresses it endures during exercise (Johnston and Back 2006). These injuries can significantly impact a horse's welfare and performance, highlighting the need for accurate diagnosis and targeted treatment strategies (Barrett et al. 2017b; Reis et al. 2024). Although radiography and ultrasound are commonly used to assess such injuries, MRI overcomes many diagnostic limitations of these modalities, providing superior visualization of both bone and soft tissue structures (Garrett 2022). It can detect subtle and subclinical lesions and is particularly valuable for examining the foot region, which remains challenging to fully assess with traditional imaging modalities (Barrett et al. 2023; Murray and Mair 2005). Standing low-field MRI, in particular, has gained popularity as a practical and non-invasive alternative to high-field MRI, eliminating the risks associated with general anesthesia while maintaining diagnostic value (Morgan et al. 2024b).

While other retrospective studies have systematically analyzed MRI findings of the equine foot in large caseloads of sport horses, few have investigated potential correlations between MRI findings and demographic factors. Furthermore, to the best of the author's knowledge, no published studies have specifically investigated MRI findings in sport horses in Ontario, Canada. McKee-Pownall Equine Services (MPES) is a veterinary practice that focuses on lameness and sports horse medicine, serving a large number of performance horses across various disciplines. Given its role as the sole provider of standing MRI in Ontario, this study presents a unique opportunity to analyze a representative caseload in this region. By analyzing retrospective MRI data from MPES, this study aims to:

1. Provide an overview of the MRI caseload over a three-year period;
2. Characterize the prevalence and nature of low-field MRI findings in the forelimb foot region;
3. Investigate lesion co-occurrence patterns, identifying frequently associated abnormalities;
4. Explore potential associations between MRI findings and demographic factors (age, sex, breed, and discipline).

As a retrospective study based on clinical MRI reports, inherent limitations include the subjective nature of MRI interpretation, variability in clinical reporting, and potential biases in case selection. Nonetheless, it aims to provide valuable insights into the prevalence and patterns of pathologies affecting the equine foot in this population, contributing to a greater understanding of MRI's role in equine diagnostics and laying the foundation for future research.

2. Materials and Methods

2.1. Study Design and Population

Medical records of 185 horses that underwent standing low-field MRI of the distal limb at MPES between January 2017 and December 2019 were retrospectively reviewed. For the purpose of this study, only horses undergoing an initial diagnostic scan were included. Follow-up assessment scans were excluded to minimize bias from treatment or progression-related findings, as well as cases without available MRI reports due to insufficient data.

To provide an overview of the MRI caseload during the study period, 172 initial diagnostic scans were characterized based on their distribution across: annual seasons, forelimbs and hindlimbs, and anatomical regions imaged.

Given the high prevalence of forelimb foot examinations and the diagnostic value of MRI for assessing this region, a subset of 149 horses presenting with unilateral or bilateral forelimb lameness who underwent imaging of the foot, was selected for further analysis including detailed characterization of MRI findings, and investigation of potential lesion co-occurrence patterns and demographic trends.

2.2. Data Collection, Classification and Analysis

Data collected from medical records included the date of examination, age, sex, breed, discipline, lame limb(s), scanned limb(s), and reported MRI findings (affected structure, nature of the abnormality, and clinical relevance). The classification of these variables is summarized in **Table 6**. MRI findings were only recorded for limbs identified as clinically lame. Each affected structure was recorded independently, and multiple abnormalities within the same structure were classified separately. Due to the retrospective nature of the study and reliance on medical records alone, information such as lameness grade, duration, response to diagnostic analgesia, and findings from other imaging modalities, was not consistently available and was therefore excluded.

Table 6 – Classification of Study Variables: demographics, affected limb(s), and MRI findings.

Category	Variable	Details
Demographics	Age	Age Groups: <5 years; 6-10 years; 11-15 years; 16-20 years.
	Sex	Mare, gelding, or stallion
	Breed	Dutch Warmblood, Canadian Warmblood, Irish Sport Horse, Quarter Horse, Hanoverian, Oldenburg, Thoroughbred, Holsteiner, Other (Draft Cross, Arabian, Cleveland Bay, Welsh Pony)
	Discipline	Show jumping, hunter, eventing, dressage, western (western pleasure, barrel racing, reining, roping), pleasure riding, other (racing, polo, fox hunting)

Lameness	Lame Limb(s)	Unilateral (RF or LF) or bilateral
Scans	Scanned Limb(s)	RF and/or LF
MRI Findings	Affected Structure	NB, NBU, DSIL, CSL, DDFT, DIP joint, CLs of the DIP joint, P3, P2, PIP joint, DDAL, and UC.
	Lesion Type	Bone marrow lesion, fiber disruption, cartilage damage, etc. Each lesion type was recorded as present (=1) or absent (=0) for each affected structure.
	Clinical Relevance	Determined based on the MRI report author's interpretation, indicating findings most likely contributing to the presenting lameness. Findings were marked as contributory (=1) or not (=0).

Abbreviations: RF, right front; **LF**, left front; **NB**, navicular bone; **NBU**, navicular bursa; **DSIL**, distal sesamoidean impar ligament; **CSL**, collateral sesamoidean ligament; **DDFT**, deep digital flexor tendon; **DIP**, distal interphalangeal; **CLs**, collateral ligaments; **P3**, distal phalanx; **P2**, middle phalanx; **PIP**, proximal interphalangeal; **DDAL**, distal digital annular ligament; **UC**, ungual cartilages.

Descriptive statistics (frequencies, percentages, and measures of central tendency, where applicable) were used to: characterize the overall MRI caseload; summarize demographic and lameness characteristics of the study population; and, determine the prevalence of MRI-detected abnormalities. Associations between demographic variables and affected anatomical structures, as well as lesion co-occurrence patterns, were assessed using chi-square tests or Fisher's exact test (or Fisher-Freeman-Halton's exact test for larger contingency tables) for categorical data comparisons. When significant, post hoc Z-tests with Bonferroni correction were applied for column proportion comparisons. All statistical analyses were performed using IBM SPSS Statistics for Windows, version 29.0 (IBM Corp., Armonk, NY, USA). Statistical significance was set at a $p<0.05$.

2.3. Magnetic Resonance Imaging

All MRI examinations were performed under sedation using a low-field standing equine MRI system (0.27T; Hallmarq Veterinary Imaging Ltd., Guildford, UK). The foot region was imaged in sagittal, transverse, and dorsal planes using standard sequences, including STIR, T2W and PD FSE, and T1W, T2*W GRE. Foot scans encompassed the region extending from the distal phalanx to the middle of the proximal phalanx, as this field of view is inherent to the equipment used. Although the proximal middle phalanx and the PIP joint lie outside the traditional anatomical definition of the foot, they were included in the analysis as these structures may contribute to foot-related lameness, and diagnostic anesthesia targeting the foot can often desensitize them inadvertently. Including them allowed for a more complete and clinically relevant assessment of the lame limb. The contralateral limb was imaged in select cases where bilateral lameness was present or for comparison to the non-lame limb. The acquired MR images were interpreted by either an ACVR board-certified radiologist (KS) or an experienced clinician (MM) at MPES. As MRI reports were originally written for clinical use rather than research, findings were extracted based on the available descriptions.

3. Results

3.1. Overview of the MRI caseload

Between January 2017 and December 2019, a total of 210 standing low-field MRI examinations were performed on 185 horses at MPES. Among these, 172 examinations (81.9%) were initial diagnostic scans, while 32 (15.2%) were follow-up assessments. Additionally, 6 examinations (2.9%) had missing MRI reports.

3.1.1. Characterization of Initial MRI examinations

A total of 172 initial diagnostic scans were conducted during the study period. MRI examinations were not evenly distributed across the year, with a statistically significant deviation from expected values ($\chi^2(3)=15.767$, $p=0.001$). The frequency of MRI scans was lowest in Winter (13.4%) and highest in Summer (32.6%) and Fall (30.8%) (**Figure 5**). A detailed breakdown of observed and expected frequencies is provided in *Appendix 1*.

Figure 5 – Distribution of initial diagnostic MRI examinations across annual seasons.

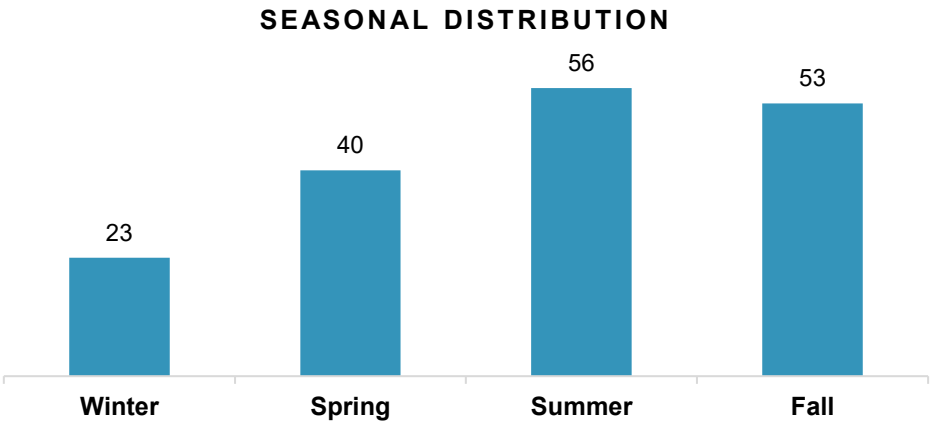

All horses underwent scanning of either the forelimbs or hindlimbs. The distribution of scanned anatomical regions (**Figure 6**) demonstrated a clear predominance of forelimb examinations, accounting for 92.1% (278/302) of all imaged limbs and involving 90.1% (155/172) of horses. In contrast, hindlimb examinations were significantly less frequent, representing only 7.9% (24/302) of imaged limbs and 9.9% (17/172) of horses. Bilateral scans were more common overall, though unilateral scans were more frequent among hindlimb examinations (*Appendix 2*).

Figure 6 – Distribution of the 172 initial scans (302 limbs) across forelimb and hindlimb examinations.

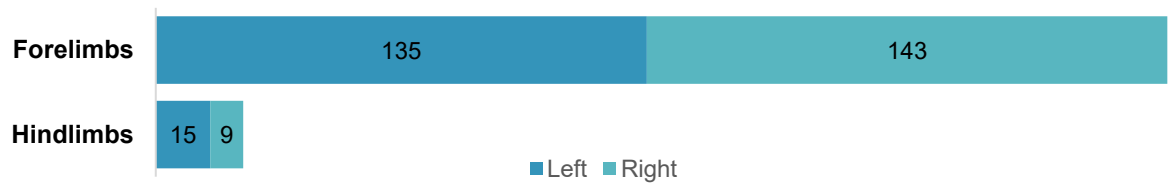

Multiple anatomical regions of the distal limb were assessed, including the foot, pastern, fetlock, proximal metacarpus, proximal metatarsus, carpus, and tarsus. **Table 7** provides an overview of the anatomical regions scanned in forelimbs and hindlimbs, including the number of horses and limbs assessed. Each limb underwent imaging of one or more anatomical regions.

Table 7 – Distribution of scanned anatomical regions among the 302 imaged limbs (172 horses).

Anatomical Regions	n Limbs	% Limbs	n Horses	% Horses
Forelimbs	**278**	**92.1**	**155**	**90.1**
Foot	261	86.4	149	86.6
Pastern	51	16.9	49	28.5
Fetlock	67	22.2	55	32.0
Proximal Metacarpus	2	0.7	1	0.6
Carpus	3	1.0	2	1.2
Hindlimbs	**24**	**7.9**	**17**	**9.9**
Foot	12	4.0	11	6.4
Pastern	5	1.7	5	2.9
Fetlock	19	6.3	13	7.6
Proximal Metatarsus	6	2.0	5	2.9
Tarsus	2	0.7	2	1.2
Total	**302**	**100.0**	**172**	**100.0**

The foot was the most commonly examined region overall, representing 90.4% (273/302) of all limb scans and assessed in 93.6% (161/172) of horses. The fetlock was the second most frequently examined region, accounting for 28.5% (86/302) of limb scans and examined in 39.5% (55/172) of horses.

In forelimbs, the foot was the primary region of interest (93.9%, 261/278), with most horses undergoing isolated foot scans, followed by combinations with the pastern and the fetlock (*Appendix 2*). In contrast, the fetlock was the most frequently imaged region in the hindlimbs (79.2%, 19/24), most often in combination with other anatomical regions (*Appendix 3*). Scans of more proximal regions were less frequent overall, comprising only 3% (9/302) of all imaged limbs. Notably, these scans were disproportionately represented in hindlimbs, with 25% (6/24) including the proximal metatarsus and/or tarsus, compared to just 1.1% (3/278) of forelimb scans that included the proximal metacarpus and/or carpus (**Figure 7**).

Figure 7 – Comparison of scanned anatomical regions among forelimbs and hindlimbs.

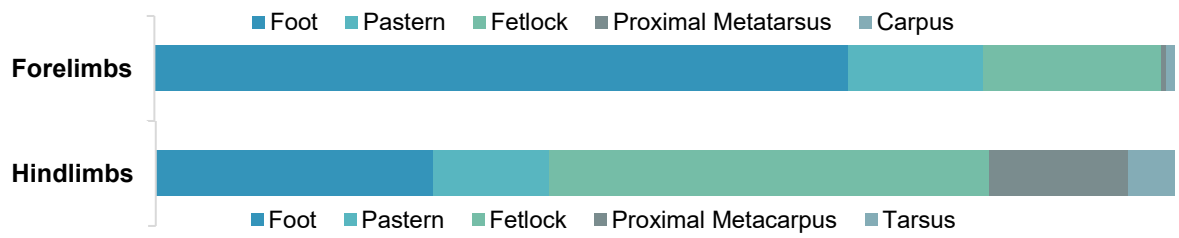

3.2. The Forelimb Foot Region

3.2.1. Demographics

This section of the study focused on the 149 horses that underwent initial diagnostic scans of the forelimb foot region. The population ranged from 2 to 20 years old, with a mean of 10.6 years (± 3.8) and a median of 11 years. Most horses were in the middle age categories, with 40.9% aged 6-10 years and 40.3% aged 11-15 years. Horses under 5 years of age were the least represented (8.7%), while older horses (16-20 years) represented 10.1% of the population. Geldings were more prevalent than mares, comprising 59.1% and 40.9% of the population, respectively, while stallions were not represented.

Dutch Warmblood was the predominant breed (18.1%), followed by Canadian Warmblood (13.4%), Irish Sport Horse (13.4%), and Quarter Horse (12.8%). The remaining breeds (Hanoverian, Oldenburg, Thoroughbred, Holsteiner, and Others, including Draft Cross, Arabian, Cleveland Bay, Welsh Pony) were each represented by less than 10% of the population. The horses were primarily used in jumping disciplines, with show jumpers (32.2%) and hunters (26.8%) being the most common. Other disciplines included dressage (12.1%), eventing (10.1%), and western (9.4%). A smaller proportion of horses were used for pleasure riding (6.7%) and other less frequent activities (2.7%). The demographic distribution is summarized in **Table 8** and illustrated in **Figure 8**.

Table 8 – Summary of demographic characteristics of the study population.

Demographics	**n**	**%**		**n**	**%**
Age ***in years***			**Sex**		
< 5	13	8.7	Gelding	88	59.1
6 – 10	61	40.9	Mare	61	40.9
11 – 15	60	40.3			
16 - 20	15	10.1			
Breed			**Discipline**		
Dutch Warmblood	27	18.1	Show Jumping	48	32.2
Canadian Warmblood	20	13.4	Hunter	40	26.8
Irish Sport Horse	20	13.4	Dressage	18	12.1
Quarter Horse	19	12.8	Eventing	15	10.1
Hanoverian	14	9.4	Western	14	9.4
Oldenburg	14	9.4	Pleasure Riding	10	6.7
Thoroughbred	13	8.7	Other	4	2.7
Holsteiner	12	8.1			
Other	10	6.7			
Total	**149**	**100.0**		**149**	**100.0**

Figure 8 – Distribution of the study population across demographic groups (149 horses).

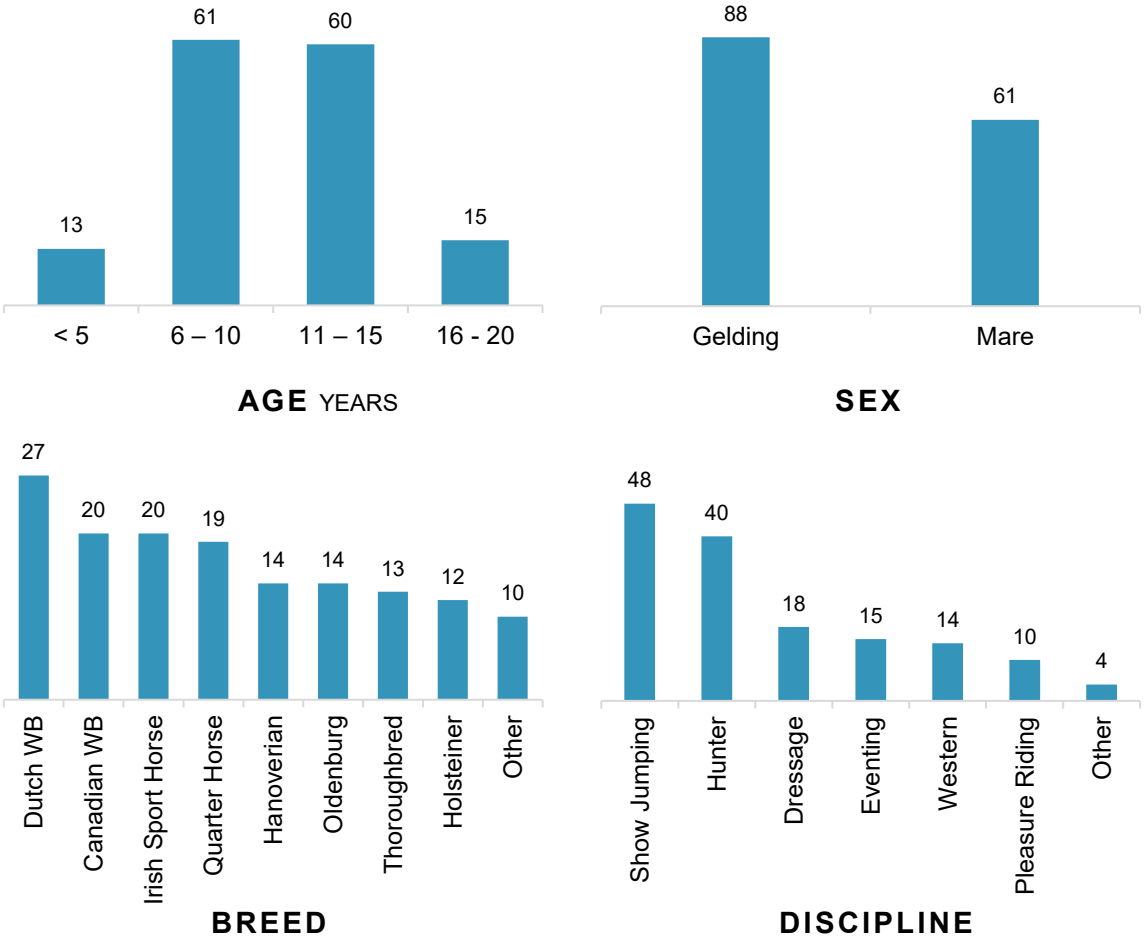

3.2.2. Lameness Distribution and Scanning Patterns

Unilateral lameness was the predominant clinical presentation, observed in 79.9% (119/149) of horses, while bilateral lameness was observed in 20.1% (30/149). Despite the predominance of unilateral lameness, bilateral imaging was performed in the majority of horses (75.2%, 112/149) (**Figure 9**). In total, 261 forelimb feet were scanned, including 179 clinically lame limbs and 82 non-lame contralateral limbs. Additionally, the distribution between left and right limbs was nearly equal for both lameness presentation (LF=75; RF=74) and scanning frequency (LF=126; RF=135) (*Appendix 3*).

Figure 9 – Distribution of lameness and scanning patterns among study population (149 horses).

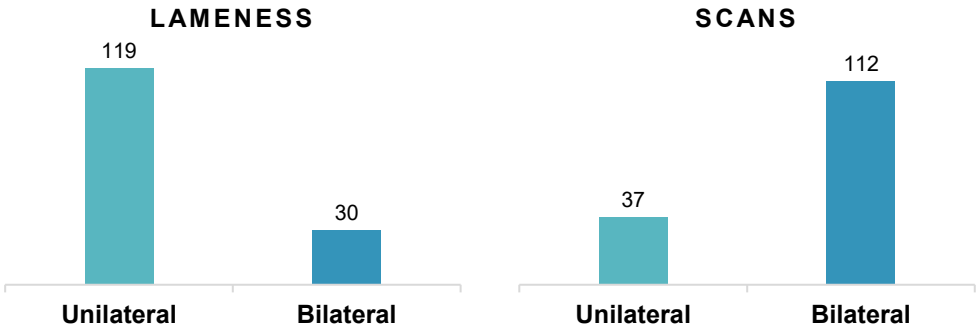

3.3. Characterization of MRI Findings

The MRI findings from the 179 clinically lame limbs of the 149 horses that underwent forefoot imaging are summarized in **Table 9**.

Table 9 – Summary of abnormal MRI findings in the 179 lame limbs of 149 horses.

Abnormal MRI Findings	Limbs Affected		Horses Affected		Contributory to Lameness	
	n	%	n	%	n	%
Navicular Bone	**96**	**53.6**	**85**	**57.0**	**56**	**31.3**
Altered SI in the trabecular bone	83	46.4	73	49.0	50	27.9
Enlarged synovial invaginations	16	8.9	15	10.1	5	2.8
Flexor surface erosions	12	6.7	11	7.4	11	6.1
Distal border fragmentation	4	2.2	4	2.7	4	2.2
Navicular Bursa	**108**	**60.3**	**92**	**61.7**	**23**	**12.8**
Effusion	69	38.5	66	44.3	14	7.8
Synovial proliferation and capsular thickening	70	39.1	59	39.6	17	9.5
DSIL	**30**	**16.8**	**28**	**18.8**	**13**	**7.3**
Desmopathy	4	2.2	4	2.7	0	0
Enthesopathy	30	16.8	28	18.8	13	7.3
CSL	**7**	**3.9**	**7**	**4.7**	**0**	**0**
Desmopathy	7	3.9	7	4.7	0	0
DDFT	**103**	**57.5**	**87**	**58.4**	**63**	**35.2**
Tendinopathy	88	49.2	73	49.0	53	29.6
Enthesopathy	24	13.4	22	14.8	14	7.8
DIP Joint	**166**	**92.7**	**138**	**92.6**	**43**	**24.0**
Effusion and synovitis	154	86.0	130	87.2	12	6.7
Osteoarthritis	76	42.5	57	38.3	31	17.3
CLs of DIP Joint	**47**	**26.3**	**41**	**27.5**	**22**	**12.3**
Desmopathy	39	21.8	35	23.5	19	10.6
Enthesopathy	19	10.6	17	11.4	7	3.9
Distal Phalanx	**66**	**36.9**	**62**	**41.6**	**43**	**24.0**
Altered SI in the trabecular bone	59	33.0	55	36.9	35	19.6
Fractures	7	3.9	7	4.7	6	3.4
Middle Phalanx	**10**	**5.6**	**10**	**6.7**	**7**	**3.9**
Altered SI in the trabecular bone	10	5.6	10	6.7	7	3.9
PIP joint	**39**	**21.8**	**37**	**24.8**	**8**	**4.5**
Effusion and synovitis	6	3.4	6	4.0	0	0
Osteoarthritis	36	20.1	34	22.8	8	4.5
Ungual Cartilages	**17**	**9.5**	**15**	**10.1**	**0**	**0**
Ossification of the collateral cartilages of the foot	17	9.5	15	10.1	0	0
DDAL	**7**	**3.9**	**6**	**4.0**	**0**	**0**
Desmopathy	7	3.9	6	4.0	0	0
Enthesopathy	2	1.1	2	1.3	0	0

SI, signal intensity; **DSIL**, distal sesamoidean impar ligament; **CSL**, collateral sesamoidean ligament; **DDFT**, deep digital flexor tendon; **DIP** joint, distal interphalangeal joint; **CLs DIP** joint, collateral ligaments of the distal interphalangeal joint; **PIP** joint, proximal interphalangeal joint; **DDAL**, distal digital annular ligament.

All lame limbs had abnormalities in more than one structure of the foot, though not all were deemed contributory to lameness. A primary lesion was identified in 36.3% (65/179) of limbs, with additional secondary abnormalities present in other structures. Primary injuries most commonly involved the DDFT, distal phalanx, and navicular bone. In 51.4% (92/179) of limbs, injuries in multiple structures were thought to be equally contributing to lameness without a clear primary lesion. These included variable combinations of injury, most often involving damage to two or three of the following structures: DDFT, navicular bone, DIP joint, distal phalanx, navicular bursa and collateral ligaments of the DIP joint. Additionally, in 9.5% (17/179) of cases the primary injury was located outside the foot, in the fetlock region. The remaining 2.8% (5/179) of cases had inconclusive findings on MRI.

The DIP joint and navicular bursa were the most frequently affected structures overall (**Table 9**). However, fluid distension in these synovial structures was most often considered a secondary change or incidental finding rather than a primary cause of lameness. Conversely, lesions in DDFT, navicular bone, distal phalanx, and collateral ligaments of the DIP joint were more frequently considered contributory to the presenting lameness. Abnormalities in other foot structures were observed in less than 25% of limbs.

3.3.1. Navicular Bone

Navicular bone abnormalities were identified in 96 limbs (53.6%) across 85 horses (57%) (**Table 9**). In 56 limbs (31.3%), these lesions were deemed contributory to lameness, with 12 cases (6.7%) classified as primary lesions.

Bone marrow lesions, characterized by abnormal fluid signal within the trabecular bone, were the most frequently observed pathology, affecting 83 limbs (46.4%). The fluid signal was most commonly diffuse throughout the spongiosa, or localized close to and parallel to the palmar flexor surface. Less common focal patterns included increased fluid signal near the distal, dorsal, proximal, or central aspects of the bone. In 16 limbs (8.9%), increased fluid signal was limited to enlarged and more numerous synovial invaginations along the distal border, with increased fluid signal in the adjacent trabecular bone.

Flexor surface erosions were observed in 12 limbs (6.7%), typically along the sagittal midline, with most affecting the middle or distal thirds of the bone. These defects measured 1-8 mm in diameter and were frequently associated with surrounding fluid signal and/or sclerosis. One case involved communication with a prominent cyst-like lesion in the mid-third of the bone. Distal border fragmentation occurred in 4 limbs (2.2%), presenting as either a single, larger fragment or multiple small fragments originating at the medial or lateral angles within the DSIL attachment site.

Navicular bone pathology was frequently associated with concurrent abnormalities in the DDFT (67.7%, 65/96). Increased fluid signal along the flexor surface of the navicular bone was

significantly more prevalent in limbs with DDF tendinopathy (20.5%, 18/88) than in those without (5.5%, 5/91; p=0.003). Similarly, an increase in size and number of the synovial invaginations along the distal border occurred at a significantly higher rate in limbs with DDF tendinopathy (14.8%, 13/88) compared to those without (3.3%, 3/91; p=0.007). Moreover, erosions in the flexor surface of the navicular bone were significantly more common in limbs with DDF tendinopathy (12.5%, 11/88), compared to those without (1.1%, 1/91; p=0.002). A detailed breakdown of lesion co-occurrence is provided in *Appendix 4*.

Association between Demographics and Navicular Bone pathology

The distribution of navicular bone pathology across demographic groups is shown in **Figure 10** and a detailed breakdown is provided in *Appendix 5*. No significant associations were found with age (p=0.095), sex (p=0.946), breed (p=0.190), or discipline (p=0.181). Though they did not reach statistical significance, the following distribution patterns were observed.

Age-related trends showed a consistently higher prevalence of affected cases in young and middle-aged horses (<5 years: 61.5%, 8/13; 6-10 years: 59.0%, 36/61; 11-15 years: 61.7%, 37/60), whereas this pattern reversed in the oldest age group, with horses aged 16-20 years exhibiting a substantially lower prevalence of navicular bone pathology (26.7%, 4/15). Sex differences were minimal, with proportions of affected cases nearly identical between geldings (56.8%, 50/88) and mares (57.4%, 35/61). Among breeds, Dutch Warmbloods had the lowest proportion of affected cases (40.7%, 11/27), notably lower than other breeds such as Quarter Horses (73.7%, 14/19) and Oldenburgs (78.6%, 11/14). Regarding discipline, eventers (80%, 12/15) and western horses (78.6%, 11/14) had the highest proportion of pathology, while hunters (47.5%, 19/40) had the lowest.

Figure 10 – Distribution of navicular bone pathology across demographic groups.

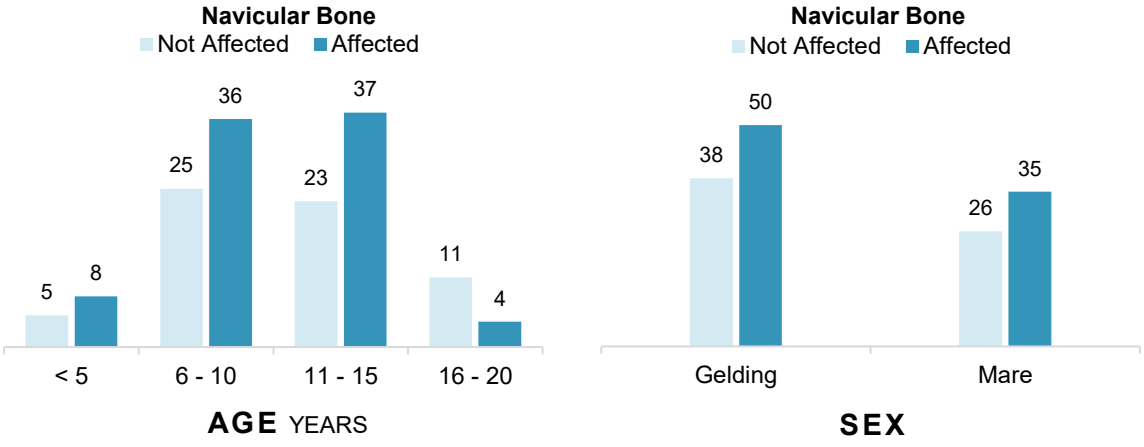

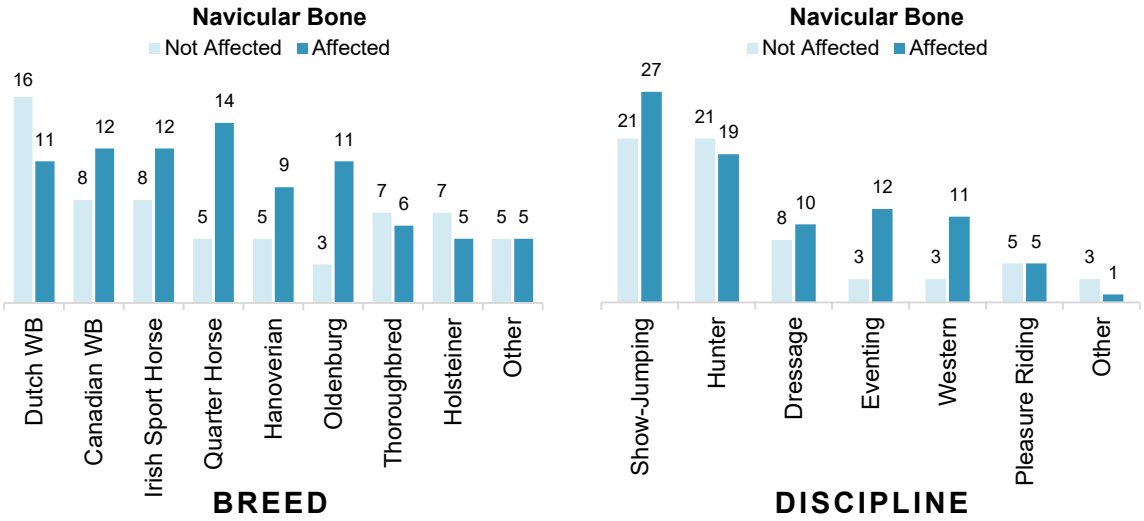

3.3.2. Navicular Bursa

Navicular bursa abnormalities were identified in 108 limbs (60.3%) of 92 horses (61.7%) (**Table 9**). Among these, only 23 limbs (12.8%) had changes considered contributory to lameness. Observed pathological changes included effusion, synovial proliferation, and capsular thickening. Effusion was the most frequently observed abnormality affecting 69 limbs (38.5%). In most cases, fluid accumulation was mild to moderate, with severe bursal effusion observed in 13% (9/69) of affected cases. Synovial proliferation and/or capsular thickening was seen in 70 limbs (39.1%), with or without bursal effusion. Among these, 15.7% (11/70) exhibited severe intrathecal soft tissue proliferation, resulting in minimal fluid accumulation.

All 108 limbs with navicular bursa pathology had concurrent abnormalities in the podotrochlear apparatus. Moreover, synovial proliferation and/or capsular thickening was significantly more prevalent in limbs with DDFT tendinopathy (67%, 59/88), particularly in lesions extending from mid-P2 to the level of the navicular bone, compared to those without (12.1%, 11/91; $p<0.001$). Similarly, synovial proliferation and/or capsular thickening was significantly more common in limbs with increased trabecular fluid signal within the navicular bone (53%, 44/83) than in those without (27.1%, 26/96; $p<0.001$). In contrast, navicular bursa effusion/synovitis did not show significant associations with any specific DDFT or navicular bone injuries ($p>0.05$ for all comparisons). A detailed breakdown of lesion co-occurrence is provided in *Appendix 6*.

Association between Demographics and Navicular Bursa pathology

The distribution of navicular bursa pathology across demographic groups is shown in **Figure 11**, and a detailed breakdown is provided in *Appendix 7*. No significant associations were found with age ($p=0.420$), sex ($p=0.137$), breed ($p=0.057$), or discipline ($p=0.148$). Though they did not reach statistical significance, the following distribution patterns were observed.

Similar to the navicular bone, young and middle-aged horses displayed higher prevalence of navicular bursa pathology (<5 years: 69.2%, 9/13; 6-10 years: 67.2%, 41/61; 11-15 years: 58.3%, 35/60), whereas horses aged 16-20 years had a lower proportion of affected cases (46.7%, 7/15). Regarding sex, mares were more frequently affected (68.9%, 42/61) than geldings (56.8%, 50/88). Among breeds, Quarter Horses (84.2%, 16/19) and Canadian Warmbloods (80.0%, 16/20) had the highest prevalence, while Thoroughbreds had the lowest (38.5%, 5/13). By discipline, western horses (85.7%, 12/14) and show-jumpers (70.8%, 34/48) had the highest proportions of affected cases, whereas dressage horses (44.4%, 8/18) had the lowest.

Figure 11 – Distribution of navicular bursa pathology across demographic groups.

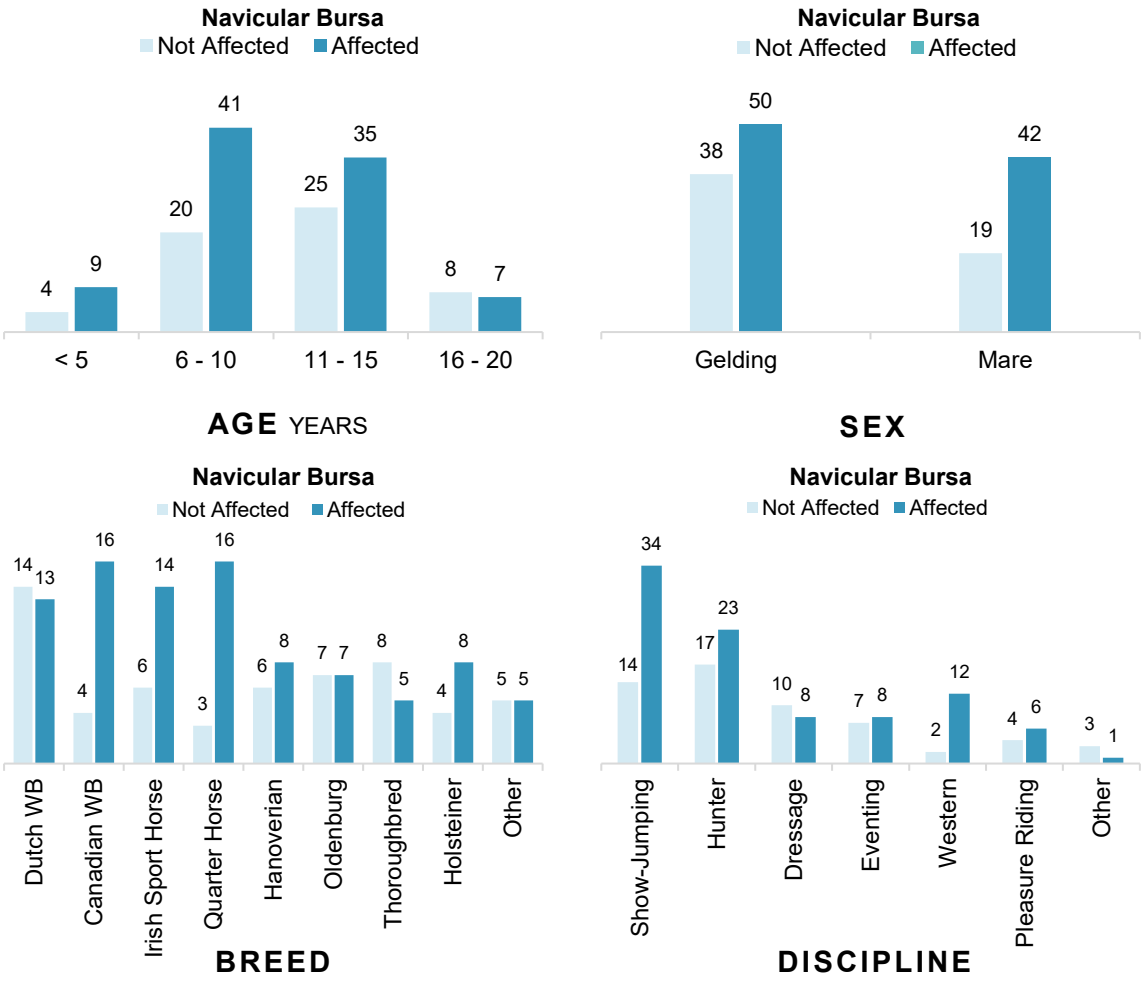

3.3.3. Distal Sesamoidean Impar Ligament

Abnormalities involving the DSIL were identified in 30 limbs (16.6%) of 28 horses (18.8%) (**Table 9**). DSIL desmopathy was observed in only 4 limbs (2.2%), characterized by moderate, diffuse thickening of the ligament. In contrast, insertional enthesopathy at the palmar aspect of the distal phalanx was more frequent, affecting 30 limbs (16.8%) of 28 horses (18.8%), with 13 cases (7.3%) deemed contributory to lameness. This was typically characterized by focal

fluid signal and/or sclerosis at the ligament's insertion site, often accompanied by focal bone resorption. Two cases of avulsion injuries were observed, both associated with significant fiber disruption and bone fluid at the insertion site on the distal phalanx.

Pathologic changes of the DSIL were frequently associated with navicular bone pathology (80%, 24/30). Increased diffuse fluid signal in the navicular bone was significantly more prevalent in limbs with DSIL abnormalities (50%, 15/30) than in those without (24.2%, 36/149; p=0.004). Similarly, an increase in size and number of the synovial invaginations along the distal border of the navicular bone occurred at a significantly higher rate in limbs with DSIL pathology (20%, 6/30) compared to those without (6.7%, 10/149; p=0.032). A breakdown of lesion co-occurrence patterns is provided in *Appendix 8*.

Association between Demographics and DSIL pathology

The distribution of DSIL pathology across demographic groups is shown in **Figure 12**, and a detailed breakdown is provided in *Appendix 9*. No significant associations were found with age (p=0.948), sex (p=0.279), breed (p=0.701), or discipline (p=0.130).

The proportion of affected cases was relatively consistent across age groups, with horses aged 6-15 years showing slightly higher prevalence (6–10 years: 21.3%, 13/61; 11–15 years: 18.3%, 11/60) than younger (<5 years: 15.4%, 2/13) and older horses (16-20 years: 13.3%, 2/15). Mares showed a slightly higher prevalence of DSIL pathology (23%, 14/61) than geldings (15.9%, 14/88). Among breeds, Quarter Horses showed the highest prevalence of affected cases (36.8%, 7/19), which was noticeably higher than other breeds, in which the prevalence of DSIL pathology ranged from 8.3% (1/12) in Holsteiners to 21.4% (3/14) in Hanoverians and Oldenburgs. By discipline, western horses had the highest proportion of affected cases (50%, 7/14), substantially higher than other disciplines, which ranged from 10% (1/10) in pleasure riding horses to 18.8% (9/48) in show-jumpers.

Figure 12 – Distribution of distal sesamoidean impar ligament pathology across demographic groups.

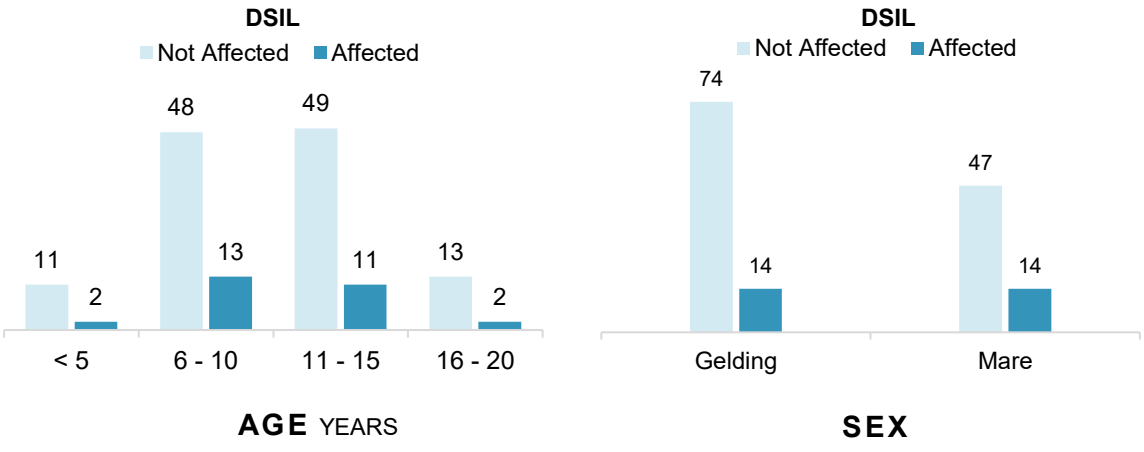

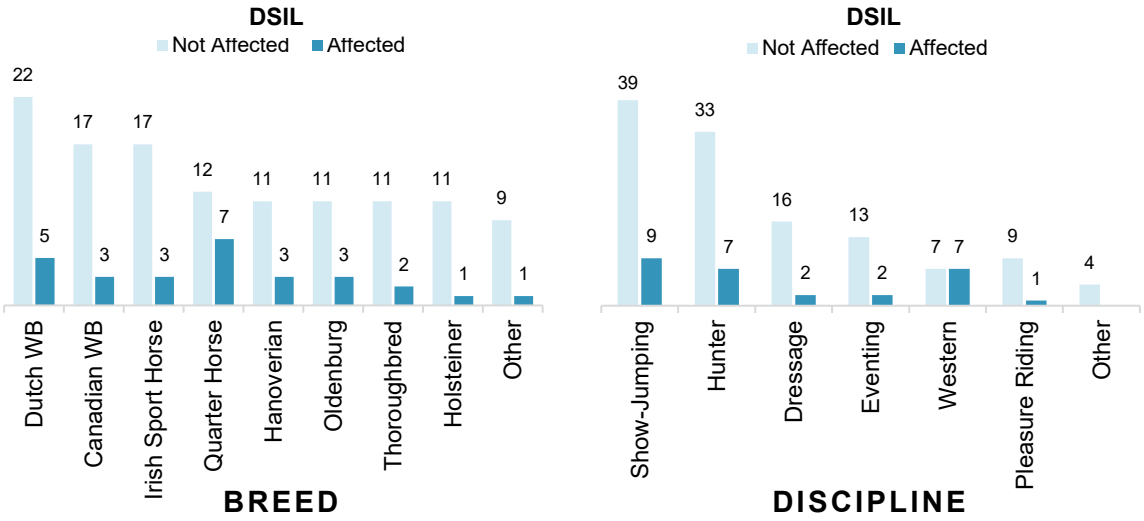

3.3.4. Collateral Sesamoidean Ligaments

Desmopathy of the CSL was identified in 7 limbs (3.9%) of 7 horses (4.7%), with none of these lesions deemed contributory to the presenting lameness (**Table 9**). The most common finding, observed in 4 limbs (2.2%), was diffuse thickening of the ligament body and/or branches without alteration of the normal signal pattern. Two partial-thickness tears were detected: one located just proximal to the navicular bone near the insertion, and other located in the lateral branch, which was associated with a concurrent split in the adjacent DDFT. One case exhibited focal dystrophic mineralization, presenting as a mineralized ovoid area within the lateral branch, without evidence of tearing. No cases of CSL enthesopathy were identified.

Association between Demographics and CSL pathology

The distribution of CSL pathology across demographic groups is shown in **Figure 13**, and a detailed breakdown is provided in *Appendix 10*. Due to the very low prevalence of CSL pathology in the study population (4.7%, 7/149) no statistically meaningful associations were possible to detect with age, sex, breed, or discipline.

Across age groups, only horses aged 6-15 years were affected (6-10 years: 3.3%, 2/61; 11-15 years: 8.3%, 5/60). The proportion of affected cases was nearly identical between geldings (4.5%, 4/88) and mares (4.9%, 3/61). Affected breeds included Irish Sport Horses (15.0%, 3/20), Quarter Horses (10.5%, 2/19), Hanoverians (7.1%, 1/14), and Oldenburgs (7.1%, 1/14). Among disciplines, dressage was the only group without affected cases, with prevalence ranging from 4.2% (2/48) in show-jumping to 10% (1/10) in pleasure riding.

Figure 13 – Distribution of collateral sesamoidean ligament pathology across demographic groups.

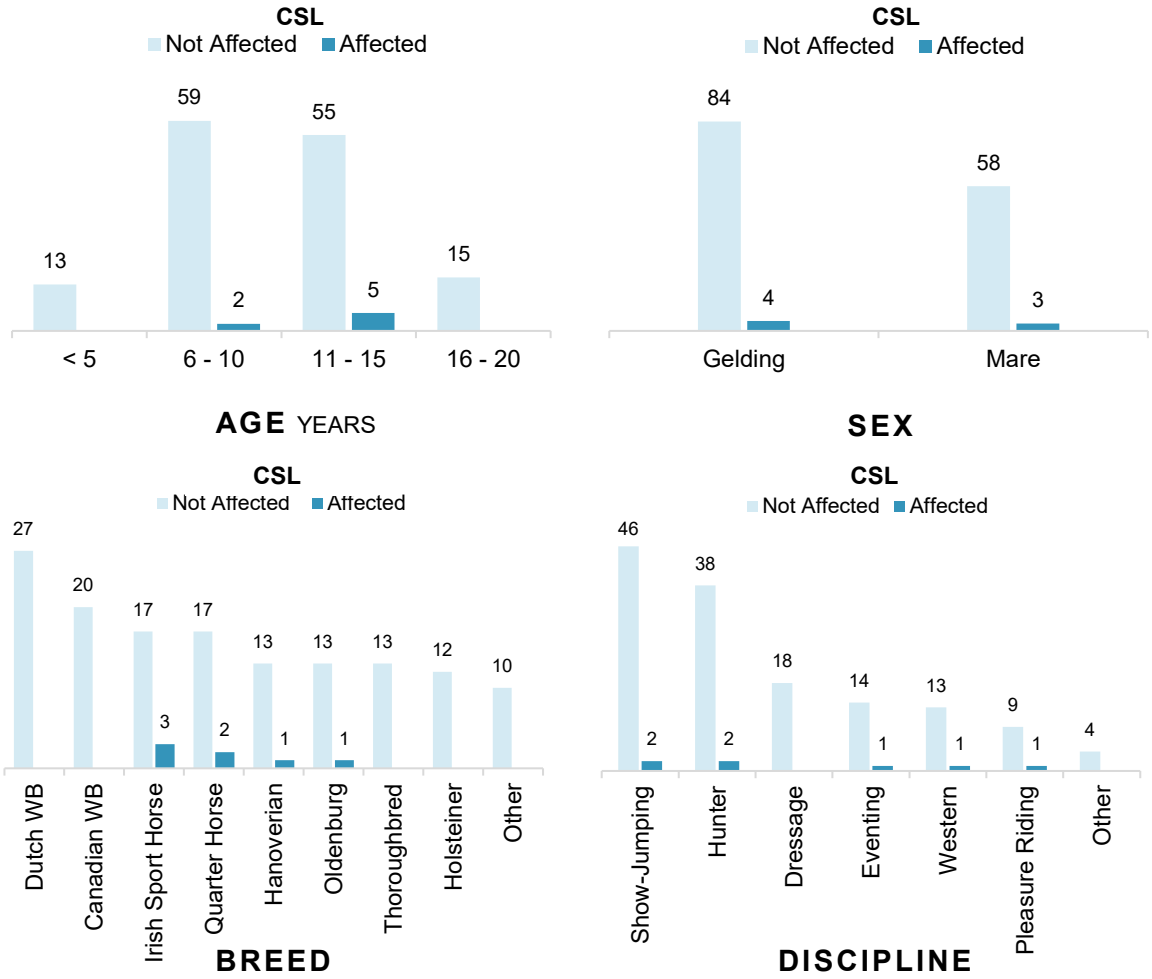

3.3.5. Deep Digital Flexor Tendon

DDF tendinopathies within the foot were identified in 88 limbs (49.2%) of 73 horses (49%) (**Table 9**). Among these, lesions in 53 limbs (29.6%) were deemed contributory to lameness, with 19 cases (10.6%) classified as primary abnormalities. Lesions varied in size and configuration, typically appearing as areas of increased signal intensity within one or both tendon lobes, with or without associated enlargement.

Lesions occurred at one or more sites along the tendon. The most frequently identified location was proximal to the navicular bone (81.8%, 72/88), especially at the level of the proximal recess of the navicular bursa and the CSL. The level of the navicular bone itself was the second most affected site (60.2%, 53/88), followed by fewer cases seen at the level of the PIP joint (19.3%, 17/88), distal to the navicular bone (15.9%, 14/88), and at the level of the proximal phalanx (10.2%, 9/88). In limbs with lesions involving multiple locations, lesions commonly extended from the middle phalanx to the navicular bone or to the insertion on the distal phalanx, sometimes originating as proximally as the limb was imaged.

Four different types of lesions were identified: dorsal border tears or fibrillation (71.6%, 63/88), (para)sagittal splits and tears (43.2%, 38/88), core lesions (14.8%, 13/88), and

insertional lesions (12.5%, 11/88). Combinations of these lesion types were common, with specific lesion types more prevalent at certain locations: core lesions were predominant along the proximal phalanx and PIP joint; (para)sagittal splits and tears were most mostly seen extending from the middle phalanx and distally to the navicular bone, though dorsal border damage was prevalent just proximally to the navicular bone. At the insertion level, fiber abnormalities were generally not classified into specific lesion types, but fiber damage and/or enlargement were noted, including one case of avulsion injury. Additionally, findings included abnormal thinning over the flexor surface of the navicular bone (3.9%, 7/179), and presumable adhesions (7.8%, 14/179). These were characterized by strands of low-signal tissue between the dorsal margins of the DDFT and: the navicular bursa (13 limbs), the CSL (7 limbs), and an erosion of the flexor surface of the navicular bone (2 limbs).

DDFT enthesopathy, observed in 24 limbs (13.4%) of 22 horses (14.8%) (**Table 9**), was characterized by abnormal fluid signal and/or sclerosis at the insertion site on the palmar aspect of the distal phalanx, associated with stress remodeling.

Association between Demographics and DDFT pathology

The distribution of DDFT pathology across demographic groups is shown in **Figure 14**, and detailed breakdown is provided in *Appendix 11*. No significant associations were found with age (p=0.667), sex (p=0.069), breed (p=0.335), or discipline (p=0.660).

Among age groups, the youngest horses (<5 years) had the highest prevalence of affected cases (69.2%, 9/13), whereas horses aged 16-20 years had the lowest (46.7%, 7/15). Regarding sex, mares had a higher prevalence of DDFT pathology (67.2%, 41/61) compared to geldings (52.3%, 46/88). Among breeds, Quarter Horses (78.9%, 15/19), Canadian Warmbloods (70%, 14/20), and Irish Sport Horses (65%, 13/20) showed the highest prevalence of DDFT pathology, while Dutch Warmbloods were the only breed in which non-affected cases outnumbered affected cases (44.4%, 12/27). Across disciplines, western horses showed the highest prevalence DDFT pathology (78.6%, 11/14), while in the remaining disciplines proportion of affected cases ranged between 50% to 60%.

Figure 14 – Distribution of DDFT pathology across demographic groups.

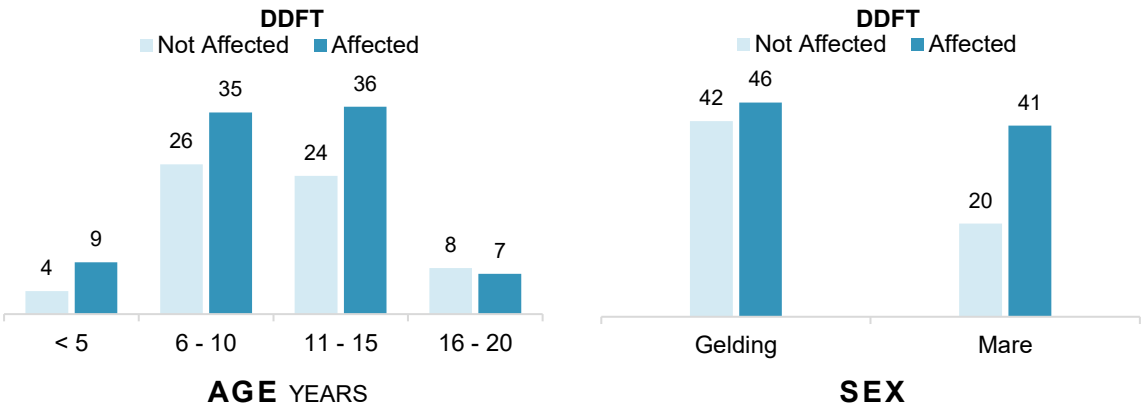

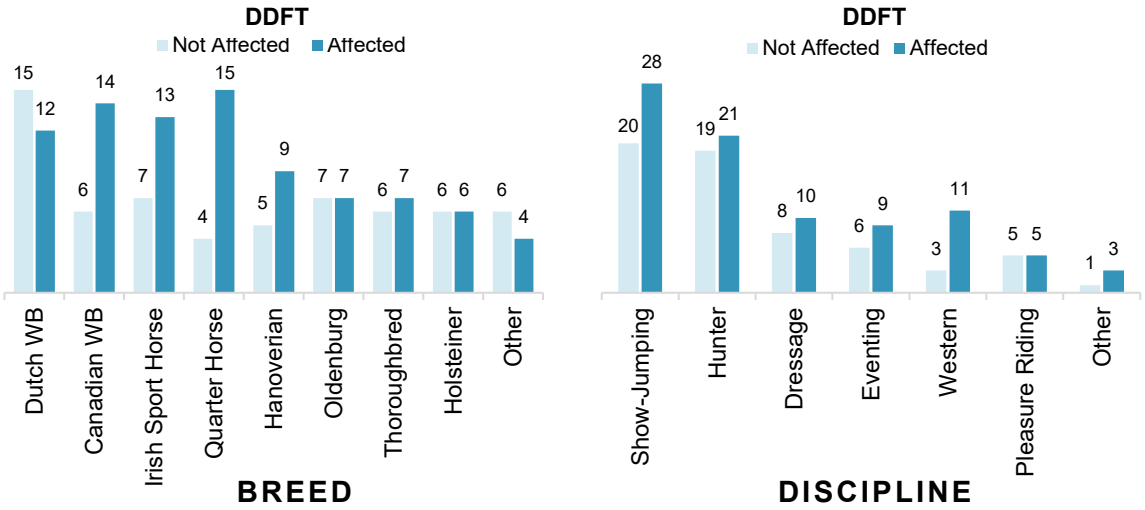

3.3.6. Distal Interphalangeal Joint

Pathological changes involving the DIP joint were observed in 166 limbs (92.7%) of 138 horses (92.6%) (**Table 9**). However, these were deemed contributory to lameness in only 43 limbs (24%), and considered primary lesions in 9 of them (5%).

The most common finding was effusion, with or without concurrent synovial proliferation, observed in 154 limbs (86%). Fluid distension was generally mild to moderate, with severe synovitis noted in only 13% (20/154) of affected cases. Moreover, chronic synovitis with extensive synovial proliferation and capsular thickening was observed in 2% (3/154) of affected cases, resulting in loss of the dorsal fluid space.

Osteoarthritis was diagnosed in 76 limbs (42.5%), characterized by articular cartilage damage, subchondral bone changes, and/or periarticular osteophyte formation, often accompanied by joint effusion. Three full-thickness focal articular cartilage defects in the sagittal midline of the distal phalanx were identified, ranging between 2-4 mm, characterized by pooling of synovial fluid and a concave defect in the subchondral bone. Three multilobular osseous cyst-like lesions (OCLLs) were detected, also located in the sagittal midline of the distal phalanx (n=2) and middle phalanx (n=1), characterized by variable fluid signal intensity, well-demarcated or irregular margins, and with an average size of 10 mm in diameter. All lesions were associated with surrounding subchondral bone sclerosis, and two showed communication with articular surface defects. In another three limbs, subchondral bone fluid signal was seen extending continuously across the distal and middle phalanges along the midline without visible cartilage damage. Diffuse cartilage thinning with joint space narrowing was observed in three other limbs. Osteophyte formation (69 limbs, 38.5%) predominantly affected the dorsodistal aspect of the middle phalanx and the extensor process of the distal phalanx. Less common sites included the dorsoproximal aspect of the navicular bone, the palmar distal aspect of the middle phalanx, and the joint capsule insertion on the dorsoproximal aspect of the middle phalanx.

Among limbs with DIP joint abnormalities, 77.7% (129/166) limbs had concurrent alterations in the podotrochlear apparatus, 27.7% (46/166) had collateral desmopathy and/or enthesopathy of the DIP joint, and 4.8% (8/166) had increased diffuse fluid signal within the trabecular bone of either the distal aspect of the middle phalanx or the extensor process extending distally into the distal phalanx.

Association between Demographics and DIP joint pathology

The distribution of DIP joint pathology across demographic groups is shown in **Figure 15**, and a detailed breakdown is provided in *Appendix 12*. Due to the high overall prevalence of DIP joint abnormalities in the study population (92.6%, 138/149), statistically meaningful associations with age, sex, breed, or discipline were not possible to detect.

Horses aged 16-20 years showed a slightly lower prevalence of affected cases (86.7%, 13/15) compared to younger groups, which had a prevalence of approximately 93% (<5 years: 92.3%, 12/13; 6-10 years: 93.4%, 57/61; 11-15 years: 93.3%, 56/60). Regarding sex, geldings (93.2%, 82/88) and mares (91.8%, 56/61) had similar proportions of affected cases. DIP joint pathology was highly prevalent across all breeds and disciplines, with Holsteiners (83.3%, 17/20) and show-jumpers (87.5%, 42/48) showing the lowest prevalence of affected cases, respectively.

Figure 15 – Distribution of DIP Joint pathology across demographic groups.

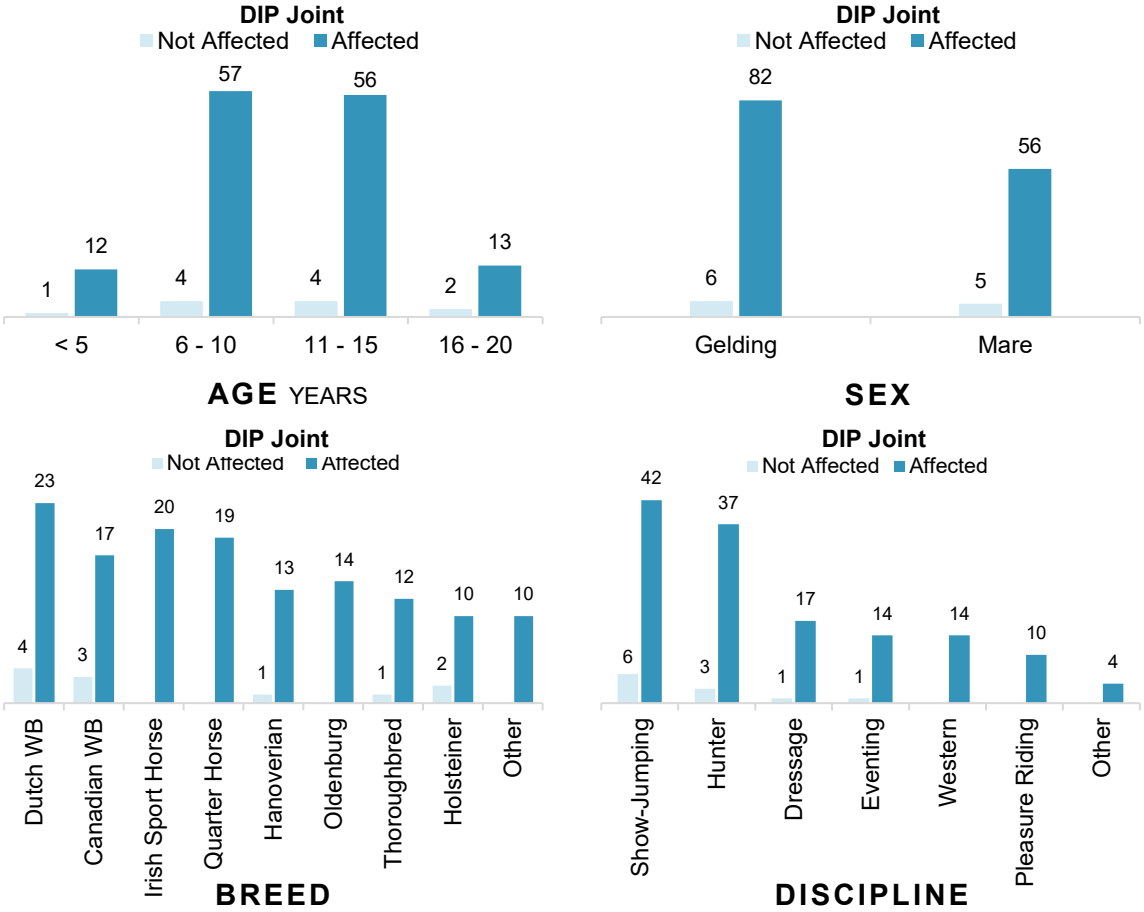

3.3.7. Collateral Ligaments of the DIP Joint

Collateral desmopathy of the DIP joint was identified in 39 limbs (21.8%) of 35 horses (23.5%) (**Table 9**). Lesions were deemed contributory to lameness in 19 limbs (10.6%), of which 3 (1.7%) were considered primary injuries. Abnormalities included enlargement and/or increased signal intensity within the ligament, often accompanied by periligamentous thickening. A diffuse mottled signal pattern on T2-weighted images, consistent with degenerative changes was seen in 25.6% (10/39) of affected limbs. Abnormalities were predominantly diffuse throughout the ligament, although focal changes were also observed, more often in the proximal third. Lesions in the distal third of the ligament were less frequent and typically manifested as fiber disruption or fraying near the insertion on the distal phalanx. Lateral CL desmopathy (43.6%) was slightly more prevalent than medial CL desmopathy (35.9%) or biaxial desmopathy (28.2%). Concurrent DIP joint abnormalities were observed in 97.4% (38/39) of affected limbs, of which 46.2% (18/39) had signs of osteoarthritis.

Collateral enthesopathy was identified in 19 limbs (10.6%) of 17 horses (11.4%), with 7 cases (3.9%) deemed contributory to lameness (**Table 9**). Insertional enthesopathy was characterized by cortical irregularity of the attachment fossae of the distal phalanx, and occasionally by abnormal fluid signal extending into the underlying trabecular bone. The lateral and medial attachment sites were equally affected. Only two cases of CL enthesopathy at the origin on the middle phalanx were recorded, presenting as focal bone resorption and extensive new bone proliferation at the ligament's attachment sites. Concurrent CL desmopathy was present in 57.9% (11/19) of cases.

Association between Demographics and CLs of DIP joint pathology

The distribution of CLs of DIP joint pathology across demographic groups is shown in **Figure 16**, and a detailed breakdown is provided in *Appendix 13*. No significant associations were found with age (p=0.413), sex (p=0.074), breed (p=0.389), or discipline (p=0.575).

Horses aged 11-15 years had slightly higher prevalence of affected cases (35%, 21/60) compared to other age groups (<5 years: 23.1%, 3/13; 6-10 years: 21.3%, 13/61; 16-20 years: 26.7%, 4/15). Geldings showed a higher prevalence of affected cases (33%, 29/88) compared to mares (19.7%, 12/61). Among breeds, the highest prevalence of affected cases was observed in Irish Sport Horses (40%, 8/20) and Oldenburgs (35.7%, 5/14), while the lowest prevalence was noted in Holsteiners (8.3%, 1/12) and Quarter Horses (10.5%, 2/19). Across disciplines, hunters (35.0%, 14/40) and eventing horses (33.3%, 5/15) showed the highest prevalence, whereas pleasure horses (10.0%, 1/10) and western horses (14.3%, 2/14) had the lowest prevalence.

Figure 16 – Distribution of CLs of the DIP joint pathology across demographic groups.

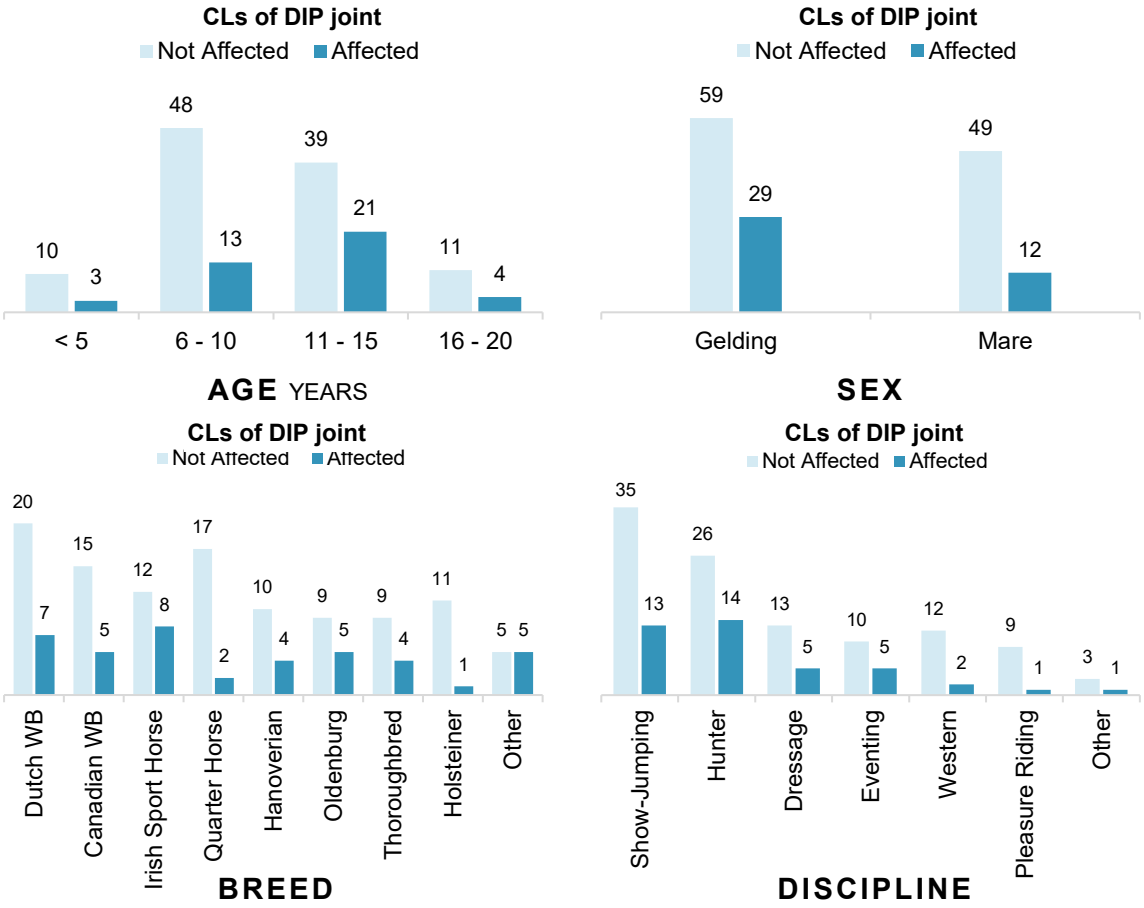

3.3.8. Distal Phalanx

Abnormalities of the distal phalanx were observed in 66 lame limbs (36.9%) of 62 horses (41.6%) (**Table 9**). These were deemed contributory to lameness in 43 cases (24%), with 15 cases (8.4%) classified as primary lesions.

Bone marrow lesions were the most common finding, observed in 58 limbs (32.4%). These lesions appeared as abnormal fluid signal within the trabecular bone and were either diffuse throughout the spongiosa or localized to specific regions, including one or both palmar processes, the toe, the mid-to-palmar aspect, and the medial or lateral quarters. Fluid signal in the toe region was frequently associated with inflammation and chronic thickening of the dorsal laminar attachment site. In two other cases, it was linked to a solar margin and overlying laminar defect, consistent with keratoma. Bone marrow lesions in the distal phalanx were seen clustered in one side of the bone, often extending into the navicular bone and middle phalanx.

The palmar processes were the most frequently affected sites. In addition to bone marrow lesions, 3 limbs (1.7%) exhibited cortical irregularity and sclerosis compatible with remodeling; and 6 limbs (3.4%) had evidence of incomplete non-articular fractures. Four oblique fractures extended distally from the base of the ungual cartilage to the palmar process, often involving the collateral ligament fossae. Three transverse fractures occurred at the base of an ungular cartilage. Six of these fractures were associated with severe ossification of the

ipsilateral ungual cartilage. Additionally, one case exhibited a transverse articular fracture extending from the medial palmar articular margin to the solar margin.

Association between Demographics and Distal Phalanx pathology

The distribution of distal phalanx pathology across demographic groups is shown in **Figure 17**, and a detailed breakdown is provided in *Appendix 14*. A near-significant association was found between age and the presence of distal phalanx pathology ($\chi^2(3)=7.777$, $p=0.051$). Horses under 5 years of age showed a notably higher proportion of affected cases (76.9%; 10/13) compared to older age groups (6-10 years: 41%, 25/61; 11-15 years: 35%, 21/60; 16-20 years: 40%, 6/15). Additionally, a significant association was found with sex ($\chi^2(1)=4.654$; $p=0.031$), in which geldings showed a significantly higher proportion of affected cases (48.9%; 43/88) compared to mares (31.1%, 19/61).

Conversely, no significant associations were found between pathology prevalence and breed ($p=0.977$) or discipline ($p=0.687$). The proportion of affected horses across breeds ranged from 35% (7/20) in Canadian Warmbloods to 50% (10/20) in Irish Sport Horses. Among disciplines, pleasure riding horses exhibited the lowest prevalence of pathology (20%; 2/10), whereas western horses showed the highest (50%; 7/14), though these differences were not statistically significant.

Figure 17 – Distribution of distal phalanx pathology across demographic groups.

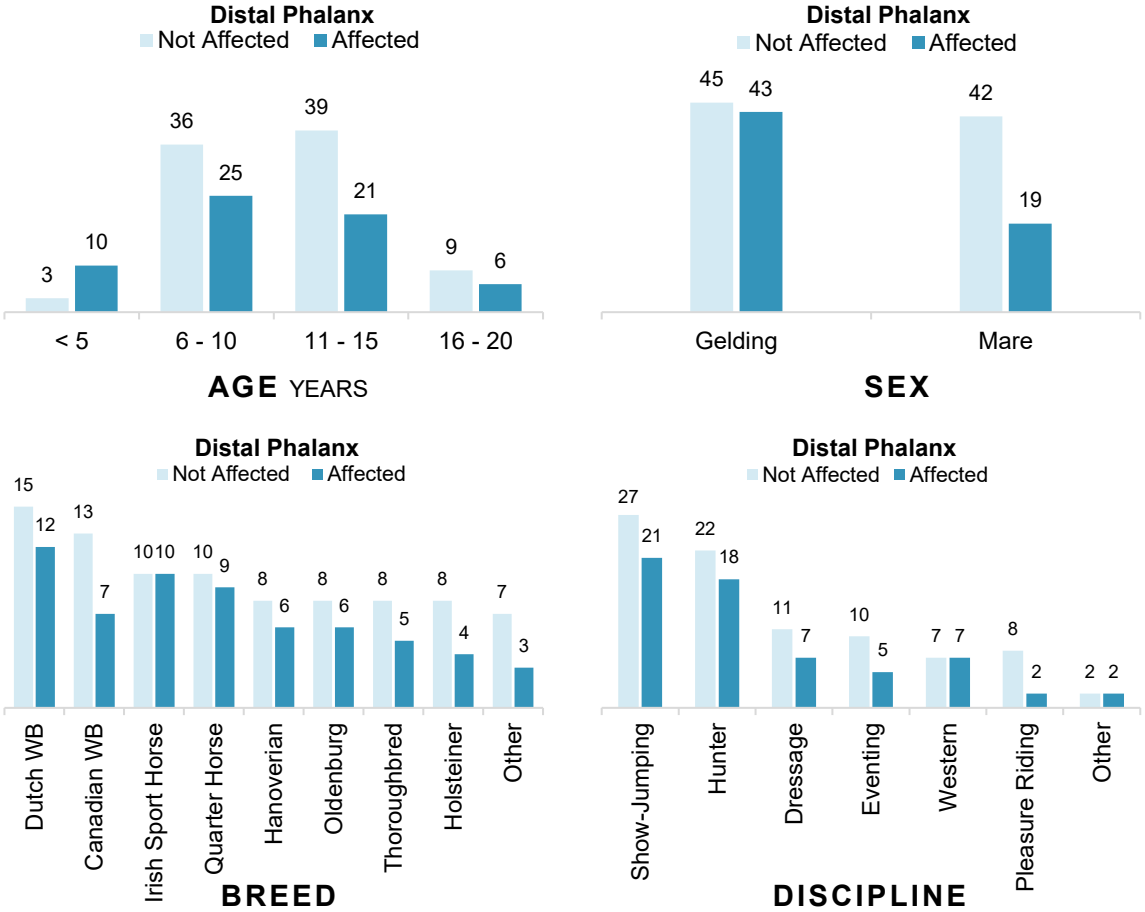

3.3.9. Middle Phalanx

Abnormalities of the middle phalanx were identified in 10 limbs (5.6%) from 10 horses (6.7%), with 7 cases (3.9%) considered contributory to the presenting lameness (**Table 9**). All observed abnormalities were bone marrow lesions, primarily affecting the trabecular bone of the proximal and distal regions, occasionally extending to the subchondral bone. The proximal region was the most frequently affected, particularly the dorsal aspect. A smaller subset of cases exhibited focal fluid signal localized to the mid-dorsal region.

Association between Demographics and Middle Phalanx pathology

The distribution of middle phalanx pathology across demographic groups is shown in **Figure 18**, and a detailed breakdown is provided in *Appendix 15*. Due to the very low prevalence of middle phalanx pathology in the study population (6.7%, 10/149), statistically meaningful associations with age, sex, breed, or discipline were not possible to detect.

The prevalence of middle phalanx abnormalities was similar across age groups, ranging from 6.6% (4/61) in the 6-10 years group to 7.7% (1/13) in horses under 5 years old. Similarly, there was no notable difference between geldings (5.7%; 5/88) and mares (8.2%; 5/61) in the prevalence pathology. Regarding breed, Quarter Horses showed a higher proportion of affected cases than expected (21.1%, 4/19). Other affected breeds included Thoroughbred (15.4%, 2/13), Hanoverian (7.1%, 1/14), and Dutch Warmblood (7.4%, 2/27). Among disciplines, western horses had the highest proportion of affected cases (21.4%, 3/14), while eventing and pleasure riding horses were not affected.

Figure 18 – Distribution of middle phalanx pathology across demographic groups.

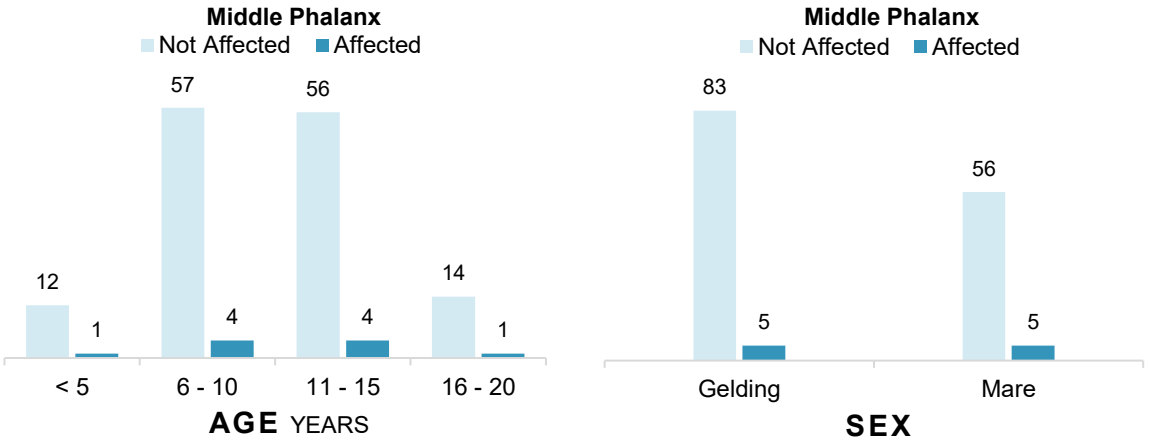

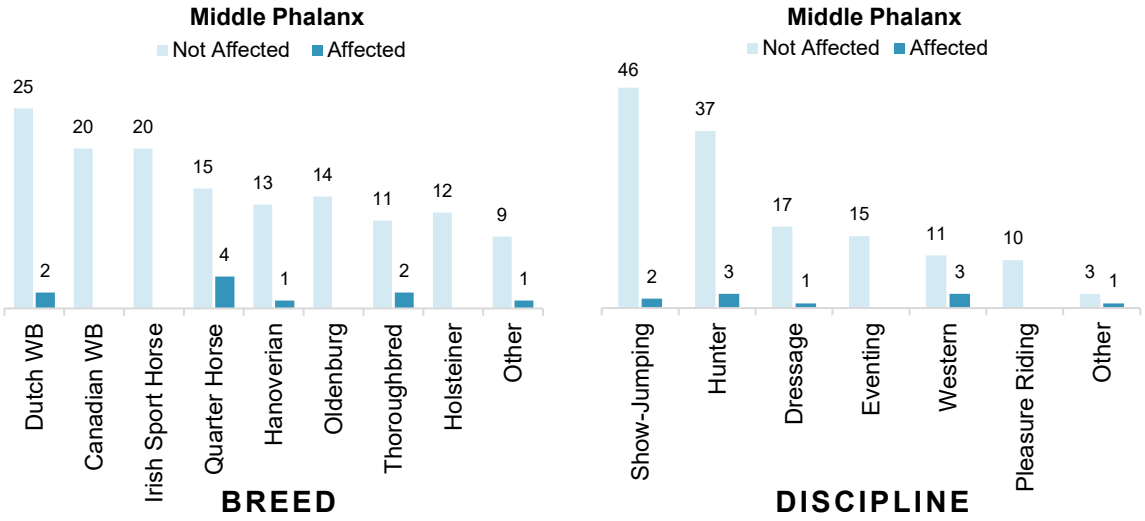

3.3.10. Proximal Interphalangeal Joint

Pathological changes involving the PIP joint were observed in 39 limbs (21.8%) of 37 horses (24.8%), with only 8 cases (4.5%) considered contributory to lameness (**Table 9**).

Effusion was rare, observed in 6 limbs (3.4%) of 6 horses (4%), and was typically mild to moderate in severity. Osteoarthritis was diagnosed in 35 limbs (19.6%) of 34 horses (22.8%). Among these, osteophyte formation (32 limbs, 17.9%) was the most frequent finding, predominantly seen at the dorsoproximal margin of the middle phalanx. Subchondral bone changes were noted in 7 limbs (3.9%). These included: three subchondral OCLLs communicating with the articular surface (3 limbs, 1.7%), located in the mid-to-palmar aspect of the middle phalanx and in the central aspect of the proximal phalanx; areas of subchondral bone fluid signal and/or sclerosis affecting both phalanges equally (3 limbs, 1.7%); and a shallow, concave subchondral bone defect bordered by sclerosis located in the distolateral aspect of the proximal phalanx (2 limbs, 1.1%). Additional findings included, joint space narrowing (2 limbs, 1.1%), distodorsal fragmentation of the proximal phalanx (1 limb, 0.6%), and secondary joint effusion (3 limbs, 1.7%).

Association between Demographics and PIP joint pathology

The distribution of PIP joint pathology across demographic groups is shown in **Figure 19**, and a detailed breakdown is provided in *Appendix 16*. A statistically significant association was found between age and the presence of pathology in the PIP joint ($\chi^2(3)=22.536$, $p<0.001$), in which the prevalence of pathology increased substantially with age, ranging from no affected horses under 5 years to 66.7% (10/15) affected horses aged 16-20 years.

No significant association was found with sex (p=0.742), breed (p=0.594), or discipline (p=0.336). However, the following distribution patterns were observed. Regarding sex, the proportion of affected cases was comparable between geldings (23.9%, 21/88) and mares (26.2%, 16/61). Among breeds, Quarter Horses had a lower prevalence of affected cases

(10.5%, 2/19), especially compared to Dutch Warmbloods which had the highest proportion of affected cases (37%, 10/27). Across disciplines, pleasure riding horses showed the highest prevalence of PIP pathology (50%, 5/10), and western horses showed the lowest (7.1%, 1/14), while the remaining disciplines had a prevalence of approximately 25%.

Figure 19 – Distribution of PIP Joint pathology across demographic groups.

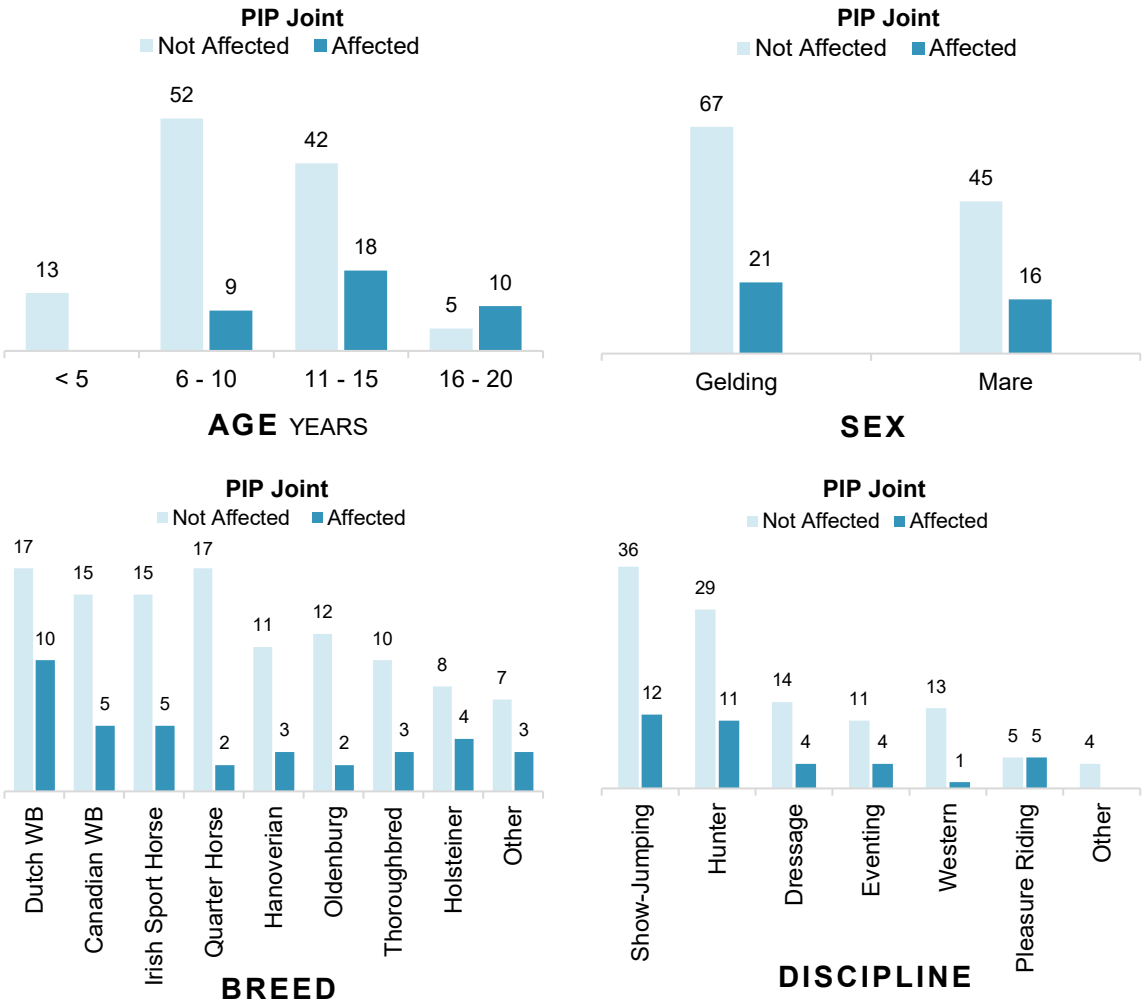

3.3.11. Other Findings

Additional abnormalities identified in lame limbs included varying degrees of ossification of the collateral cartilages of the foot, observed in 17 limbs (9.5%) from 15 horses (10%), and thickening of the DDAL was noted in 7 limbs (3.9%) from 6 horses (4%), with concurrent enthesopathy at the proximal attachment on the proximal phalanx in 2 limbs (1.1%) from 2 horses (1.3%).

4. Discussion

This retrospective study aimed to describe the clinical use of standing low-field MRI of the equine distal limb, in a population of horses presented to the only equine practice in Ontario, Canada that provides this service. Moreover, it sought to characterize the observed MRI findings in the forelimb foot in terms of their prevalence, nature, co-occurrence patterns, and distribution across demographic groups, including age, sex, breed, and discipline. Over a three-year period, standing MRI was primarily used to investigate forelimb lameness, with the foot representing the most commonly scanned anatomical region. Among the lame feet examined, abnormalities in the DIP joint, navicular bursa, DDFT, and navicular bone were the most prevalent findings. All feet exhibited abnormalities in more than one anatomical structure, and in approximately half of the cases, multiple structures were deemed to have pathological changes equally contributory to the presenting lameness. Few statistically significant associations were identified between affected structures and demographic factors, but clinical differences in pathology distribution were observed across groups.

4.1. Overview of the MRI Caseload

Between 2017 and 2019, a total of 210 MRI examinations were performed on 185 horses at MPES. Among these, 172 (81.9%) were initial diagnostic scans, while 32 (15.2%) were follow-up assessments, suggesting that approximately 1 in 7 MRI scans at MPES are recheck examinations, with the remainder serving diagnostic purposes. This distribution reflects the current primary role of MRI as an advanced diagnostic tool, which is to detect injuries that may not be visible on more conventional imaging modalities (Garrett 2022; Schramme and Zimmerman 2022). The value of recheck examinations for monitoring progression and response to treatment, and consequently, optimizing case management, as emphasized by Werpy (2012), was also recognized. Certain lesions may become visible using conventional imaging modalities after an initial MRI diagnosis, but the same level of anatomical detail and lesion characterization may not be achievable (Werpy 2012). Therefore, the frequency of follow-up scans likely reflects a combination of clinical necessity, strategic use of other imaging modalities, and factors such as client motivation and financial considerations.

Over the three-year study period, the frequency of initial examinations varied significantly, with the highest number of scans conducted in the Summer (32.6%) and Fall (30.8%), and the lowest in Winter (13.4%). This seasonal pattern may reflect variations in training intensity imposed by competition schedules, as lameness tends to appear or worsen during periods of increased athletic demand (Wilson and Weller 2011). In Ontario, the main competition season for many equestrian disciplines spans from May to October, aligning with the observed peak in MRI use, particularly towards the end of season. In addition, during the Winter months, many performance horses relocate to Florida for the Winter show season,

reducing the caseload locally. For those that remain, colder weather and snow may pose a challenge for transporting horses to the clinic, potentially delaying advanced diagnostics until conditions improve or performance becomes a more immediate concern.

Analysis of scanned anatomical regions revealed a marked predominance of forelimb imaging, involving 90.1% of horses compared to 9.9% undergoing hindlimb scans. Furthermore, the foot was the most frequently scanned region overall, with 93.6% of horses having at least one foot imaged. However, the primary region of interest differed between limbs: while the foot stood out as the primary focus within forelimbs (93.9%, 261/278), fetlock region scans were more prevalent within hindlimbs (79.2%, 19/24), though hind foot scans followed closely behind (50%, 12/24). This distribution pattern is consistent with the well-known primary clinical application of MRI, which is to examine the foot when conventional imaging modalities often fail to provide a conclusive diagnosis (Schramme and Zimmerman 2022). MRI's ability to visualize all structures of the foot with great detail and across multiple planes makes it the gold standard modality for diagnosing equine foot pathology, whereas radiography can only evaluate bone and is limited by superimposition, and ultrasonography's ability to assess soft-tissues is significantly limited by the hoof capsule (Dyson and Murray 2007; Schramme and Zimmerman 2022). While the distribution of limb involvement and the location of lameness is heavily influenced by factors such as sport discipline and breed conformation (Murray et al. 2006b; Baxter et al. 2020), the relatively low proportion of hindlimb studies may be explained by the fact that hindlimb foot lameness is generally less common than forelimb foot lameness (Ross 2011b). Hindlimb injuries tend to occur more proximally within the limb, often affecting the proximal metatarsus/distal metatarsus or the stifle (Baxter et al. 2020), where radiography and ultrasonography are often sufficient to achieve a definitive diagnosis, reducing the need for advanced diagnostics (Garrett 2022; Schramme and Zimmerman 2022). Additionally, susceptibility for motion artifacts in standing MRI is higher in more proximal regions, as well as in the hindlimbs, due to patient movement or wobbling motion under sedation (Murray and Dyson 2007). As a result, MRI under general anesthesia may be preferred in these cases to improve diagnostic quality of the images obtained from these regions.

4.2. Prevalence and Co-occurrence Patterns of MRI Findings

The following discussion focuses on the pathological findings identified within the 179 clinically lame forefeet of the 149 horses examined using standing low-field (0.27T) MRI in this study. Several previous studies have evaluated the prevalence and nature of MRI findings in horses with foot pain using both low-field and high-field systems and examining diverse populations, providing a basis for comparison (Dyson et al. 2005; Mitchell et al. 2006; Dyson and Murray 2007; Sherlock et al. 2007; Sampson et al. 2009; Gutierrez-Nibeyro et al. 2012;

Gutierrez-Nibeyro et al. 2020). Comparative studies between low-field and high-field MRI systems have consistently shown that, despite the inherent relatively lower image resolution of low-field MRI, it remains highly effective in detecting a wide range of clinically relevant foot lesions, while avoiding the risks and logistical challenges associated with general anesthesia (Werpy 2007; Murray et al. 2009; Bolen et al. 2010; Byrne et al. 2021). Nonetheless, the reported limitations in evaluating the foot in these studies have included difficulty in assessing the articular cartilage of the DIP joint, the flexor surface of the navicular bone, and the DSIL; reduced sensitivity for detecting small or subtle lesions; and increased susceptibility to image artifacts in the DDFT and the CLs of the DIP joint.

Among the 149 horses that underwent forefoot MRI in the current study, the most frequently observed findings included abnormalities of the DIP joint (92.6%), navicular bursa (61.7%), DDFT (58.4%), and navicular bone (57%). This pattern of lesion distribution is consistent with the most commonly affected structures reported in similar standing MRI studies of the same field strength, but the prevalence rates varied (Mitchell et al. 2006; Gutierrez-Nibeyro et al. 2012; Gutierrez-Nibeyro et al. 2020). These differences may reflect true variation in lesion occurrence across populations, but are also likely influenced by methodological differences between studies, such as the diagnostic thresholds used to define and categorize abnormal findings, as well as variation in case selection, demographic characteristics, and the duration and grade of lameness prior to imaging.

Abnormalities involving the DIP joint and navicular bursa primarily consisted of mild to moderate fluid distension, with or without synovial proliferation, and were rarely considered contributory to lameness. Previous studies have also noted that effusion of the DIP joint and navicular bursa is a common finding in both lame and sound feet, suggesting it most often represents a non-specific finding, typically secondary to other pathologies within the foot (Dyson et al. 2005; Mitchell et al. 2006; Dyson and Murray 2007; Sherlock et al. 2007; Gutierrez-Nibeyro et al. 2012; Gutierrez-Nibeyro et al. 2020). Conversely, DDFT pathology has long been recognized as a major contributor to distal forelimb lameness (Dyson et al. 2003; Mair and Kinns 2005; Dyson and Murray 2007), and the findings from the current study further reinforce its clinical importance, with DDFT tendinopathy considered the most clinically significant finding overall. In the navicular bone, increased signal intensity on fluid-sensitive sequences, consistent with bone marrow lesions (BMLs), was the most common finding and considered the second most significant pathological change after DDFT tendinopathy. This abnormality may reflect a variety of underlying pathologies, including acute inflammation, interstitial edema, hemorrhage, or early microtrabecular injury in recently lame horses, but may also represent chronic changes such as medullary fibrosis, osteonecrosis, or trabecular remodeling depending on duration and signal distribution (Busoni et al. 2005; Dyson et al. 2012). Severe or extensive BMLs have been more strongly associated with lameness than

lower-grade changes, which may be observed in sound limbs (Schramme and Segard-Weisse 2020). BMLs were also frequently identified in the distal phalanx, and less commonly in the middle phalanx. While these may represent the same underlying processes as those observed in the navicular bone, osseous fluid in the phalanges is most commonly attributed to bone bruising due to acute trauma, but may also represent chronic overload or secondary changes associated with osteoarthritis or soft tissue injury (Olive et al. 2009). MRI's ability to detect BMLs is a major advantage as it allows for the identification of pathological changes that are often not visible on radiographs (Werpy 2010; Garrett 2022). However, distinguishing simple contusion or physiological remodeling from degenerative disease, most often requires a recheck examination, as the former typically resolves with rest, while the latter tends to persist or progress over time (Werpy 2012). Abnormalities affecting other anatomical structures, including the CLs of the DIP joint, PIP joint, DSIL, CSL, DDAL, and ungual cartilages, were observed in less than 25% of the population individually. While some of these findings were occasionally deemed clinically significant, the majority were not classified as primary injuries, but were instead affected in conjunction with other lesions considered equally contributory to lameness.

A significant finding of this study, consistent with previous MRI investigations of equine foot pain, was the high prevalence of pathology involving multiple anatomical structures within the same foot (Dyson et al. 2005; Mitchell et al. 2006; Dyson and Murray 2007; Sherlock et al. 2008; Sampson et al. 2009; Gutierrez-Nibeyro et al. 2012; Gutierrez-Nibeyro et al. 2020). All examined limbs exhibited abnormalities in more than one structure, and in over half of the cases (51.4%), lesions in multiple structures were considered clinically significant, having not been possible to determine a primary injury, which underscores the complex and multifactorial nature of foot pain and the utility of MRI for a comprehensive evaluation.

The introduction of MRI in equine clinical practice substantially improved the understanding of what was once broadly termed as "navicular syndrome" and is now recognized as "podotrochlosis". By allowing the detailed visualization of both osseous and soft tissue structures within the foot, MRI revealed that foot pain frequently arises from multiple co-occurring pathologies, rather than a disease of the navicular bone alone (Dyson et al. 2011). While a definitive etiology remains inconclusive, the current understanding is that when the normal biomechanical forces within the foot become imbalanced, whether due to excessive or abrupt loading, working on hard or uneven surfaces, poor conformation, or inadequate shoeing, the repetitive abnormal mechanical stress placed on any of the structures within the podotrochlear apparatus over time exceeds the tissue's capacity to adapt and repair (Dyson et al. 2011). This initiates a cascade of compensatory changes in the interconnected structures, often beginning with an acute inflammatory response that, if not properly managed, may advance to chronic degenerative changes (Dyson et al. 2011).

The frequent co-existence of lesions within the podotrochlear apparatus, including the DDFT, navicular bone, navicular bursa, CSL, and DSIL, is well-documented and reflects the close anatomical and functional relationship between them (Dyson 2015). The DDFT functions to prevent hyperextension of the DIP joint as it passes over the flexor surface of the navicular bone, cushioned by the navicular bursa, and inserts on the palmar aspect of the distal phalanx to flex the joint (Dyson 2011). During weight-bearing, particularly in the propulsive phase of the stride, the tendon exerts compressive forces against the navicular bone, creating cumulative mechanical stress along the flexor surface (Dyson 2011; Osborn et al. 2021). The CSL and DSIL, comprising the navicular suspensory apparatus, further contribute with tensile forces to prevent the displacement of the navicular bone during movement (Bowker 2011).

In the current study, DDFT tendinopathies were identified in nearly half of the horses that underwent forefoot imaging (49%). Lesions commonly extended from the middle phalanx to the navicular bone or to the insertion on the distal phalanx, often changing in morphological appearance at different levels along the course of the tendon. Dorsal border fibrillation at the level of the CSL and the proximal recess of the navicular bursa was the most frequent lesion type overall, followed by (para)sagittal splits and tears at the level of the navicular bone. This distribution is consistent with previous MRI studies, and supports the idea that chronic friction and pressure at the tendon-bone interface may predispose to surface fraying and fiber disruption of the DDFT (Dyson and Murray 2007; Sampson et al. 2009; Gutierrez-Nibeyro et al. 2012; Gutierrez-Nibeyro et al. 2020). DDFT tendinopathy was frequently accompanied by pathology in the navicular bone (69.3%) and in the navicular bursa (83%). Occasionally, strands of low-signal tissue were observed between the dorsal margins of the DDFT and these adjacent structures, presumed to be adhesions. Such adhesions generally result from chronic inflammation, and may be suggestive of advanced podotrochlear disease (Dyson 2015).

Navicular bone pathology included bone marrow lesions, flexor cortex erosions, enlarged synovial invaginations, and distal border fragmentation. There was a significant association between bone marrow lesions dorsal and parallel to the palmar cortex of the navicular bone and DDFT tendinopathy. These have been linked to primary pathology of the DDFT in previous studies (Dyson et al. 2012), and likely reflects an inflammatory response or stress reaction to the injured or mechanically abnormal tendon as it passes over the navicular bone. Additionally, synovial proliferation and capsular thickening of the navicular bursa were significantly associated with both DDFT tendinopathy and bone marrow lesions of the navicular bone in the present study. These associations are consistent with the theory that chronic mechanical overload and injury to the DDFT and navicular bone trigger a secondary inflammatory response in the navicular bursa that further contributes to biomechanical dysfunction and chronic pain within the foot (Dyson et al. 2005; Dyson and Murray 2007; Sampson et al. 2009). Flexor cortex erosions represent full-thickness degeneration of the palmar fibrocartilage that

covers the flexor surface to the extent of involving the underlying subchondral bone, and indicate advanced podotrochlear disease, generally carrying a poor prognosis (Sherlock et al. 2008; Dyson et al. 2012; Gutierrez-Nibeyro et al. 2020). In the present study, these were located in the distal third of the bone around the sagittal midline, and were frequently associated with fluid signal and/or sclerosis. In one instance, there was communication between a flexor cortex defect and an OCLL in the mid-third of the bone. A significant association was found between these defects and DDFT tendinopathy. The distal third of the navicular bone has been highlighted to be the region subjected to higher compressive forces from the DDFT (Dyson 2011; Osborn et al. 2021), and other studies have also reported that fibrocartilage degeneration in this area is strongly linked to dorsal fibrillation of the DDFT (Blunden et al. 2006; Dyson and Murray 2007). Synovial invaginations are normal extensions of the DIP joint capsule that project into the distal aspect of the navicular bone (Dyson 2015), and abnormal changes on MRI may include an enlargement of the cross-sectional area, an increase in number, and deeper penetration into the bone (McParland et al. 2023). Studies have shown that while mild changes can be found in clinically sound horses, severe alterations can be associated with pathology of both the podotrochlear apparatus and the DIP joint (McParland et al. 2023). These changes likely reflect increased pressure or inflammation within the DIP joint, or potentially chronic stress at the distal aspect of the navicular bone where the DDFT exerts major compression and associated ligaments attach, such as the DSIL. In the current study, enlarged synovial invaginations were significantly associated with DDFT tendinopathy and DSIL pathology, and frequently accompanied flexor cortex erosions or adjacent trabecular fluid signal. In a comparative study between MRI and histological findings in the navicular bone, Dyson et al. (2012) suggested alterations in the synovial invaginations are often associated with changes in architecture of the adjacent spongiosa and degenerative pathological changes of the proximal aspect of the DSIL.

Pathological changes in the CSL and DSIL in this study were rare, with CSL desmopathy identified in only 7 limbs and DSIL desmopathy in 4 limbs. Both were most commonly seen as generalized thickening without evidence of fiber disruption. While pathology of the CSL and DSIL is relatively uncommon, the observed low prevalence of findings within the DSIL may also reflect the limitations of low-field MRI, where lower resolution and thicker slices can make accurate evaluation challenging due to the ligament's small size, oblique course, and heterogenous appearance (Werpy 2007; Murray et al. 2009). However, in another comparative study of MRI and histological findings of the DSIL, Dyson et al. (2010) found that osseous abnormalities at the entheses are commonly associated with DSIL body pathology, and therefore suggested that these features may serve as useful indicators of DSIL injury when the body of the ligament cannot be evaluated on low-field images. These included the presence of cyst-like lesions and fragmentation of the distal border of the navicular bone, and increased

STIR signal intensity and enthesous new bone at the insertion on the distal phalanx. In the present study, several findings were consistent with this pattern, indicating that DSIL body pathology may have been underdiagnosed. These included changes near the origin on the navicular bone such as focal hyperintensity in the distal border, often extending diffusely into the adjacent trabecular bone, enlarged synovial invaginations, and distal border fragmentation. At the insertion on the distal phalanx, focal areas of increased fluid signal and/or sclerosis were common, sometimes associated with focal bone resorption, and two cases of partial avulsion injury were recorded. Statistical analysis also revealed a significant association between increased diffuse fluid signal in the navicular bone and DSIL abnormalities, which primarily consisted of enthesopathic changes at the insertion on the distal phalanx. This further supports the hypothesis that DSIL pathology is not an isolated occurrence, but rather contributes to, or results from, broader pathological processes affecting the podotrochlear apparatus and associated structures. Moreover, as previously discussed, the CSL and DSIL function together to stabilize the navicular bone within the foot (Bowker 2011), and their pathological changes seem to share the same biomechanical stress pathway. Dyson and Murray (2007) observed that an increased fluid signal at the origin of the DSIL often occurred alongside focal changes at the insertion of the CSL, frequently connected by a linear band of increased signal intensity through the spongiosa. In this population, however, concurrent pathology of the CSL and DSIL was not observed, and fluid signal at the origin of the DSIL was not accompanied by similar changes in the proximal aspect of the bone. Generalized thickening of both the CSL and DSIL has been associated with concurrent navicular bursitis secondary to pathology of the DDFT or the navicular bone (Schramme and Segard-Weisse 2020), and the same pattern was observed in the current study, with nearly all cases of desmopathy presenting concurrent signs of navicular bursitis, DDFT tendinopathy, and diffuse trabecular fluid signal of the navicular bone.

In addition to the podotrochlear apparatus, there are several other associated structures within the foot that play a part in its biomechanical function. The DIP joint is essential for absorbing concussive forces during movement, making it highly susceptible to injury and degenerative changes. Because articular cartilage has limited ability to heal, early diagnosis is essential to prevent irreversible damage (Van Weeren 2016). MRI offers a significant advantage in detecting early degenerative changes within the DIP joint that may not be apparent on conventional imaging. Although cartilage assessment using standing low-field MRI has advanced significantly since earlier studies, identifying small defects on the curved articular surfaces remains challenging, especially under weight-bearing conditions where joint space is reduced, making it difficult to visualize and assess the integrity of individual articular surfaces (Olive 2010; Van Zadelhoff et al. 2020; Baker et al. 2023). Observed degenerative changes consistent with osteoarthritis included articular cartilage damage, subchondral bone injuries, and osteophyte formation. Contrary to simple joint effusion, these changes are often

associated with chronic pain and poor performance (Baccarin et al. 2022). In the current study, standing low-field MRI detected only three small, full-thickness focal articular cartilage defects involving the subchondral bone along the sagittal midline of the distal phalanx, and three OCLLs also affecting the central aspect of the subchondral bone, either communicating with a defect in the articular surface, or showing abnormal signal in the overlying cartilage. Articular cartilage damage without involvement of the subchondral bone was not observed in this study, with the exception of generalized thinning and resulting joint space narrowing. It is possible that the true prevalence of cartilage lesions was underestimated in this population, due to the technical limitations of the MRI system used. Moreover, degenerative changes of the DIP joint rarely occurred as isolated findings. In the majority of cases, they were accompanied by concurrent pathology within the podotrochlear apparatus or collateral ligament abnormalities, and in a smaller proportion, by bone marrow changes affecting the adjacent phalanges. This supports the concept that DIP joint disease often develops as part of a broader pattern of biomechanical dysfunction within the foot, rather than as an isolated or independent process. Notably, similar mild osteoarthritic changes of the PIP joint were observed, often in conjunction with DIP joint osteoarthritis, but were rarely considered clinically significant in isolation. In contrast, effusion of the PIP joint was a very rare finding. These findings align with observations made by Dyson and Murray (2007).

The CLs of the DIP joint provide medial and lateral support to the joint (Van Weeren 2016). Given their anatomical function, they are exposed to substantial tensile forces, particularly during propulsion and uneven loading, making them susceptible to strain, degeneration, or traumatic injury (Dyson and Murray 2007; Dyson 2011). In the present study, abnormalities of the DIP joint collateral ligaments were not among the most common findings but were still clinically relevant, with approximately a quarter of examined limbs presenting changes consistent with desmopathy and/or enthesopathy. MRI findings included generalized thickening, increased signal intensity, and occasional fiber disruption, changes consistent with chronic degeneration or partial tearing. Degenerative signal changes, characterized by a diffuse mottled pattern on T2-weighted sequences, were a frequent observation, suggestive of chronic remodeling processes rather than acute injuries. As reported in previous studies, mild to moderate hyperintense signal in the DIP collateral ligaments must be interpreted cautiously, given the high susceptibility of these structures to image artifacts, particularly when using low-field MRI systems (Gutierrez-Nibeyro et al. 2009). However, in this population, the presence of concurrent pathology in other structures, most frequently DIP joint effusion and/or osteoarthritis and abnormal osseous changes at the insertion on the distal phalanx, reinforced the clinical relevance of these abnormalities.

Regarding abnormalities of the phalanges, as previously noted, BMLs were the most common abnormality identified in the distal phalanx and the only finding in the middle phalanx.

In the distal phalanx, fluid signal was most frequently located within the palmar processes and was occasionally accompanied by sclerosis and cortical irregularity. These findings are thought to reflect chronic bone bruising and remodeling in response to repetitive stress or trauma-related contusion, or may be associated with abnormalities at the entheses of the collateral ligaments (Schramme and Segard-Weisse 2020). Moreover, incomplete non-articular fractures were identified at the base of the ungual cartilages, often extending into the palmar processes and fossae of the collateral ligaments. These fractures were frequently observed in horses with sclerosis of the palmar processes and severe ossification of the collateral cartilages. While sidebone formation may be a normal anatomical variation as the horses ages, extensive mineralization of these structures significantly impairs their ability to absorb and dissipate concussive forces, altering the foot's biomechanics and increasing susceptibility to fractures, particularly at the bone-cartilage interface (Selberg and Werpy 2011). In the middle phalanx, although the dorsodistal aspect has been described as a common site for bone bruises (Olive et al. 2009), this pattern was observed in only one limb in the present study. Instead, lesions were more frequently localized to the dorsoproximal aspect of the bone, even though they were rare. However, Olive et al. (2009) also noted that hyperintense STIR signal not accompanied by corresponding low signal intensity on T1-weighted images, particularly at the periphery of the image, such as the proximal aspect of the middle phalanx, may represent an artifact caused by inadequate fat suppression in standing low-field MRI. As such, care must be taken not to misinterpret these patterns as true BMLs. Notably, BMLs were frequently seen clustered in one side of the foot, often involving both phalanges and the navicular bone, suggesting uneven loading or further reinforcing the theory of traumatic origin.

The DDAL forms a supportive band that stabilizes the DIP joint in its palmar aspect and maintains DDFT alignment during movement as it passes over the pastern and navicular region (Fails 2020). Pathological changes of the DDAL were uncommon, but showed close association with pathology of the podotrochlear apparatus. In this study, DDAL desmopathy was characterized by generalized moderate thickening, occasionally accompanied by enthesophyte formation at the origin and presumed adhesion formation near the mid-pastern. These findings align with a previous report by Cohen et al. (2008), where DDAL desmitis was characterized by enlargement ranging from 2.5 to 10 times the normal size, loss of normal homogenous low-signal appearance, and adhesions between the DDAL and the DDFT were common. The study demonstrated that primary DDAL desmitis may occur either alone or in association with lesions of the DDFT, even in the absence of radiographic abnormalities, and may represent a significant cause of lameness (Cohen et al. 2008). In the current study, DDAL abnormalities were not identified in isolation, but rather seen alongside concurrent chronic navicular bursitis, DDFT tendinopathy extending from the mid-pastern to the navicular bone, and DIP joint osteoarthritis. This pattern suggests that DDAL pathology may either contribute

to or result from ongoing biomechanical dysfunction and instability within the foot, and should be considered when interpreting MRI findings in horses with chronic foot pain.

4.3. Distribution and Association with Demographic Factors

The last aim of this study was to investigate the distribution and potential associations between demographic characteristics of the population and the presence of pathology on MRI within each of the anatomical structures of the foot. Understanding the factors that may predispose horses to specific musculoskeletal injuries is valuable information for developing effective prevention and management strategies. The factors analyzed included age, sex, breed, and discipline, based on their frequent mention in the literature as potential risk factors for musculoskeletal pathology. Meaningful statistical analysis regarding associations was limited for some structures (e.g., CSL, Middle Phalanx) due to their low overall prevalence, and for others (e.g., DIP joint) due to very high prevalence, preventing meaningful comparisons between groups. While only a few statistically significant associations were identified, some notable non-significant trends were observed. However, these findings should be interpreted cautiously given the retrospective nature of the study and the possibility of uneven representation across demographic groups. Furthermore, although associations may highlight predispositions, they do not establish causality.

4.3.1. Age

The aging process in horses is accompanied by a range of physiological changes within the foot and overall musculoskeletal system that transition from periods of growth, adaptation, and maturation in younger animals to the accumulation of wear and tear and degenerative changes over time (Van Weeren et al. 2000; Van Weeren and Back 2016). Ageing impacts bone density and microarchitecture, articular cartilage composition and thickness, and the flexibility and regenerative capacity of tendons and ligaments (Weeren 2024; Smith et al. 2024; Whitton 2024).

In horses under 5 years, distal phalanx pathology approached significance ($p=0.051$), with a notably higher proportion of bone marrow lesions and fractures. Other common abnormalities included navicular bone marrow lesions, focal dorsal border DDFT lesions at and just proximal to the navicular bone, and effusion and synovitis of the DIP joint and navicular bursa, generally in the absence of chronic changes. These findings may be indicative of adaptive bone remodeling and acute inflammatory processes occurring in response to early mechanical stress or trauma, potentially associated with introduction to exercise, rapid increases in training intensity, or incomplete skeletal maturity (Whitton 2024). Interestingly, flexor surface erosions, typically linked to navicular disease in mature horses (Dyson et al. 2011), were proportionally more common in this youngest group. This may indicate early onset

degenerative podotrochlosis, potentially due to genetic predisposition, poor hoof conformation, or excessive training at an early age (Dyson et al. 2011).

In horses aged 6-10 years, pathology shifted toward the development of more chronic changes. This group had the highest prevalence of navicular bone marrow lesions, increased signs of degeneration (flexor surface erosions, distal border fragmentation), and new changes like sclerosis and cortical irregularity of the palmar processes and solar margin defects. There was also a marked increase in chronic bursal changes and osteoarthritis of the DIP and PIP joints. DDFT lesions remained common, but more severe patterns were identified, including (para)sagittal splits and tears extending from the mid-pastern to the navicular bone. This group also showed the highest prevalence of DSIL enthesopathy, and the emergence of CSL and DDAL pathology. Given that horses in this age range are typically in full training or competitive work, these findings likely reflect active and cumulative biomechanical stress imposed on the foot during exercise (Van Weeren 2024; Smith et al. 2024; Whitton 2024). These results highlight a critical period of mechanical overload, during which subclinical changes may progress to clinically significant degenerative disease if not properly managed.

The 11-15 years age group had the highest overall prevalence of pathological changes, showing the highest proportion of navicular bone, CLs of the DIP joint, CSL, and DDAL lesions. The nature of the findings was similar to that of the 6-10 years age group, but changes were progressively more chronic and extensive. Chronic navicular bursitis and DDFT tendinopathy peaked in this age group, with DDFT abnormalities featuring core lesions and affecting more regions within the tendon. Horses in this age group may start to experience age-related degeneration of tissues and reduced healing capacity (Van Weeren 2024; Smith et al. 2024; Whitton 2024), increasing the susceptibility to chronic lameness and reduced performance. In general, the MRI findings in this age group suggest a phase of structural damage, where chronic degenerative lesions predominate but remain active.

Horses aged 16-20 years had a shift in the primary sites of pathology from the podotrochlear apparatus to the interphalangeal joints. There was a marked decline in navicular bone pathology and bone marrow lesions in general, with some lesions seen in younger groups now reduced or even absent, including flexor surface erosions, enlarged synovial invaginations, distal border fragmentation, palmar process fractures, navicular bursitis, CSL desmopathy, and enthesopathic changes in general. Conversely, osteoarthritis of the DIP and especially the PIP joint peaked ($p<0.001$). While it is expected to observe more osteoarthritic changes in senior horses (Van Weeren and Back 2016), the reduced frequency or absence of some lesions is surprising. This pattern may be due to a combination of reduced mechanical demand in older horses, and the retirement of severely affected horses from the athletic population, making them less likely to undergo MRI examinations.

4.3.2. Sex

While there haven't been any investigations solely focused on the influence of sex on musculoskeletal injuries in horses, it is frequently included as a potential demographic risk factor in studies for various orthopedic conditions (Parkes et al. 2013; Hitchens et al. 2019; Paris et al. 2021), although findings in the literature are not always consistent and may vary depending on the specific injury and horse population studied.

In the current study, a statistically significant association was found between sex and the presence of distal phalanx pathology (p=0.031), in which geldings exhibited a significantly higher proportion of affected cases compared to mares, with lesions including bone marrow lesions, fractures, and solar margin defects. While there are no direct comparisons in the literature linking sex to distal phalanx pathology specifically, Fürst et al. (2008) explored sex differences in bone density and microarchitecture in the radius and tibia and found no significant differences between males and females. Moreover, the study suggested that sex hormones in horses are less likely to play a role as it has been seen in humans, since unlike women after menopause, aged mares don't experience a sharp drop in estrogen, so a significantly different bone microstructure than older geldings or stallions isn't expected (Fürst et al. 2008). In contrast, another study indicated that entire males and geldings had lower bone turnover markers compared to females, which could potentially increase their susceptibility to musculoskeletal injury (Ayodele et al. 2025). Additionally, cortisol levels, a stress marker, were highest in entire males, followed by geldings, and then females, suggesting a possible link between stress and musculoskeletal injury risk in males (Ayodele et al. 2025). However, Ayodele et al. (2025) also noted that age, training history, and origin may confound the observed association between sex and injury susceptibility. For the remaining evaluated structures in the present study, no statistically significant associations with sex were detected. This lack of association aligns with another study that did not find associations between gender and foot pain (Parkes et al. 2013). However, studies have reported males, particularly geldings, to be at higher risk of developing podotrochlosis (Ackerman et al. 1977). Contrary to these findings, while differences were non-significant in the present study, mares consistently exhibited a higher proportion of affected cases across the structures of the podotrochlear apparatus.

In summary, sex was significantly associated with distal phalanx pathology, with geldings more frequently affected. The underlying reasons remain speculative and may involve a multifactorial interplay of physiological, conformational, behavioral, or discipline-related variables. The lack of significant associations for most other foot structures suggests that, in this study population, sex does not appear to be a major independent risk factor for forelimb foot pathology. However, further research is needed to investigate these potential sex-based

differences in distal phalanx characteristics, biomechanical loading, and training regimens to better understand the reasons for this observed association.

4.3.3. Breed

Breed is often considered a potential intrinsic risk factor for certain musculoskeletal conditions in horses, with breed-predispositions believed to be linked to genetic factors, conformational traits, or the specific demands placed on breeds commonly used in certain disciplines (Parkes et al. 2013). In the current study, however, statistical analysis revealed no significant associations between breed and the presence of pathology in any of the evaluated anatomical structures within the foot, although some numerical differences in lesion prevalence were observed across breeds that may warrant further investigation.

Based on the proportion of affected cases across all structures, Quarter Horses exhibited the highest overall prevalence, followed by Irish Sport Horses and Hanoverians, while Holsteiners and Thoroughbreds had the lowest. Quarter Horses had particularly high rates of podotrochlear apparatus lesions, including the highest prevalence of DDFT tendinopathy, synovial proliferation and/or capsular thickening of the navicular bursa, and DSIL enthesopathy. Although these findings did not reach statistical significance, they align with previous reports identifying podotrochlear syndrome as a common cause of forelimb lameness in Quarter Horses (Ackerman et al. 1977; Sampson et al. 2009; Dyson et al. 2011). The breed's predisposition is often attributed to its characteristic conformation, a relatively large body mass supported by small upright feet, which may predispose to abnormal load distribution and increased mechanical stress on these structures (Dyson et al. 2011). Similarly, the characteristically tall, narrow, and often asymmetrical feet of Dutch Warmbloods, as well as the commonly flat feet with low, collapsed heels seen in Thoroughbreds, are believed to contribute to these breeds' predisposition to developing podotrochlear syndrome (Ducro et al. 2009; Ducro et al. 2009a; Dyson et al. 2011). In this study, however, both breeds had relatively fewer cases of podotrochlear abnormalities, with Dutch Warmbloods exhibiting the lowest proportion of DDFT and navicular bone pathology among all breeds. Instead, bone marrow lesions within the distal phalanx and osteoarthritis of the PIP and DIP joints were especially common in this breed. In contrast, notably higher rates of pathology within the podotrochlear apparatus were observed in Canadian Warmbloods, Irish Sport Horses, Hanoverians, and Oldenburgs, with the latter showing the highest overall rate of navicular bone pathology.

This discrepancy between the observed findings and established breed predispositions for podotrochlosis could be due to potential limitations related to sample size within breed categories or reflect the specific characteristics of this study population which may not be fully representative of the entire breed populations, potential referral biases, or differences in the specific disciplines and intensity of work performed by these horses compared to populations

studied previously. Further research with larger and more homogenous breed cohorts, and controlled for discipline is needed to clarify the role of breed in equine foot pathology.

4.3.4. Discipline

Discipline has been frequently investigated as a potential extrinsic risk factor influencing the type and distribution of musculoskeletal injury (Ross and Kaneene 1996; Dyson 2002; Mitchell et al. 2006; Murray et al. 2006b; Murray et al. 2010; Swor et al. 2019). Different disciplines place distinct biomechanical stresses on specific anatomical structures due to characteristic movements, surface interactions, and workload patterns, potentially predisposing horses to discipline-specific injuries (Murray et al. 2006b). In the current study, no statistically significant associations were identified between discipline and the presence of pathology in any foot structure. However, consistent numerical trends were observed across some disciplines that align with known risk patterns.

Western performance horses exhibited the highest overall prevalence of pathology across disciplines, and the highest podotrochlear apparatus involvement, including the highest relative prevalence of abnormal findings in the DDFT, navicular bursa, DSIL, CSL, and distal and middle phalanges. All horses involved in western disciplines in this study were Quarter Horses. While this breed's conformation has been associated with susceptibility to podotrochlear syndrome (Dyson et al. 2011), the specific demands of Western performance disciplines have also been linked to lameness arising from the distal forelimb (Johnson et al. 2021). Movements such as sliding stops and sharp turns place substantial axial compression, hyperextension, and torsional forces on the DIP joint and palmar foot structures, which serve as important stabilizers for the joint (Carpenter et al. 2020). Therefore, the observed high prevalence of podotrochlear and distal phalangeal pathology in Quarter Horses participating in Western disciplines in this study, while not statistically significant for discipline as an independent factor, supports the influence of potential breed predisposition and the biomechanical demands of Western disciplines on these structures. Notably, collateral desmopathy of the DIP joint was relatively rare in Western horses.

Eventing horses had the second-highest mean pathology rate, and the highest navicular bone involvement and DIP and PIP joint osteoarthritis. They showed a broad distribution of abnormalities, reflecting the diverse demands of their sport, which includes galloping, jumping, and dressage. Traumatic joint disease, especially in the forelimbs, is common in eventers due to repeated high-impact loading associated with jumping, speed and varied terrain (Bathe 2011). According to Murray et al. (2006b), the navicular bone and associated ligaments are frequently injured across all performance levels in eventers, as well as the suspensory ligament and superficial digital flexor tendon, but these more proximal structures were not evaluated in the present study.

Show Jumping and Hunting disciplines represented the largest proportion of the study population. Both disciplines involve frequent jumping and landing, but with differing biomechanical demands. Show Jumping requires abrupt changes in speed and direction and often higher fences, while Hunting prioritizes rhythm, smoothness of gait, and consistent pacing over obstacles (Carpenter et al. 2020). Forelimb foot pain is the most common cause of lameness in both sports, most likely associated with impact and repeated hyperextension of the DIP joint on landing and respective strain on associated structures (Boswell et al. 2011). The mean pathology rates were comparable for both disciplines in this study, falling in the mid-range of the overall discipline spectrum. However, show jumpers exhibited higher involvement of the podotrochlear apparatus, with particularly high rates of navicular bursa pathology, while hunters showed higher relative prevalence of joint, collateral ligament, and phalangeal abnormalities. Damage to the DDFT within the hoof capsule has been highlighted as the most common injury in horses participating in jumping activities (Murray et al. 2006b; Boswell et al. 2011). In the current study, over half of jumpers and hunters exhibited DDFT lesions, but the observed prevalence was similar to dressage horses, and lower than eventers and western performance horses.

Dressage horses demonstrated a slightly lower than average mean prevalence of foot pathology among sport disciplines. Dressage horses are classically described as being predisposed to suspensory ligament desmitis, especially of the hindlimbs, and thoracolumbar soreness due to the discipline's emphasis on engagement, collection, and repetitive axial loading (Kold and Dyson 2011), which might explain the observed lower prevalence of forelimb foot pathology in this group in the current study. However, as Mitchell et al. (2006) and Murray et al. (2010) highlighted, foot-related issues are still common in dressage horses, and more frequently in nonelite horses, possibly due to the relatively higher loading on the forelimbs in this group, compared to higher-level horses that are more trained to transfer the weight to the hindlimbs. In this study, the most common injuries observed in dressage horses included DIP joint synovitis, navicular bone flexor surface erosions, DDFT tendinopathy, and fractures of the palmar processes.

Horses used for pleasure or recreational riding often transition to this role after retirement of careers in various competitive disciplines and are generally subjected to lower-intensity and less frequent workloads. In this study, this group included horses 11 to 20 years of age and their primary activities were unknown. While the sample size was small, they showed the lowest mean prevalence of pathology, exhibiting navicular bursa inflammation, DIP joint effusion, and PIP joint osteoarthritis as the most common findings.

5. Conclusion

This retrospective study highlights the forelimb foot as the primary region of interest for the clinical application of standing low-field MRI as a diagnostic tool in MPES, which serves a population of predominantly sport horses in Ontario, Canada. Analyzing a large caseload over a defined three-year period, this study reflects real-world clinical scenarios from the exclusive provider of standing MRI services in the province. The results of this study provide valuable insights into the spectrum of MRI findings in the forelimb foot, corroborating existing literature on the prevalence and co-occurrence patterns of injuries in this anatomical region, while introducing insights into potential demographic associations within this specific population.

Among low-field MRI-detectable abnormalities, DDFT tendinopathy and navicular bone marrow lesions were the most prevalent clinically significant findings. While effusion with or without synovial proliferation of the DIP joint and navicular bursa were the most frequent findings overall, these were often interpreted as secondary or incidental. Occurrence of abnormal changes in multiple structures was ubiquitous, with multiple lesions considered equally contributory to the presenting lameness in approximately half of the population. The significant associations observed between DDFT tendinopathy and navicular bone and bursa pathology further support the idea that imbalanced biomechanical forces acting on multiple interconnected structures may result in podotrochlosis. The observed associations between pathology in specific anatomical structures and demographic factors included distal phalanx pathology in geldings and PIP joint pathology in older horses (16-20 years). While most demographic variables were not associated with specific pathologies, some notable trends emerged, including Quarter Horses involved in western performance disciplines exhibiting the highest relative prevalence of foot MRI abnormalities.

These findings have meaningful clinical implications for the diagnosis and management of forelimb foot lameness. Knowledge of the most frequent lesions and common co-occurrence patterns can assist clinicians in targeting their diagnostic efforts more effectively. Moreover, the high prevalence of cases presenting concurrent osseous and soft tissue pathology supports the clinical utility of advanced imaging modalities like MRI for a comprehensive evaluation of the foot, to ensure the identification of all contributing lesions. Furthermore, awareness of age, breed, sex, and discipline-related trends may support earlier recognition of at-risk individuals and the implementation of specific preventative or management strategies.

To contextualize these findings and ensure accurate interpretation, limitations of this study must be acknowledged. The retrospective nature of this study and reliance on existing clinical MRI reports may introduce subjective bias due to observer interpretation and potential variability in reporting styles and the level of detail provided, as inter-observer reliability between radiologists was not formally assessed. Furthermore, the absence of consistently detailed clinical information, such as lameness grading, duration of lameness, and

comprehensive response to diagnostic analgesia or treatment, limited the ability to establish definitive correlations between specific imaging findings and clinical severity or long-term outcomes. Moreover, clinical relevance was documented based on the MRI report's description of the most relevant findings per interpretation of the radiologist. Selection bias may have also occurred, as cases referred for MRI at a single practice may not represent the broader population of lame horses, and may not be generalizable to other geographic areas or non-sport horse populations. Lastly, the inherent lower resolution of standing low-field MRI compared to high-field MRI may have resulted in an underestimation of subtle lesions, particularly those affecting articular cartilage or small ligaments like the DSIL.

In conclusion, this study contributes to the current understanding of MRI assessment of equine forelimb foot lameness, highlighting the importance of advanced imaging such as MRI for accurate diagnosis. Despite acknowledged limitations, this study's detailed characterization of lesion types, their prevalence, common co-occurrence patterns, and potential risk factors within a relevant sport horse population underscores the complexity of foot pain, thereby advocating for a holistic diagnostic approach that considers the foot as a functional unit. Ultimately, the insights gained from this study can assist clinicians in making more informed diagnostic and therapeutic decisions, and improve the overall well-being and performance outcomes for horses affected by forelimb foot lameness.

IV. REFERENCES

Ackerman N, Johnson JH, Dorn CR. Navicular disease in the horse: risk factors, radiographic changes, and response to therapy. *J Am Vet Med Assoc*. 1977;170(2):183-187.

Ayodele BA, Pagel CN, Mackie EJ, Armour F, Yamada S, Zahra P, Courtman N, Whitton RC, Hitchens PL. Differences in bone turnover markers and injury risks between local and international horses: A Victorian Spring Racing Carnival study. *Equine Vet J*. 2025;57(2):333-346. doi:10.1111/evj.14098.

Baccarin RYA, Seidel SRT, Michelacci YM, Tokawa PKA, Oliveira TM. Osteoarthritis: a common disease that should be avoided in the athletic horse's life. *Anim Front*. 2022;12(3):25-36. doi:10.1093/af/vfac026.

Baker ME, Kershaw LE, Carstens A, Daniel CR, Brown H, Roberts S, Taylor SE. T2 mapping of cartilage in the equine distal interphalangeal joint with corresponding histology using 0.27 T and 3.0 T magnetic resonance imaging. *Equine Vet J*. 2023;55(5):843-852. doi:10.1111/evj.13900.

Barrett MF, Frisbie DD, King MR, Werpy NM, Kawcak CE. A review of how magnetic resonance imaging can aid in case management of common pathological conditions of the equine foot. *Equine Vet Educ*. 2017;29(12):683-693. doi:10.1111/eve.12542.

Barrett MF, Goorchenko GE, Frisbie DD. Comparison of Ultrasound and Magnetic Resonance Imaging for Identifying Soft Tissue Abnormalities in the Palmar Aspect of the Equine Digit. *Animals (Basel)*. 2023;13(14):2328. doi:10.3390/ani13142328.

Bathe AP. Lameness in the Three Day Event Horse. In: Ross MW, Dyson SJ, editors. *Diagnosis and Management of Lameness in the Horse*. St. Louis: Elsevier; 2011. p. 1123-1137.

Baxter GM. Assessment of the Lame Horse. In: Baxter GM, editor. *Manual of Equine Lameness*. 2nd ed. Hoboken: Wiley; 2022.

Baxter GM, Stashak TS, Keegan KG. Examination for Lameness. In: Baxter GM, editor. *Adams and Stashak's Lameness in Horses*. 7th ed. Hoboken: Wiley; 2020. p. 67-188.

Berner D, Mader D, Groß C, Gerlach K. Effect of Scan Plane and Arthrography on Visibility and Interobserver Agreement of the Equine Distal Sesamoidean Impar Ligament on Magnetic Resonance Images. *J Equine Vet Sci*. 2020;94:103227. doi:10.1016/j.jevs.2020.103227

Blunden A, Dyson S, Murray R, Schramme M. Histopathology in horses with chronic palmar foot pain and age-matched controls. Part 2: The deep digital flexor tendon. *Equine Vet J*. 2006;38(1):23-27. doi:10.2746/042516406775374342

Bolas N. Basic MRI principles. In: Murray RC, editor. *Equine MRI*. 1st ed. Hoboken: Wiley; 2010. p. 1-37.

Bolen G, Audigié F, Spriet M, Vandenberghe F, Busoni V. Qualitative Comparison of 0.27T, 1.5T, and 3T Magnetic Resonance Images of the Normal Equine Foot. *J Equine Vet Sci*. 2010;30(1):9-20. doi:10.1016/j.jevs.2009.11.002

Boorman S, Hofmeister EH, Ross MW, Ralston S, Bell G, Mackie S, Ortved K. Influence of osteochondrosis on the longevity and racing performance of standardbred trotters and pacers. *Vet Surg*. 2021;50(3):507-516. doi:10.1111/vsu.13568

Boswell RP, Mitchell RD, Ober TR, Benoit PH, Miller CB, Dyson SJ. Lameness in the Show Hunter and Show Jumper. In: Ross MW, Dyson SJ, editors. *Diagnosis and Management of Lameness in the Horse*. St. Louis: Elsevier; 2011. p. 1096-1112.

Bowker RM. Functional Anatomy of the Palmar Aspect of the Foot. In: Ross MW, Dyson SJ, editors. *Diagnosis and Management of Lameness in the Horse*. St. Louis: Elsevier; 2011. p. 320-323.

Busoni V, Heimann M, Trenteseaux J, Snaps F, Dondelinger RF. Magnetic resonance imaging findings in the equine deep digital flexor tendon and distal sesamoid bone in advanced navicular disease—an ex vivo study. *Vet Radiol Ultrasound*. 2005;46(4):279-286. doi:10.1111/j.1740-8261.2005.00051.x

Byrne CA, Marshall JF, Voute LC. Clinical magnetic resonance image quality of the equine foot is significantly influenced by acquisition system. *Equine Vet J*. 2021;53(3):469-480. doi:10.1111/evj.13330

Carpenter R, Johnston K, Nickels FA, Goodman NL, Overly LR, Dabareiner RM, Maher O, Holbrook TC, Johnson SA, Frisbie DD, et al. Occupational-related lameness conditions. In: Baxter GM, editor. *Adams and Stashak's Lameness in Horses*. 1st ed. Hoboken: Wiley; 2020. p. 949-1031.

Fails AD. Functional anatomy of the equine musculoskeletal system. In: Baxter GM, editor. *Adams and Stashak's Lameness in Horses*. 1st ed. Hoboken: Wiley; 2020. p. 1-65.

Fürst A, Meier D, Michel S, Schmidlin A, Held L, Laib A. Effect of age on bone mineral density and microarchitecture in the radius and tibia of horses: an Xtreme computed tomographic study. *BMC Vet Res*. 2008;4(1):3. doi:10.1186/1746-6148-4-3

Gallastegui A. Imaging the equine foot. *Vet Clin North Am Equine Pract*. 2021;37(3):563-579. doi:10.1016/j.cveq.2021.07.003

Garrett KS. How to understand differences between high- and low-field standing magnetic resonance imaging. In: Proceedings of the 61st Annual Convention of the American Association of Equine Practitioners; 2015 Dec; Las Vegas, NV. Vol. 61. Lexington (KY): AAEP; 2015. p. 416–417.

Garrett KS. When radiography and ultrasonography are not enough: the use of computed tomography and magnetic resonance imaging for equine lameness cases. *J Am Vet Med Assoc*. 2022;260(10):1113–1123. doi:10.2460/javma.22.03.0136

Gerard MP. Anatomy and physiology of the equine foot. *Vet Clin North Am Equine Pract*. 2021;37(3):529–548. doi:10.1016/j.cveq.2021.07.002

Giorio ME. Referral of the lameness case for standing magnetic resonance imaging. *UK-Vet Equine*. 2018;2(1):22–26. doi:10.12968/ukve.2018.2.1.22

Gold SJ. How to interpret a distal limb magnetic resonance imaging report. In: Proceedings of the 61st Annual Convention of the American Association of Equine Practitioners; 2015 Dec; Las Vegas, NV. Vol. 61. Lexington (KY): AAEP; 2015. p. 360–369.

Gutierrez-Nibeyro S, Werpy N, White NA II. Standing low-field magnetic resonance imaging in horses with chronic foot pain. *Aust Vet J*. 2012;90(3):75–83. doi:10.1111/j.1751-0813.2011.00875.x

Gutierrez-Nibeyro SD, Werpy NM, Gold SJ, Olguin S, Schaeffer DJ. Standing MRI lesions of the distal interphalangeal joint and podotrochlear apparatus occur with a high frequency in Warmblood horses. *Vet Radiol Ultrasound*. 2020;61(3):336–345. doi:10.1111/vru.12855

Gutierrez-Nibeyro SD, White NA, Werpy NM, Tyrrell L, Allen KA, Sullins KE, Mitchell RD. Magnetic resonance imaging findings of desmopathy of the collateral ligaments of the equine distal interphalangeal joint. *Vet Radiol Ultrasound*. 2009;50(1):21–31. doi:10.1111/j.1740-8261.2008.01485.x

Hitchens PL, Morrice-West AV, Stevenson MA, Whitton RC. Meta-analysis of risk factors for racehorse catastrophic musculoskeletal injury in flat racing. *Vet J*. 2019;245:29–40. doi:10.1016/j.tvjl.2018.11.014

Horne CR, Tufts S. Advances in imaging techniques to guide therapies and monitor response to the treatment of musculoskeletal injuries. *Vet Clin North Am Equine Pract*. 2023;39(3):489–501. doi:10.1016/j.cveq.2023.06.001

Jaskólska M, Adamiak Z, Zhalniarovich Y, Holak P, Przyborowska P. Magnetic resonance protocols in equine lameness examination, used sequences, and interpretation. *Pol J Vet Sci*. 2013;16(4):803–811. doi:10.2478/pjvs-2013-0115

Johnson SA, Donnell JR, Donnell AD, Frisbie DD. Retrospective analysis of lameness localisation in Western Performance Horses: a ten-year review. *Equine Vet J*. 2021;53(6):1150–1158. doi:10.1111/evj.13397

Johnston C, Back W. Hoof-ground interaction: when biomechanical stimuli challenge the tissues of the distal limb. *Equine Vet J*. 2006;38(7):634–641. doi:10.2746/042516406X158341

Kold SE, Dyson SJ. Lameness in the dressage horse. In: Ross MW, Dyson SJ, editors. *Diagnosis and Management of Lameness in the Horse*. St. Louis: Elsevier; 2011. p. 1112–1123.

Labens R, Schramme MC, Murray RC, Bolas N. Standing low-field MRI of the equine proximal metacarpal/metatarsal region is considered useful for diagnosing primary bone pathology and makes a positive contribution to case management: a prospective survey study. *Vet Radiol Ultrasound*. 2020;61(2):197–205. doi:10.1111/vru.12824

Lepeule J, Seegers H, Rondeau V, Robert C, Denoix JM, Bareille N. Risk factors for the presence and extent of developmental orthopaedic disease in the limbs of young horses: insights from a count model. *Prev Vet Med*. 2011;101(1–2):96–106. doi:10.1016/j.prevetmed.2011.05.009

Mair TS, Kinns J. Deep digital flexor tendonitis in the equine foot diagnosed by low-field magnetic resonance imaging in the standing patient: 18 cases. *Vet Radiol Ultrasound*. 2005;46(6):458–466. doi:10.1111/j.1740-8261.2005.00084.x

Mair TS, Kinns J, Jones RD, Bolas NM. Magnetic resonance imaging of the distal limb of the standing horse. *Equine Vet Educ*. 2005;17(2):74–78. doi:10.1111/j.2042-3292.2005.tb00340.x

Mata F, Franca I, Araújo J, Paixão G, Lesniak K, Cerqueira JL. Investigating associations between horse hoof conformation and presence of lameness. *Animals*. 2024;14(18):2697. doi:10.3390/ani14182697

McIlwraith CW, Kawcak C, Baxter GM, Goodrich LR, Valberg SJ. Principles of musculoskeletal disease. In: Baxter GM, editor. *Adams and Stashak's Lameness in Horses*. 1st ed. Hoboken: Wiley; 2020. p. 801–874.

McKnight AL. Introduction to equine MRI. *J Equine Vet Sci*. 2012a;32(10):655–661. doi:10.1016/j.jevs.2012.08.209

McKnight AL. MRI of the equine stifle—61 clinical cases. *J Equine Vet Sci*. 2012b;32(10):672. doi:10.1016/j.jevs.2012.08.215

McParland TJ, Horne CR, Robertson JB, Schnabel LV, Nelson NC. Alterations to the synovial invaginations of the navicular bone are associated with pathology of both the navicular apparatus and distal interphalangeal joint when evaluated using high field MRI. *Vet Radiol Ultrasound*. 2023;64(1):9–17. doi:10.1111/vru.13140

Metzger J, Distl O. Genetics of equine orthopedic disease. *Vet Clin North Am Equine Pract*. 2020;36(2):289–301. doi:10.1016/j.cveq.2020.03.008

Mitchell RD, Edwards RB, Makkreel LD, Oliveira TD. Standing MRI lesions identified in jumping and dressage horses with lameness isolated to the foot. In: Proceedings of the 52nd Annual Convention of the American Association of Equine Practitioners; 2006 Dec; San Antonio, TX. Vol. 52. Lexington (KY): AAEP; 2006. p. 422–426.

Morgan JM, Aceto H, Manzi T, Davidson EJ. Incidence and risk factors for complications associated with equine general anaesthesia for elective magnetic resonance imaging. *Equine Vet J*. 2024;56(5):944–951. doi:10.1111/evj.14026

Murray R, Mair T. Use of magnetic resonance imaging in lameness diagnosis in the horse. *In Pract*. 2005;27(3):138–146. doi:10.1136/inpract.27.3.138

Murray RC, Dyson S. Image interpretation and artifacts. *Clin Tech Equine Pract*. 2007;6(1):16–25. doi:10.1053/j.ctep.2006.11.002

Murray RC, Dyson SJ, Tranquille C, Adams V. Association of type of sport and performance level with anatomical site of orthopaedic injury diagnosis. *Equine Vet J*. 2006;38(S36):411–416. doi:10.1111/j.2042-3306.2006.tb05578.x

Murray RC, Mair TS, Sherlock CE, Blunden AS. Comparison of high-field and low-field magnetic resonance images of cadaver limbs of horses. *Vet Rec*. 2009;165(10):281–288. doi:10.1136/vr.165.10.281

Murray RC, Walters JM, Snart H, Dyson SJ, Parkin TDH. Identification of risk factors for lameness in dressage horses. *Vet J*. 2010;184(1):27–36. doi:10.1016/j.tvjl.2009.03.020

Nagy A, Dyson S. Magnetic resonance anatomy of the carpus of the horse described from images acquired from low-field and high-field magnets. *Vet Radiol Ultrasound*. 2011;52(3):273–283. doi:10.1111/j.1740-8261.2010.01773.x

NEHS. Lameness the most commonly reported health problem in horses. *Vet Rec*. 2016;179(15):370. doi:10.1136/vr.i5514

Olive J. Distal interphalangeal articular cartilage assessment using low-field magnetic resonance imaging: low-field MR of distal interphalangeal cartilage. *Vet Radiol Ultrasound*. 2010;51(3):259–266. doi:10.1111/j.1740-8261.2009.01663.x

Olive J, Mair TS, Charles B. Use of standing low-field magnetic resonance imaging to diagnose middle phalanx bone marrow lesions in horses. *Equine Vet Educ*. 2009;21(3):116–123. doi:10.2746/095777309X383612

Osborn ML, Cornille JL, Blas-Machado U, Uhl EW. The equine navicular apparatus as a premier enthesis organ: functional implications. *Vet Surg*. 2021;50(4):713–728. doi:10.1111/vsu.13620

Paris A, Beccati F, Pepe M. Type, prevalence, and risk factors for the development of orthopedic injuries in endurance horses during training and competition. *J Am Vet Med Assoc*. 2021;258(10):1109–1118. doi:10.2460/javma.258.10.1109

Parkes RS, Richard Newton J, Dyson SJ. An investigation of risk factors for foot-related lameness in a United Kingdom referral population of horses. *Vet J*. 2013;196(2):218–225. doi:10.1016/j.tvjl.2012.09.006

Parks AH. Aspects of functional anatomy of the distal limb. In: Proceedings of the 58th Annual Convention of the American Association of Equine Practitioners; 2012 Dec; Anaheim, CA. Vol. 58. Lexington (KY): AAEP; 2012. p. 132–137.

Porter EG, Werpy NM. New concepts in standing advanced diagnostic equine imaging. *Vet Clin North Am Equine Pract*. 2014;30(1):239–268. doi:10.1016/j.cveq.2013.11.001

Reis IL, Lopes B, Sousa P, Sousa AC, Caseiro AR, Mendonça CM, Santos JM, Atayde LM, Alvites RD, Maurício AC. Equine musculoskeletal pathologies: clinical approaches and therapeutical perspectives—a review. *Vet Sci*. 2024;11(5):190. doi:10.3390/vetsci11050190

Ribitsch I, Oreff GL, Jenner F. Regenerative medicine for equine musculoskeletal diseases. *Animals (Basel)*. 2021;11(1):234. doi:10.3390/ani11010234

Ross MW. The lameness examination. In: Ross MW, Dyson SJ, editors. *Diagnosis and Management of Lameness in the Horse*. 2nd ed. St. Louis: Elsevier; 2011. p. 1–167.

Ross MW. The hind foot and pastern. In: Ross MW, Dyson SJ, editors. *Diagnosis and Management of Lameness in the Horse*. 2nd ed. St. Louis: Elsevier; 2011. p. 475–480.

Ross WA, Kaneene JB. An individual-animal-level prospective study of risk factors associated with the occurrence of lameness in the Michigan (USA) equine population. *Prev Vet Med*. 1996;29(1):59–75. doi:10.1016/S0167-5877(96)01055-0

Sampson SN, Schneider RK, Gavin PR, Ho CP, Tucker RL, Charles EM. Magnetic resonance imaging findings in horses with recent onset navicular syndrome but without

radiographic abnormalities. *Vet Radiol Ultrasound*. 2009;50(4):339–346. doi:10.1111/j.1740-8261.2009.01547.x

Schramme M, Segard-Weisse E. Diagnostic imaging. In: Baxter GM, editor. *Adams and Stashak's Lameness in Horses*. 7th ed. Hoboken: Wiley; 2020. p. 387–429.

Schramme M, Zimmerman M. The role of magnetic resonance imaging. In: Proceedings of the 68th Annual Convention of the American Association of Equine Practitioners; 2022 Dec; San Diego, CA. Vol. 68. Lexington (KY): AAEP; 2022. p. 141–150.

Selberg K, Werpy N. Fractures of the distal phalanx and associated soft tissue and osseous abnormalities in 22 horses with ossified sclerotic ungual cartilages diagnosed with magnetic resonance imaging. *Vet Radiol Ultrasound*. 2011;52(4):394–401. doi:10.1111/j.1740-8261.2011.01813.x

Sherlock C, Mair T, Blunden T. Deep erosions of the palmar aspect of the navicular bone diagnosed by standing magnetic resonance imaging. *Equine Vet J*. 2008;40(7):684–692. doi:10.2746/042516408X330365

Sherlock CE. What has MRI taught us about foot lameness? In: Proceedings of the NAVC Conference; 2015 Jan; Orlando, FL. Vol. 29. NAVC Large Animal Edition; 2015. p. 243–245.

Sherlock CE, Kinns J, Mair TS. Evaluation of foot pain in the standing horse by magnetic resonance imaging. *Vet Rec*. 2007;161(22):739–744. doi:10.1136/vr.161.22.739

Smith M. Diagnosing causes of foot pain in the horse. *Equine Health*. 2015;23:32–35. doi:10.12968/eqhe.2015.23.32

Smith MA, Dyson SJ, Murray RC. Reliability of high- and low-field magnetic resonance imaging systems for detection of cartilage and bone lesions in the equine cadaver fetlock. *Equine Vet J*. 2012;44(6):684–691. doi:10.1111/j.2042-3306.2012.00561.x

Smith RKW, Birch HL, Sinclair C, Goodship AE. Tendon and ligament physiology. In: Hinchcliff KW, Kaneps AJ, Geor RJ, editors. *Equine Sports Medicine and Surgery*. 3rd ed. London: Elsevier; 2024. p. 252–279.

Swor TM, Dabareiner RM, Honnas CM, Cohen ND, Black JB. Musculoskeletal problems associated with lameness and poor performance in cutting horses: 200 cases (2007–2015). *J Am Vet Med Assoc*. 2019;254(5):619–625. doi:10.2460/javma.254.5.619

Tucker RL, Sampson SN. Magnetic resonance imaging protocols for the horse. *Clin Tech Equine Pract*. 2007;6(1):2–15. doi:10.1053/j.ctep.2006.11.001

Uprichard KL, Boden LA, Marshall JF. An online survey to characterise spending patterns of horse owners and to quantify the impact of equine lameness on a pleasure horse population. *Equine Vet J*. 2014;46(S47):4–4. doi:10.1111/evj.12323_7

Van Weeren PR. General anatomy and physiology of joints. In: Frisbie DD, McIlwraith CW, editors. *Joint Disease in the Horse*. 2nd ed. London: Elsevier; 2016. p. 1–24.

Van Weeren PR, Back W. Musculoskeletal disease in aged horses and its management. *Vet Clin North Am Equine Pract*. 2016;32(2):229–247. doi:10.1016/j.cveq.2016.04.003

Van Weeren PR. Joint physiology: response to exercise and training. In: Hinchcliff KW, Kaneps AJ, Geor RJ, editors. *Equine Sports Medicine and Surgery*. 3rd ed. London: Elsevier; 2024. p. 280–291.

Van Weeren PR, Brama PAJ, Barneveld A. Exercise at young age may influence the final quality of the equine musculoskeletal system. In: Proceedings of the 46th Annual Convention of the American Association of Equine Practitioners; 2000 Dec; San Antonio, TX. Vol. 46. Lexington (KY): AAEP; 2000. p. 29–35.

Van Zadelhoff C, Schwarz T, Smith S, Engerand A, Taylor S. Identification of naturally occurring cartilage damage in the equine distal interphalangeal joint using low-field magnetic resonance imaging and magnetic resonance arthrography. *Front Vet Sci*. 2020;6:508. doi:10.3389/fvets.2019.00508

Waselau M, McKnight A, Kasparek A. Magnetic resonance imaging of equine stifles: technique and observations in 76 clinical cases. *Equine Vet Educ*. 2020;32(S10):85–91. doi:10.1111/eve.13248

Weishaupt MA. Adaptation strategies of horses with lameness. *Vet Clin North Am Equine Pract*. 2008;24(1):79–100. doi:10.1016/j.cveq.2007.11.010

Werpy NM. Magnetic resonance imaging for diagnosis of soft tissue and osseous injuries in the horse. *Clin Tech Equine Pract*. 2004;3(4):389–398. doi:10.1053/j.ctep.2005.02.017

Werpy NM. Magnetic resonance imaging of the equine patient: a comparison of high- and low-field systems. *Clin Tech Equine Pract*. 2007;6(1):37–45. doi:10.1053/j.ctep.2006.11.004

Werpy NM. Equine imaging modalities. In: Proceedings of the 56th Annual Convention of the American Association of Equine Practitioners; 2010 Dec; Baltimore, MD. Vol. 56. Lexington (KY): AAEP; 2010. p. 297–306.

Werpy NM. Recheck magnetic resonance imaging examinations for evaluation of musculoskeletal injury. *Vet Clin North Am Equine Pract*. 2012;28(3):659–680. doi:10.1016/j.cveq.2012.09.003

Werpy NM, Ho CP, Kawcak CE, Rantanen NW, McIlwraith CW. Review of principles and clinical applications of magnetic resonance imaging in the horse. In: Proceedings of the 52nd Annual Convention of the American Association of Equine Practitioners; 2006 Dec; San Antonio, TX. Vol. 52. Lexington (KY): AAEP; 2006. p. 427–440.

Whitton C. Skeletal physiology: responses to exercise and training. In: Hinchcliff KW, Kaneps AJ, Geor RJ, editors. *Equine Sports Medicine and Surgery*. 3rd ed. London: Elsevier; 2024. p. 233–251.

Wilson A, Weller R. The biomechanics of the equine limb and its effect on lameness. In: Ross MW, Dyson SJ, editors. *Diagnosis and Management of Lameness in the Horse*. 2nd ed. St. Louis: Elsevier; 2011. p. 270–281.

Winter MD. The basics of musculoskeletal magnetic resonance imaging. *Vet Clin North Am Equine Pract*. 2012;28(3):599–616. doi:10.1016/j.cveq.2012.09.001

V. APPENDIX

Appendix 1 – Distribution of MRI examinations across the year.

Appendix 1.1 – MRI examination distribution by season.

SEASONAL DISTRIBUTION			
	Observed N	**Expected N**	**Residual**
Winter	23	43,0	-20,0
Spring	40	43,0	-3,0
Summer	56	43,0	13,0
Fall	53	43,0	10,0
Total	**172**		

Appendix 2.2 – MRI examination distribution by month.

MONTHLY DISTRIBUTION			
	Observed N	**Expected N**	**Residual**
January	6	14,3	-8,3
February	5	14,3	-9,3
March	11	14,3	-3,3
April	9	14,3	-5,3
May	20	14,3	5,7
June	14	14,3	-,3
July	22	14,3	7,7
August	20	14,3	5,7
September	16	14,3	1,7
October	22	14,3	7,7
November	15	14,3	,7
December	12	14,3	-2,3
Total	**172**		

Appendix 2 – Scanning patterns of all initial MRI examinations.

Appendix 3.1 – Distribution of bilateral and unilateral scans.

Limb(s) Scanned	N	%
Bilateral		
RF + LF	123	71,5%
RH + LH	7	4,1%
Unilateral		
RF	20	11,6%
LF	12	7,0%
LH	8	4,7%
RH	2	1,2%
Total	**172**	**100,0%**

Appendix 4.2 – Scan patterns: combinations of scanned anatomical regions.

Initial Scans	n Limbs	% Limbs	n Horses	% Horses
Forelimbs				
Foot;	191	63,2%	111	64,5%
Foot; Pastern;	18	6,0%	17	9,9%
Foot; Pastern; Fetlock;	29	9,6%	29	16,9%
Foot; Fetlock;	22	7,3%	21	12,2%
Foot; Pastern; Fetlock; Carpus;	1	0,3%	1	0,6%
Pastern; Fetlock;	3	1,0%	3	1,7%
Fetlock;	12	4,0%	10	5,8%
Proximal Metacarpus; Carpus;	2	0,7%	1	0,6%
Hindlimbs				
Foot;	4	1,3%	4	2,3%
Foot; Pastern; Fetlock;	3	1,0%	3	1,7%
Foot; Fetlock;	3	1,0%	3	1,7%
Foot; Fetlock; Proximal Metatarsus;	1	0,3%	1	0,6%
Foot;Pastern; Fetlock;Proximal Metatarsus;Tarsus;	1	0,3%	1	0,6%
Pastern; Fetlock;	1	0,3%	1	0,6%
Fetlock;	7	2,3%	5	2,9%
Fetlock; Proximal Metatarsus;	3	1,0%	2	1,2%
Proximal Metatarsus; Tarsus;	1	0,3%	1	0,6%
Total	**302**	**100,0%**	**172**	**100,0%**

Appendix 3 – Lameness presentation and scanning patterns of forefeet examinations.

Appendix 3 – Distribution of Lameness Presentation, Scanning Patterns, and Laterality.

Lameness		n	%	Scanned Limbs		n	%
Unilateral		**119**	**79.9**	**Unilateral**		**37**	**24.8**
	LF	60	40.3		**LF**	14	9.4
	RF	59	39.6		**RF**	23	15.4
Bilateral		**30**	**20.1**	**Bilateral**		**112**	**75.2**
Total		**149**	**100.0**			**149**	**100.0**

Appendix 4 – Association between navicular bone and DDFT pathology.

Appendix 4.1 – Association between fluid signal along the flexor surface of the navicular bone and DDF tendinopathy.

		DDF tendinopathy				
		Absent	**Present**	**Total**	X^2	p
NB fluid signal along flexor surface	**Absent**	**86**$_a$	**70**$_b$	**156**	8.941	0.003
	% within DDFT	94.5	40.8	87.2		
	Present	**5**$_a$	**18**$_b$	**23**		
	% within DDFT	5.5	20.5	12.8		
	Total	**91**	**88**	**179**		
	% within DDFT	100.0	100.0	100.0		

Each subscript letter denotes a subset of DDFT categories whose column proportions do not differ significantly from each other at the .05 level.

Appendix 4.2 – Association between enlarged synovial invaginations in the navicular bone and DDF tendinopathy.

		DDF tendinopathy				
		Absent	**Present**	**Total**	X^2	p
NB enlarged synovial invaginations	**Absent**	**88**$_a$	**75**$_b$	**163**	7.239	0.007
	% within DDFT	96.7	85.2	91.1		
	Present	**3**$_a$	**13**$_b$	**16**		
	% within DDFT	3.3	14.8	8.9		
	Total	**91**	**88**	**179**		
	% within DDFT	100.0	100.0	100.0		

Each subscript letter denotes a subset of DDFT categories whose column proportions do not differ significantly from each other at the .05 level.

Appendix 4.3 – Association between flexor surface erosions of the navicular bone and DDF tendinopathy.

		DDF tendinopathy				
		Absent	**Present**	**Total**	X^2	p
NB flexor surface erosion	**Absent**	**90**$_a$	**77**$_b$	**167**	9.298	0.002
	% within DDFT	98.9	87.5	93.3		
	Present	**1**$_a$	**11**$_b$	**12**		
	% within DDFT	1.1	12.5	6.7		
	Total	**91**	**88**	**179**		
	% within DDFT	100.0	100.0	100.0		

Each subscript letter denotes a subset of DDFT categories whose column proportions do not differ significantly from each other at the .05 level.

Appendix 5 – Association between demographics and navicular bone pathology.

Appendix 5.1 – Association between Age and Navicular Bone Pathology.

	Navicular Bone							
	Not Affected		Affected		Total			
Age Group	n	%	n	%	n	%	X^2	p
< 5 years	5	7.8	8	9.4	13	8.7	6,376	0.095
6 – 10 years	25	39.1	36	42.4	61	40.9		
11 – 15 years	23	35.9	37	43.5	60	40.3		
16 – 20 years	11	17.2	4	4.7	15	10.1		
Total	**64**		**85**		**149**			

Appendix 5.2 – Association between Sex and Navicular Bone Pathology.

	Navicular Bone							
	Not Affected		Affected		Total			
Sex	n	%	n	%	n	%	X^2	p
Gelding	38	37.8	50	58.8	88	59.1	0.005	0.946
Mare	26	40.6	35	34.8	61	40.9		
Total	**64**		**85**		**149**			

Appendix 5.3 – Association between Breed and Navicular Bone Pathology.

	Navicular Bone							
	Not Affected		Affected		Total			
Breed	n	%	n	%	n	%	X^2	p
Dutch Warmblood	16	25.0	11	12.9	27	18.1	9.968	0.190
Canadian Warmblood	8	12.5	12	14.1	20	13.4		
Irish Sport Horse	8	12.5	12	14.1	20	13.4		
Quarter Horse	5	7.8	14	16.5	19	12.8		
Hanoverian	5	7.8	9	10.6	14	9.4		
Oldenburg	3	4.7	11	12.9	14	9.4		
Thoroughbred	7	10.9	6	7.1	13	8.7		
Holsteiner	7	10.9	5	5.9	12	8.1		
Other	5	7.8	5	5.9	10	6.7		
Total	**64**		**85**		**149**			

Appendix 5.4 – Association between Discipline and Navicular Bone Pathology.

	Navicular Bone							
	Not Affected		Affected		Total			
Discipline	n	%	n	%	n	%	X^2	p
Show Jumping	21	32.8	27	31.8	48	32.2	7.586	0.181
Hunter	21	32.8	19	22.4	40	26.8		
Dressage	8	12.5	10	11.8	18	12.1		
Eventing	3	4.7	12	14.1	15	10.1		
Western	3	4.7	11	12.9	14	9.4		
Pleasure Riding	5	7.8	5	5.9	10	6.7		
Other	3	4.7	1	1.2	4	2.7		
Total	**64**		**85**		**149**			

Appendix 6 – Association between navicular bursa and DDFT and NB pathology.

Appendix 6.1 – Association between synovial proliferation/thickening of the navicular bursa and DDF tendinopathy.

		DDF tendinopathy				
		Absent	**Present**	**Total**	X^2	p
NBU synovial proliferation/	**Absent**	**80**$_a$	**29**$_b$	**109**	56.742	<0.001
thickening	% within DDFT	87.9	33.0	60.9		
	Present	**11**$_a$	**59**$_b$	**70**		
	% within DDFT	12.1	67.0	39.1		
	Total	**91**	**88**	**179**		
	% within DDFT	100.0	100.0	100.0		

Each subscript letter denotes a subset of DDFT categories whose column proportions do not differ significantly from each other at the .05 level.

Appendix 6.2 – Association between synovial proliferation/thickening of the navicular bursa and abnormal navicular bone trabecular fluid signal.

		NB diffuse fluid signal				
		Absent	**Present**	**Total**	X^2	p
NBU synovial proliferation/	**Absent**	**70**$_a$	**26**$_b$	**96**	12.567	<0.001
thickening	% within NB	64.2	37.1	53.6		
	Present	**39**$_a$	**44**$_b$	**83**		
	% within NB	35.8	62.9	46.4		
	Total	**109**	**70**	**179**		
	% within NB	100.0	100.0	100.0		

Each subscript letter denotes a subset of Navicular Bone categories whose column proportions do not differ significantly from each other at the .05 level.

Appendix 7 – Association between demographics and navicular bursa pathology.

Appendix 7.1 – Association between Age and Navicular Bursa Pathology.

	Navicular Bursa							
	Not Affected		Affected		Total			
Age Group	n	%	n	%	n	%	X^2	p
< 5 years	4	7.0	9	9.8	13	8.7	2.820	0.420
6 – 10 years	20	35.1	41	44.6	61	40.9		
11 – 15 years	25	43.9	35	38.0	60	40.3		
16 – 20 years	8	14.0	7	7.6	15	10.1		
Total	**57**		**92**		**149**			

Appendix 7.2 – Association between Sex and Navicular Bursa Pathology.

	Navicular Bursa							
	Not Affected		Affected		Total			
Sex	n	%	n	%	n	%	X^2	p
Gelding	38	37.8	50	58.8	88	59.1	2.209	0.137
Mare	19	33.3	42	37.7	61	40.9		
Total	**64**		**85**		**149**			

Appendix 7.3 – Association between Breed and Navicular Bursa Pathology.

	Navicular Bursa							
	Not Affected		Affected		Total			
Breed	n	%	n	%	n	%	X^2	p
Dutch Warmblood	14	24.6	13	14.1	27	18.1	13.699	0.057
Canadian Warmblood	4	7.0	16	17.4	20	13.4		
Irish Sport Horse	6	10.5	14	15.2	20	13.4		
Quarter Horse	3	5.3	16	17.4	19	12.8		
Hanoverian	6	10.5	8	8.7	14	9.4		
Oldenburg	7	12.3	7	7.6	14	9.4		
Thoroughbred	8	14.0	5	5.4	13	8.7		
Holsteiner	4	7.0	8	8.7	12	8.1		
Other	5	8.8	5	5.4	10	6.7		
Total	**57**		**92**		**149**			

Appendix 7.4 – Association between Discipline and Navicular Bursa Pathology.

	Navicular Bursa							
	Not Affected		Affected		Total			
Discipline	n	%	n	%	n	%	X^2	p
Show Jumping	14	24.6	34	37.0	48	32.2	8.155	0.148
Hunter	17	29.8	23	25.0	40	26.8		
Dressage	10	17.5	8	8.7	18	12.1		
Eventing	7	12.3	8	8.7	15	10.1		
Western	2	3.5	12	13.0	14	9.4		
Pleasure Riding	4	7.0	6	6.5	10	6.7		
Other	3	5.3	1	1.1	4	2.7		
Total	**57**		**92**		**149**			

Appendix 8 – Association between DSIL and navicular bone pathology.

Appendix 8.1 – Association between DSIL enthesopathy and diffuse fluid signal within the navicular bone.

		NB diffuse fluid signal				
		Absent	**Present**	**Total**	X^2	p
DSIL enthesopathy	**Absent**	**113**$_a$	**36**$_b$	**149**	8.183	0.004
	% within NB	88.3	70.6	83.2		
	Present	**15**$_a$	**15**$_b$	**30**		
	% within NB	35.8	62.9	46.4		
	Total	**128**	**51**	**179**		
	% within NB	100.0	100.0	100.0		

Each subscript letter denotes a subset of Navicular Bone categories whose column proportions do not differ significantly from each other at the .05 level.

Appendix 8.1 – Association between DSIL enthesopathy and enlarged synovial invaginations in the navicular bone.

		NB enlarged synovial invaginations				
		Absent	**Present**	**Total**	X^2	p
DSIL enthesopathy	**Absent**	**139**$_a$	**10**$_b$	**149**	5.418	0.032
	% within NB	85.3	62.5	83.2		
	Present	**24**$_a$	**6**$_b$	**30**		
	% within NB	14.7	37.5	16.8		
	Total	**128**	**51**	**179**		
	% within NB	100.0	100.0	100.0		

Each subscript letter denotes a subset of Navicular Bone categories whose column proportions do not differ significantly from each other at the .05 level.

Appendix 9 – Association between demographics and DSIL pathology.

Appendix 9.1 – Association between Age and DSIL Pathology.

	DSIL							
	Not Affected		Affected		Total			
Age Group	n	%	n	%	n	%	X^2	p
< 5 years	11	9.1	2	7.1	13	8.7	0.507	0.948
6 – 10 years	48	39.7	13	46.4	61	40.9		
11 – 15 years	49	40.5	11	39.3	60	40.3		
16 – 20 years	13	10.7	2	7.1	15	10.1		
Total	**121**		**28**		**149**			

Appendix 9.2 – Association between Sex and DSIL Pathology.

	DSIL							
	Not Affected		Affected		Total			
Sex	n	%	n	%	n	%	X^2	p
Gelding	74	61.2	14	50.0	88	59.1	1.171	0.279
Mare	47	38.8	14	50.0	61	40.9		
Total	**121**		**28**		**149**			

Appendix 9.3 – Association between Breed and DSIL Pathology.

	DSIL							
	Not Affected		Affected		Total			
Breed	n	%	n	%	n	%	X^2	p
Dutch Warmblood	22	18.2	5	17.9	27	18.1	4.753	0.701
Canadian Warmblood	17	14.0	3	10.7	20	13.4		
Irish Sport Horse	17	14.0	3	10.7	20	13.4		
Quarter Horse	12	9.9	7	25.0	19	12.8		
Hanoverian	11	9.1	3	10.7	14	9.4		
Oldenburg	11	9.1	3	10.7	14	9.4		
Thoroughbred	11	9.1	2	7.1	13	8.7		
Holsteiner	11	9.1	1	3.6	12	8.1		
Other	9	7.4	1	3.6	10	6.7		
Total	**121**		**28**		**149**			

Appendix 9.4 – Association between Discipline and DSIL Pathology.

	DSIL							
	Not Affected		Affected		Total			
Discipline	n	%	n	%	n	%	X^2	p
Show Jumping	39	32.2	9	32.1	48	32.2	8.103	0.130
Hunter	33	27.3	7	25.0	40	26.8		
Dressage	16	13.2	2	7.1	18	12.1		
Eventing	13	10.7	2	7.1	15	10.1		
Western	7	5.8	7	25.0	14	9.4		
Pleasure Riding	9	7.4	1	3.6	10	6.7		
Other	4	3.3	0	0.0	4	2.7		
Total	**121**		**28**		**149**			

Appendix 10 – Association between demographics and CSL pathology.

Appendix 10.1 – Association between Age and CSL Pathology.

	CSL					
	Not Affected		Affected		Total	
Age Group	n	%	n	%	n	%
< 5 years	13	9.2	0	0	13	8.7
6 – 10 years	59	41.5	2	28.6	61	40.9
11 – 15 years	55	38.7	5	71.4	60	40.3
16 – 20 years	15	10.6	0	0	15	10.1
Total	**142**		**7**		**149**	

Appendix 10.2 – Association between Sex and CSL Pathology.

	CSL					
	Not Affected		Affected		Total	
Sex	n	%	n	%	n	%
Gelding	84	59.2	4	57.1	88	59.1
Mare	58	40.8	3	42.9	61	40.9
Total	**142**		**7**		**149**	

Appendix 10.3 – Association between Breed and CSL Pathology.

	CSL					
	Not Affected		Affected		Total	
Breed	n	%	n	%	n	%
Dutch Warmblood	27	19.0	0	0.0	27	18.1
Canadian Warmblood	20	14.1	0	0.0	20	13.4
Irish Sport Horse	17	12.0	3	42.9	20	13.4
Quarter Horse	17	12.0	2	28.6	19	12.8
Hanoverian	13	9.2	1	14.2	14	9.4
Oldenburg	13	9.2	1	14.2	14	9.4
Thoroughbred	13	9.2	0	0.0	13	8.7
Holsteiner	12	8.5	0	0.0	12	8.1
Other	10	7.0	0	0.0	10	6.7
Total	**142**		**7**		**149**	

Appendix 10.4 – Association between Discipline and CSL Pathology.

	CSL					
	Not Affected		Affected		Total	
Discipline	n	%	n	%	n	%
Show Jumping	46	32.4	2	28.6	48	32.2
Hunter	38	26.8	2	28.6	40	26.8
Dressage	18	12.7	0	0.0	18	12.1
Eventing	14	9.9	1	14.3	15	10.1
Western	13	9.2	1	14.3	14	9.4
Pleasure Riding	9	6.3	1	14.3	10	6.7
Other	4	2.8	0	0.0	4	2.7
Total	**142**		**7**		**149**	

Appendix 11 – Association between demographics and DDFT pathology.

Appendix 11.1 – Association between Age and DDFT Pathology.

	DDFT							
	Not Affected		Affected		Total			
Age Group	n	%	n	%	n	%	X^2	p
< 5 years	4	6.5	9	10.3	13	8.7	1.567	0.667
6 – 10 years	26	41.9	35	40.2	61	40.9		
11 – 15 years	24	38.7	36	41.4	60	40.3		
16 – 20 years	8	12.9	7	8.0	15	10.1		
Total	**62**		**87**		**149**			

Appendix 11.2 – Association between Sex and DDFT Pathology.

	DDFT							
	Not Affected		Affected		Total			
Sex	n	%	n	%	n	%	X^2	p
Gelding	42	67.7	46	52.9	88	59.1	3.310	0.069
Mare	20	32.3	41	47.1	61	40.9		
Total	**62**		**87**		**149**			

Appendix 11.3 – Association between Breed and DDFT Pathology.

	DDFT							
	Not Affected		Affected		Total			
Breed	n	%	n	%	n	%	X^2	p
Dutch Warmblood	15	24.2	12	13.8	27	18.1	7.978	0.335
Canadian Warmblood	6	9.7	14	16.1	20	13.4		
Irish Sport Horse	7	11.3	13	14.9	20	13.4		
Quarter Horse	4	6.5	15	17.2	19	12.8		
Hanoverian	5	8.1	9	10.3	14	9.4		
Oldenburg	7	11.3	7	8.0	14	9.4		
Thoroughbred	6	9.7	7	8.0	13	8.7		
Holsteiner	6	9.7	6	6.9	12	8.1		
Other	6	9.7	4	4.6	10	6.7		
Total	**62**		**87**		**149**			

Appendix 11.4 – Association between Discipline and DDFT Pathology.

	DDFT							
	Not Affected		Affected		Total			
Discipline	n	%	n	%	n	%	X^2	p
Show Jumping	20	32.3	28	32.2	48	32.2	3.261	0.660
Hunter	19	30.6	21	24.1	40	26.8		
Dressage	8	12.9	10	11.5	18	12.1		
Eventing	6	9.7	9	10.3	15	10.1		
Western	3	4.8	11	12.6	14	9.4		
Pleasure Riding	5	8.1	5	5.7	10	6.7		
Other	1	1.6	3	3.4	4	2.7		
Total	**62**		**87**		**149**			

Appendix 12 – Association between demographics and DIP Joint pathology.

Appendix 12.1 – Association between Age and DIP Joint Pathology.

	DIP joint					
	Not Affected		Affected		Total	
Age Group	n	%	n	%	n	%
< 5 years	1	9.1	12	8.7	13	8.7
6 – 10 years	4	36.4	57	41.3	61	40.9
11 – 15 years	4	36.4	56	40.6	60	40.3
16 – 20 years	2	18.2	13	9.4	15	10.1
Total	**11**		**138**		**149**	

Appendix 12.2 – Association between Sex and DIP Joint Pathology.

	DIP joint					
	Not Affected		Affected		Total	
Sex	n	%	n	%	n	%
Gelding	6	54.5	82	59.4	88	59.1
Mare	5	45.5	56	40.6	61	40.9
Total	**11**		**138**		**149**	

Appendix 12.3 – Association between Breed and DIP Joint Pathology.

	DIP joint					
	Not Affected		Affected		Total	
Breed	n	%	n	%	n	%
Dutch Warmblood	4	36.4	23	16.7	27	18.1
Canadian Warmblood	3	27.3	17	12.3	20	13.4
Irish Sport Horse	0	0.0	20	14.5	20	13.4
Quarter Horse	0	0.0	19	13.8	19	12.8
Hanoverian	1	9.1	13	9.4	14	9.4
Oldenburg	0	0.0	14	10.1	14	9.4
Thoroughbred	1	9.1	12	8.7	13	8.7
Holsteiner	2	18.2	10	7.2	12	8.1
Other	0	0.0	10	7.2	10	6.7
Total	**11**		**138**		**149**	

Appendix 12.4 – Association between Discipline and DIP Joint Pathology.

	DIP joint					
	Not Affected		Affected		Total	
Discipline	n	%	n	%	n	%
Show Jumping	6	54.5	42	30.4	48	32.2
Hunter	3	27.3	37	26.8	40	26.8
Dressage	1	9.1	17	12.3	18	12.1
Eventing	1	9.1	14	10.1	15	10.1
Western	0	0.0	14	10.1	14	9.4
Pleasure Riding	0	0.0	10	7.2	10	6.7
Other	0	0.0	4	2.9	4	2.7
Total	**11**		**138**		**149**	

Appendix 13 – Association between demographics and CLs of DIP Joint pathology.

Appendix 13.1 – Association between Age and CLs of DIP Joint Pathology.

	CLs of DIP joint							
	Not Affected		Affected		Total			
Age Group	n	%	n	%	n	%	X^2	p
< 5 years	10	9.3	3	7.3	13	8.7	2.929	0.413
6 – 10 years	48	44.4	13	31.7	61	40.9		
11 – 15 years	39	36.1	21	51.2	60	40.3		
16 – 20 years	11	10.2	4	9.8	15	10.1		
Total	**108**		**41**		**149**			

Appendix 13.2 – Association between Sex and CLs of DIP Joint Pathology.

	CLs of DIP joint							
	Not Affected		Affected		Total			
Sex	n	%	n	%	n	%	X^2	p
Gelding	59	54.6	29	70.7	88	59.1	3.187	0.074
Mare	49	45.4	12	29.3	61	40.9		
Total	**108**		**41**		**149**			

Appendix 13.3 – Association between Breed and CLs of DIP Joint Pathology.

	CLs of DIP joint							
	Not Affected		Affected		Total			
Breed	n	%	n	%	n	%	X^2	p
Dutch Warmblood	20	18.5	7	17.1	27	18.1	7.356	0.389
Canadian Warmblood	15	13.9	5	12.2	20	13.4		
Irish Sport Horse	12	11.1	8	19.5	20	13.4		
Quarter Horse	17	15.7	2	4.9	19	12.8		
Hanoverian	10	9.3	4	9.8	14	9.4		
Oldenburg	9	8.3	5	12.2	14	9.4		
Thoroughbred	9	8.3	4	9.8	13	8.7		
Holsteiner	11	10.2	1	2.4	12	8.1		
Other	5	4.6	5	12.2	10	6.7		
Total	**108**		**41**		**149**			

Appendix 13.4 – Association between Discipline and CLs of DIP Joint Pathology.

	CLs of DIP joint							
	Not Affected		Affected		Total			
Discipline	n	%	n	%	n	%	X^2	p
Show Jumping	35	32.4	13	31.7	48	32.2	3.883	0.575
Hunter	26	24.1	14	34.1	40	26.8		
Dressage	13	12.0	5	12.2	18	12.1		
Eventing	10	9.3	5	12.2	15	10.1		
Western	12	11.1	2	4.9	14	9.4		
Pleasure Riding	9	8.3	1	2.4	10	6.7		
Other	3	2.8	1	2.4	4	2.7		
Total	**108**		**41**		**149**			

Appendix 14 – Association between demographics and Distal Phalanx pathology.

Appendix 14.1 – Association between Age and Distal Phalanx Pathology.

	Distal Phalanx							
	Not Affected		Affected		Total			
Age Group	n	%	n	%	n	%	X^2	p
< 5 years	3[a]	3.4	10[b]	16.1	13	8.7	7.777	0.051
6 – 10 years	36	41.4	25	40.3	61	40.9		
11 – 15 years	39	44.8	21	33.9	60	40.3		
16 – 20 years	9	10.3	6	9.7	15	10.1		
Total	**87**		**62**		**149**			

Each subscript letter denotes a subset of Distal Phalanx categories whose column proportions do not differ significantly from each other.

Appendix 14.2 – Association between Sex and Distal Phalanx Pathology.

	Distal Phalanx							
	Not Affected		Affected		Total			
Sex	n	%	n	%	n	%	X^2	p
Gelding	45[a]	51.7	43[b]	69.4	88	59.1	4.654	0.031
Mare	42[a]	48.3	19[b]	30.6	61	40.9		
Total	**87**		**62**		**149**			

Each subscript letter denotes a subset of Distal Phalanx categories whose column proportions do not differ significantly from each other.

Appendix 14.3 – Association between Breed and Distal Phalanx Pathology.

	Distal Phalanx							
	Not Affected		Affected		Total			
Breed	n	%	n	%	n	%	X^2	p
Dutch Warmblood	15	17.2	12	19.4	27	18.1	1.648	0.977
Canadian Warmblood	13	14.9	7	11.3	20	13.4		
Irish Sport Horse	10	11.5	10	16.1	20	13.4		
Quarter Horse	10	11.5	9	14.5	19	12.8		
Hanoverian	8	9.2	6	9.7	14	9.4		
Oldenburg	8	9.2	6	9.7	14	9.4		
Thoroughbred	8	9.2	5	8.1	13	8.7		
Holsteiner	8	9.2	4	6.5	12	8.1		
Other	7	8.0	3	4.8	10	6.7		
Total	**87**		**62**		**149**			

Appendix 14.4 – Association between Discipline and Distal Phalanx Pathology.

	Distal Phalanx							
	Not Affected		Affected		Total			
Discipline	n	%	n	%	n	%	X^2	p
Show Jumping	27	31.0	21	33.9	48	32.2	3.087	0.687
Hunter	22	25.3	18	29.0	40	26.8		
Dressage	11	12.6	7	11.3	18	12.1		
Eventing	10	11.5	5	8.1	15	10.1		
Western	7	8.0	7	11.3	14	9.4		
Pleasure Riding	8	9.2	2	3.2	10	6.7		
Other	2	2.3	2	3.2	4	2.7		
Total	**87**		**62**		**149**			

Appendix 15 – Association between demographics and Middle Phalanx pathology.

Appendix 15.1 – Association between Age and Middle Phalanx Pathology.

	Middle Phalanx					
	Not Affected		Affected		Total	
Age Group	n	%	n	%	n	%
< 5 years	12	8.6	1	10.0	13	8.7
6 – 10 years	57	41.0	4	40.0	61	40.9
11 – 15 years	56	40.3	4	40.0	60	40.3
16 – 20 years	14	10.1	1	10.0	15	10.1
Total	**139**		**10**		**149**	

Appendix 15.2 – Association between Sex and Middle Phalanx Pathology.

	Middle Phalanx					
	Not Affected		Affected		Total	
Sex	n	%	n	%	n	%
Gelding	83	59.7	5	50	88	59.1
Mare	56	40.3	5	50	61	40.9
Total	**139**		**10**		**149**	

Appendix 15.3 – Association between Breed and Middle Phalanx Pathology.

	Middle Phalanx					
	Not Affected		Affected		Total	
Breed	n	%	n	%	n	%
Dutch Warmblood	25	18.0	2	20.0	27	18.1
Canadian Warmblood	20	14.4	0	0.0	20	13.4
Irish Sport Horse	20	14.4	0	0.0	20	13.4
Quarter Horse	15	10.8	4	40.0	19	12.8
Hanoverian	13	9.4	1	10.0	14	9.4
Oldenburg	14	10.1	0	0.0	14	9.4
Thoroughbred	11	7.9	2	20.0	13	8.7
Holsteiner	12	8.6	0	0.0	12	8.1
Other	9	6.5	1	10.0	10	6.7
Total	**139**		**10**		**149**	

Appendix 15.4 – Association between Discipline and Middle Phalanx Pathology.

	Middle Phalanx					
	Not Affected		Affected		Total	
Discipline	n	%	n	%	n	%
Show Jumping	46	33.1	2	20.0	48	32.2
Hunter	37	26.6	3	30.0	40	26.8
Dressage	17	12.2	1	10.0	18	12.1
Eventing	15	10.8	0	0.0	15	10.1
Western	11	7.9	3	30.0	14	9.4
Pleasure Riding	10	7.2	0	0.0	10	6.7
Other	3	2.2	1	10.0	4	2.7
Total	**139**		**10**		**149**	

Appendix 16 – Association between demographics and PIP joint pathology.

Appendix 16.1 – Association between Age and PIP Joint Pathology.

	PIP joint							
	Not Affected		Affected		Total			
Age Group	n	%	n	%	n	%	X^2	p
< 5 years	13[a]	11.6	0[b]	0.0	13	8.7	20.814	<0.001
6 – 10 years	52[a]	46.4	9[b]	24.3	61	40.9		
11 – 15 years	42	37.5	18	48.6	60	40.3		
16 – 20 years	5[a]	4.5	10[b]	27.0	15	10.1		
Total	**112**		**37**		**149**			

Each subscript letter denotes a subset of PIP Joint categories whose column proportions do not differ significantly from each other.

Appendix 16.2 – Association between Sex and PIP Joint Pathology.

	PIP joint							
	Not Affected		Affected		Total			
Sex	n	%	n	%	n	%	X^2	p
Gelding	67	59.8	21	56.8	88	59.1	0.108	0.742
Mare	45	40.2	16	43.2	61	40.9		
Total	**112**		**37**		**149**			

Appendix 16.3 – Association between Breed and PIP Joint Pathology.

	PIP joint							
	Not Affected		Affected		Total			
Breed	n	%	n	%	n	%	X^2	p
Dutch Warmblood	17	15.2	10	27.0	27	18.1	5.589	0.594
Canadian Warmblood	15	13.4	5	13.5	20	13.4		
Irish Sport Horse	15	13.4	5	13.5	20	13.4		
Quarter Horse	17	15.2	2	5.4	19	12.8		
Hanoverian	11	9.8	3	8.1	14	9.4		
Oldenburg	12	10.7	2	5.4	14	9.4		
Thoroughbred	10	8.9	3	8.1	13	8.7		
Holsteiner	8	7.1	4	10.8	12	8.1		
Other	7	6.3	3	8.1	10	6.7		
Total	**112**		**37**		**149**			

Appendix 16.4 – Association between Discipline and PIP Joint Pathology.

	PIP joint							
	Not Affected		Affected		Total			
Discipline	n	%	n	%	n	%	X^2	p
Show Jumping	36	32.1	12	32.4	48	32.2	5.651	0.336
Hunter	29	25.9	11	29.7	40	26.8		
Dressage	14	12.5	4	10.8	18	12.1		
Eventing	11	9.8	4	10.8	15	10.1		
Western	13	11.6	1	2.7	14	9.4		
Pleasure Riding	5	4.5	5	13.5	10	6.7		
Other	4	3.6	0	0.0	4	2.7		
Total	**112**		**37**		**149**			